UNCLASSIFIED
SECURITY CLASSIFICATION OF THIS PAGE

(2)

DTIC ELECTE AUG 10 1989 D

REPORT DOCUMENTATION PAGE

1a REPORT SECURITY CLASSIFICATION UNCLASSIFIED	1b. RESTRICTIVE MARKINGS
2a SECURITY CLASSIFICATION AUTHORITY	3. DISTRIBUTION / AVAILABILITY OF REPORT APPROVED FOR PUBLIC RELEASE; DISTRIBUTION UNLIMITED
2b	
4. AD-A211 116	5. MONITORING ORGANIZATION REPORT NUMBER(S) AFOSR-TR- 89-1093
6a. NAME OF PERFORMING ORGANIZATION WEA, Ltd.	6b. OFFICE SYMBOL (If applicable)
6c. ADDRESS (City, State, and ZIP Code) P.O. Box 260, MIT Branch Cambridge, MA 02139	7a. NAME OF MONITORING ORGANIZATION AFOSR
	7b. ADDRESS (City, State, and ZIP Code) AFOSR/NA BLDG 410 Bolling AFB DC 20332-6448
8a. NAME OF FUNDING / SPONSORING ORGANIZATION AIR FORCE OFFICE OF SCIENTIFIC RESEARCH	8b. OFFICE SYMBOL (If applicable) AFOSR/NA
	9. PROCUREMENT INSTRUMENT IDENTIFICATION NUMBER F49620-88-C-0036
8c. ADDRESS (City, State, and ZIP Code) AFOSR/NA, BLDG 410 BOLLING AFB, DC 20332	10. SOURCE OF FUNDING NUMBERS

PROGRAM ELEMENT NO.	PROJECT NO.	TASK NO.	WORK UNIT ACCESSION NO.
61102F	2302	B1	

11. TITLE (Include Security Classification)
Wave-Mode Coordinate Analysis of "L" Junction in LSS (Unclassified)

12. PERSONAL AUTHOR(S)
Williams, James H., Jr. and Webb, Derrick S.

13a. TYPE OF REPORT	13b. TIME COVERED	14. DATE OF REPORT (Year, Month, Day)	15. PAGE COUNT
~~TECHNICAL~~ FINAL	FROM 88 Jan 15 TO 89 Mar 30	1989, March, 30	71

16. SUPPLEMENTARY NOTATION

17. COSATI CODES			18. SUBJECT TERMS (Continue on reverse if necessary and identify by block number)
FIELD	GROUP	SUB-GROUP	Wave-Mode Analysis, Large Space Structure, L Lattice Junction

19. ABSTRACT (Continue on reverse if necessary and identify by block number)

The propagation of structural disturbances through large space structures is of practical interest in the design and nondestructive evaluation of such large space systems. Many wave propagation analyses of large space structures must consider the reflection and transmission of waves at interconnecting junctions. Using the concepts of wave-mode coordinate analysis, a frequency domain study of wave propagation through an "L" lattice junction is conducted. Each lattice member is modeled as a combined longitudinal rod and Timoshenko beam. The joint in the assembly is modeled as a rigid mass of negligible geometric extent with mass rotary inertia. In order to determine the input wave-mode vector, the joint coupling matrix is applied to a point along a lattice member which is subjected to externally applied sinusoidal loads. The input wave-mode vector contains a mathematical description of the waves generated by the applied sinusiodal loads. The joint coupling matrix for the rigid joint with mass and rotary inertia is presented and used to obtain the scattering matrix of the "L" junction. The scattering matrix contains the reflection and transmission coefficients
(continued on reverse)

20. DISTRIBUTION / AVAILABILITY OF ABSTRACT	21. ABSTRACT SECURITY CLASSIFICATION
☒ UNCLASSIFIED/UNLIMITED ☐ SAME AS RPT ☐ DTIC USERS	UNCLASSIFIED

22a. NAME OF RESPONSIBLE INDIVIDUAL	22b TELEPHONE (Include Area Code)	22c. OFFICE SYMBOL
ANTHONY K. AMOS	202/767-4937	AFOSR/NA

DD FORM 1473, 84 MAR 83 APR edition may be used until exhausted. All other editions are obsolete.

SECURITY CLASSIFICATION OF THIS PAGE
UNCLASSIFIED

19. ABSTRACT (continued)

which the incoming waves will encounter as they enter the joint. Finally, the frequency response function of each Fourier transformed state variable of the transmitted waves is presented analytically. The results show that up to three independent waves may be generated in the lattice assembly by externally applied sinusiodal loads: one, a nondispersive propagating longitudinal wave; two, a dispersive propagating mode 1 flexural wave and; three, a mode 2 flexural wave. The mode 2 flexural wave exhibits a characteristic cutoff frequency. For frequencies less than the cutoff, the mode 2 flexural wave is a nonpropagating spatially decaying, evanescent, wave. For frequencies greater than the cutoff, the mode 2 flexural wave is a dispersive propagating wave. From the scattering matrix, the "L" lattice junction exhibits dispersive wave scattering and wave mode conversion. These features are illustrated graphically through magnitude and phase plots of the reflection and transmission coefficients.

ACKNOWLEDGMENTS

The Air Force Office of Scientific Research (Project Monitor, Dr. Anthony K. Amos) is gratefully acknowledged for its support of this research.

NOTICE

This document was prepared under the sponsorship of the Air Force. Neither the US Government nor any person acting on behalf of the US Government assumes any liability resulting from the use of the information contained in this document. This notice is intended to cover WEA, Ltd. as well.

Introduction

Many design proposals for large orbital space systems incorporate lattice type structures. Modeled as a network of joints and slender beams, such structures may exhibit low vibrational damping and low global stiffness compared with conventional lattice structures used on earth. In order to design and control such structures effectively, comprehensive dynamic analyses may be required. The propagation of structural disturbances through large lattice systems is of practical interest for design and nondestructive evaluation. Many wave propagation analyses of large lattice type space structures must consider the reflection and transmission of waves through interconnecting junctions. This report presents an analysis, using wave-mode coordinates, of wave propagation through a two-dimensional "L" junction with mass and mass rotary inertia.

A wave propagation analysis, using wave-mode coordinates, of a two-dimensional "L" lattice junction is presented. The configuration consists of two perpendicular semi-infinite members which are joined by a rigid joint as shown in Fig. 1. Each member is modeled as a combined longitudinal rod and Timoshenko beam. The corresponding geometric and material properties of each member are identical. The joint is modeled as a mass (m) of negligible geometric extent with mass rotary iner (I_{rz}). The junction is two-dimensional because the members attached to the joint exhibit both axial and flexural elastic properties such that the junction may translate and rotate only in one plane. Points 1 and 4, shown in Fig. 1, are placed equidistant from the geometric center of the rigid joint. The system is subjected to an externally applied sinusoidal axial force $\bar{F}_N$, shear force $\bar{F}_V$ and bending moment $\bar{F}_M$ at point 1 (refer to Fig. 2a), where the overbar denotes the Fourier transform of the time domain applied load.

This report is presented in four major sections. In the first section, the concept of the joint coupling matrix is applied to point 1 in order to determine the input wave-mode vector which represents the waves generated by the applied sinusoidal loads. The second section

introduces the joint coupling relationship for the two-dimensional rigid joint with mass and rotary inertia. The scattering matrix of the junction is developed and presented both analytically and graphically. In the third section, the results of the previous two sections are used to establish the frequency response function of each Fourier transformed state variable at point 4. Finally, a summary of the conclusions and recommendations is presented.

This report has three objectives: one; to illustrate the use of wave-mode coordinates to study the propagation of waves through an "L" lattice assembly as shown in Fig. 1; two, to examine the reflection and transmission coefficients of longitudinal and flexural waves in an "L" lattice assembly at various frequencies and; three, to illustrate the phenomenon of wave-mode conversion; that is, a propagating mode 1 flexural wave may reflect and/or transmit as an evanescent mode 2 flexural wave and vice versa.

Waves Induced by Sinusoidal Loading in Continuous Lattice Member

In this section, the concept of the joint coupling matrix is applied to point 1 of Fig. 1. The wave-mode vector which contains the waves generated by the applied loads at point 1 is determined. The notation and definitions presented throughout this report will follow those given in [1]. For convenience, a brief presentation of the concepts and nomenclature used in wave-mode coordinate analysis for wave propagation studies is given in Appendix A.

Joint Coupling Matrix

A rigid massless joint with no spatial extent is simulated at point 1 as shown in Fig. 2a. Points L and R are located just to the left and just to the right of point 1, respectively.

The explicit form of the joint coupling matrix for arbitrary two-dimensional rigid joints is given in [2]. It is important to note that the positive orientation of the internal shear force of the lattice member used in the development of the generalized joint coupling matrix in [2] is opposite to the convention used in the derivation of the transfer matrix of the lattice member [3]. It is necessary that the two systems be consistent. Therefore, the polarity of the shear force components of the joint coupling matrix given by [2] must be modified accordingly. From [2], the joint coupling relationship for the rigid joint with zero mass and zero spatial extent shown in Fig. 2a is

$$\underline{B}\begin{Bmatrix}\underline{\bar{z}}_L\\ \underline{\bar{z}}_R\end{Bmatrix}=\begin{Bmatrix}0\\0\\0\\\bar{F}_M\\\bar{F}_V\\\bar{F}_N\end{Bmatrix} \tag{1}$$

where

$$\underline{B} = \begin{pmatrix} 1 & 0 & 0 & 0 & 0 & 0 & -1 & 0 & 0 & 0 & 0 & 0 \\ 0 & 1 & 0 & 0 & 0 & 0 & 0 & -1 & 0 & 0 & 0 & 0 \\ 0 & 0 & 1 & 0 & 0 & 0 & 0 & 0 & -1 & 0 & 0 & 0 \\ 0 & 0 & 0 & 1 & 0 & 0 & 0 & 0 & 0 & -1 & 0 & 0 \\ 0 & 0 & 0 & 0 & (-1) & 0 & 0 & 0 & 0 & 0 & (1) & 0 \\ 0 & 0 & 0 & 0 & 0 & 1 & 0 & 0 & 0 & 0 & 0 & -1 \end{pmatrix} \tag{2}$$

is the joint coupling matrix of the massless joint, and

$$\overline{\underline{z}}_L^T = \{\overline{u}_L \quad \overline{y}_L \quad \overline{\psi}_L \quad \overline{M}_L \quad \overline{V}_L \quad \overline{N}_L\} \tag{3}$$

$$\overline{\underline{z}}_R^T = \{\overline{u}_R \quad \overline{y}_R \quad \overline{\psi}_R \quad \overline{M}_R \quad \overline{V}_R \quad \overline{N}_R\} \tag{4}$$

are the Fourier transformed state vectors at points L and R, respectively, and the superscript ^{T} denotes the transpose. The two elements of the joint coupling matrix $\underline{B}$ which are enclosed in parentheses are the modified terms which ensure that the sign conventions for the joint coupling matrix and the transfer matrix of the lattice member are consistent.

The joint coupling relationship contains the force dynamic and geometric compatibility requirements at the joint. Substituting eqns. (2) through (4) into eqn. (1) and writing out each scalar equation give

$$\overline{u}_L - \overline{u}_R = 0 \tag{5}$$

$$\overline{y}_L - \overline{y}_R = 0 \tag{6}$$

$$\overline{\psi}_L - \overline{\psi}_R = 0 \tag{7}$$

$$\overline{M}_L - \overline{M}_R = \overline{F}_M \tag{8}$$

$$-\overline{V}_L + \overline{V}_R = \overline{F}_V \tag{9}$$

$$\overline{N}_L - \overline{N}_R = \overline{F}_N \tag{10}$$

Eqns. (5) through (7) represent the compatibility requirements at the joint and eqns. (8) through (10) represent the force dynamic requirements at the joint.

Scattering and Wave-Mode Generation Matrix

The input-output relationship of a joint may be stated as [2]

$$\overline{\underline{w}}_{OUT} = \underline{S}(\omega)\overline{\underline{w}}_{IN} + \underline{G}(\omega)\overline{\underline{F}}_{ext} \tag{11}$$

where the matrix $\underline{S}(\omega)$ is called the scattering matrix of the joint, and the matrix $\underline{G}(\omega)$ is called the wave-mode generation matrix of the joint. The process of transforming eqn. (1) into a scattering relationship of the form of eqn. (11) is presented below.

The state vectors at points L and R in Fig. 2a are related to the wave-mode coordinates at points L and R, respectively, by

$$\underline{\bar{z}}_L = \underline{Y}(\omega)\underline{\bar{wL}} \tag{12}$$

$$\underline{\bar{z}}_R = \underline{Y}(\omega)\underline{\bar{wR}} \tag{13}$$

where [1,4,5]

$$\underline{Y}(\omega) = \begin{pmatrix} 1 & 0 & 0 \\ 0 & 1 & 1 \\ 0 & -j\dfrac{(\lambda_2^2-\sigma)}{l\lambda_2} & -\dfrac{(\lambda_3^2+\sigma)}{l\lambda_3} \\ 0 & -EI\dfrac{(\lambda_2^2-\sigma)}{l^2} & EI\dfrac{(\lambda_3^2+\sigma)}{l^2} \\ 0 & j\dfrac{EI\beta^4}{l^3\lambda_2} & -\dfrac{EI\beta^4}{l^3\lambda_3} \\ -j\dfrac{AE\lambda_1}{l} & 0 & 0 \end{pmatrix}$$

$$\begin{pmatrix} 0 & 0 & 1 \\ 1 & 1 & 0 \\ \dfrac{(\lambda_3^2+\sigma)}{l\lambda_3} & j\dfrac{(\lambda_2^2-\sigma)}{l\lambda_2} & 0 \\ EI\dfrac{(\lambda_3^2+\sigma)}{l^2} & -EI\dfrac{(\lambda_2^2-\sigma)}{l^2} & 0 \\ \dfrac{EI\beta^4}{l^3\lambda_3} & -j\dfrac{EI\beta^4}{l^3\lambda_2} & 0 \\ 0 & 0 & j\dfrac{AE\lambda_1}{l} \end{pmatrix} \tag{14}$$

is the wave-mode matrix of the lattice member, and

$$\underline{\overline{wL}}^T = \{\overline{wL_1^+} \quad \overline{wL_2^+} \quad \overline{wL_3^+} \quad \overline{wL_3^-} \quad \overline{wL_2^-} \quad \overline{wL_1^-}\} \tag{15}$$

$$\underline{\overline{wR}}^T = \{\overline{wR_1^+} \quad \overline{wR_2^+} \quad \overline{wR_3^+} \quad \overline{wR_3^-} \quad \overline{wR_2^-} \quad \overline{wR_1^-}\} \tag{16}$$

are the wave-mode vectors at points L and R, respectively. A summary of the variables which constitute eqn. (14) is given in Appendix A.

Substituting eqns. (12) and (13) into eqn. (1) gives

$$\underline{B}\begin{pmatrix} \underline{Y}(\omega) & 0 \\ 0 & \underline{Y}(\omega) \end{pmatrix}\begin{Bmatrix} \underline{\overline{w}}_L \\ \underline{\overline{w}}_R \end{Bmatrix} = \begin{Bmatrix} 0 \\ 0 \\ 0 \\ \overline{F}_M \\ \overline{F}_V \\ \overline{F}_N \end{Bmatrix} \tag{17}$$

Substituting eqn. (14) into eqn. (17) and multiplying out give

$$\begin{pmatrix} 1 & 0 & 0 & 0 & 0 & 1 & -1 & 0 & 0 & 0 & 0 & -1 \\ 0 & 1 & 1 & 1 & 1 & 0 & 0 & -1 & -1 & -1 & -1 & 0 \\ 0 & Y_{32} & Y_{33} & -Y_{33} & -Y_{32} & 0 & 0 & -Y_{32} & -Y_{33} & Y_{33} & Y_{32} & 0 \\ 0 & Y_{42} & Y_{43} & Y_{43} & Y_{42} & 0 & 0 & -Y_{42} & -Y_{43} & -Y_{43} & -Y_{42} & 0 \\ 0 & -Y_{52} & -Y_{53} & Y_{53} & Y_{52} & 0 & 0 & Y_{52} & Y_{53} & -Y_{53} & -Y_{52} & 0 \\ Y_{61} & 0 & 0 & 0 & 0 & -Y_{61} & -Y_{61} & 0 & 0 & 0 & 0 & Y_{61} \end{pmatrix}\begin{Bmatrix} \underline{\overline{w}}_L \\ \underline{\overline{w}}_R \end{Bmatrix} = \begin{Bmatrix} 0 \\ 0 \\ 0 \\ \overline{F}_M \\ \overline{F}_V \\ \overline{F}_N \end{Bmatrix} \tag{18}$$

where Y_{ij} represents the element located at row i and column j of the wave-mode matrix $\underline{Y}(\omega)$ given by eqn. (14).

From Fig. 2b, two wave-mode vectors which represent waves leaving and entering the massless joint may be written as

$$\underline{\overline{w}}_{OUT}^T = \{\overline{wL_1^-} \quad \overline{wL_2^-} \quad \overline{wL_3^-} \quad \overline{wR_3^+} \quad \overline{wR_2^+} \quad \overline{wR_1^+}\} \tag{19}$$

$$\underline{\overline{w}}_{IN}^T = \{\overline{wL_1^+} \quad \overline{wL_2^+} \quad \overline{wL_3^+} \quad \overline{wR_3^-} \quad \overline{wR_2^-} \quad \overline{wR_1^-}\} \tag{20}$$

The wave-mode coordinate $\overline{wL_i^{\pm}}$ and $\overline{wR_i^{\pm}}$ represents a type i wave (i=1,2,3) which, given a plus (+) sign, travels along increasing x (toward the rigid joint with mass and rotary inertia) or, given a minus (-) sign, travels along decreasing x (away from the rigid joint with mass and rotary inertia), at points L and R, respectively.

Rearranging the order of the scalar equations of eqn. (18) gives

$$\begin{pmatrix} 1 & 0 & 0 & 0 & 0 & -1 & 1 & 0 & 0 & 0 & 0 & -1 \\ 0 & 1 & 1 & -1 & -1 & 0 & 0 & 1 & 1 & -1 & -1 & 0 \\ 0 & -Y_{32} & -Y_{33} & -Y_{33} & -Y_{32} & 0 & 0 & Y_{32} & Y_{33} & Y_{33} & Y_{32} & 0 \\ 0 & Y_{42} & Y_{43} & -Y_{43} & -Y_{42} & 0 & 0 & Y_{42} & Y_{43} & -Y_{43} & -Y_{42} & 0 \\ 0 & Y_{52} & Y_{53} & Y_{53} & Y_{52} & 0 & 0 & -Y_{52} & -Y_{53} & -Y_{53} & -Y_{52} & 0 \\ -Y_{61} & 0 & 0 & 0 & 0 & -Y_{61} & Y_{61} & 0 & 0 & 0 & 0 & Y_{61} \end{pmatrix} \begin{Bmatrix} \overline{w}_{OUT} \\ \overline{w}_{IN} \end{Bmatrix} = \begin{Bmatrix} 0 \\ 0 \\ 0 \\ \overline{F}_M \\ \overline{F}_V \\ \overline{F}_N \end{Bmatrix} \tag{21}$$

Eqn. (21) is equivalent to

$$\underline{D}_{OUT} \begin{Bmatrix} \overline{wL}_1^- \\ \overline{wL}_2^- \\ \overline{wL}_3^- \\ \overline{wR}_3^+ \\ \overline{wR}_2^+ \\ \overline{wR}_1^+ \end{Bmatrix} + \underline{D}_{IN} \begin{Bmatrix} \overline{wL}_1^+ \\ \overline{wL}_2^+ \\ \overline{wL}_3^+ \\ \overline{wR}_3^- \\ \overline{wR}_2^- \\ \overline{wR}_1^- \end{Bmatrix} = \begin{Bmatrix} 0 \\ 0 \\ 0 \\ \overline{F}_M \\ \overline{F}_V \\ \overline{F}_N \end{Bmatrix} \tag{22}$$

where

$$\underline{D}_{OUT} = \begin{pmatrix} 1 & 0 & 0 & 0 & 0 & -1 \\ 0 & 1 & 1 & -1 & -1 & 0 \\ 0 & -Y_{32} & -Y_{33} & -Y_{33} & -Y_{32} & 0 \\ 0 & Y_{42} & Y_{43} & -Y_{43} & -Y_{42} & 0 \\ 0 & Y_{52} & Y_{53} & Y_{53} & Y_{52} & 0 \\ -Y_{61} & 0 & 0 & 0 & 0 & -Y_{61} \end{pmatrix} \tag{23}$$

and

$$\underline{D}_{IN} = \begin{pmatrix} 1 & 0 & 0 & 0 & 0 & -1 \\ 0 & 1 & 1 & -1 & -1 & 0 \\ 0 & Y_{32} & Y_{33} & Y_{33} & Y_{32} & 0 \\ 0 & Y_{42} & Y_{43} & -Y_{43} & -Y_{42} & 0 \\ 0 & -Y_{52} & -Y_{53} & -Y_{53} & -Y_{52} & 0 \\ Y_{61} & 0 & 0 & 0 & 0 & Y_{61} \end{pmatrix} \tag{24}$$

The inverse of the matrix $\underline{D}_{OUT}$ is determined using the computer program called MACSYMA [6]. MACSYMA is a symbolic math processor that can perform symbolic matrix inversions and various matrix operations. It is available on M.I.T.'s Honeywell DPS 8/70M computer running under the MULTICS operating system.

Rearranging eqn. (22) and premultiplying both sides by $\underline{D}_{OUT}^{-1}$ give

$$\begin{Bmatrix} \overline{wL_1^-} \\ \overline{wL_2^-} \\ \overline{wL_3^-} \\ \overline{wR_3^+} \\ \overline{wR_2^+} \\ \overline{wR_1^+} \end{Bmatrix} = \underline{S}(\omega) \begin{Bmatrix} \overline{wL_1^+} \\ \overline{wL_2^+} \\ \overline{wL_3^+} \\ \overline{wR_3^-} \\ \overline{wR_2^-} \\ \overline{wR_1^-} \end{Bmatrix} + \underline{G}(\omega) \begin{Bmatrix} 0 \\ 0 \\ 0 \\ \overline{F}_M \\ \overline{F}_V \\ \overline{F}_N \end{Bmatrix} \tag{25}$$

where

$$\underline{S}(\omega) = -\underline{D}_{OUT}^{-1}\underline{D}_{IN} = \begin{pmatrix} 0 & 0 & 0 & 0 & 0 & 1 \\ 0 & 0 & 0 & 0 & 1 & 0 \\ 0 & 0 & 0 & 1 & 0 & 0 \\ 0 & 0 & 1 & 0 & 0 & 0 \\ 0 & 1 & 0 & 0 & 0 & 0 \\ 1 & 0 & 0 & 0 & 0 & 0 \end{pmatrix} \tag{26}$$

is the scattering matrix of the massless joint at point 1, and

$$\underline{G}(\omega) = \underline{D}_{OUT}^{-1} = \frac{1}{2}\begin{pmatrix} 1 & 0 & 0 \\ 0 & \dfrac{Y_{43}}{Y_{43}-Y_{42}} & \dfrac{-Y_{53}}{Y_{32}Y_{53}-Y_{33}Y_{52}} \\ 0 & \dfrac{-Y_{42}}{Y_{43}-Y_{42}} & \dfrac{Y_{52}}{Y_{32}Y_{53}-Y_{33}Y_{52}} \\ 0 & \dfrac{Y_{42}}{Y_{43}-Y_{42}} & \dfrac{Y_{52}}{Y_{32}Y_{53}-Y_{33}Y_{52}} \\ 0 & \dfrac{-Y_{43}}{Y_{43}-Y_{42}} & \dfrac{-Y_{53}}{Y_{32}Y_{53}-Y_{33}Y_{52}} \\ -1 & 0 & 0 \end{pmatrix}$$

$$\begin{pmatrix} 0 & 0 & -\dfrac{1}{Y_{61}} \\ -\dfrac{1}{Y_{43}-Y_{42}} & \dfrac{-Y_{33}}{Y_{32}Y_{53}-Y_{33}Y_{52}} & 0 \\ \dfrac{1}{Y_{43}-Y_{42}} & \dfrac{Y_{32}}{Y_{32}Y_{53}-Y_{33}Y_{52}} & 0 \\ -\dfrac{1}{Y_{43}-Y_{42}} & \dfrac{Y_{32}}{Y_{32}Y_{53}-Y_{33}Y_{52}} & 0 \\ \dfrac{1}{Y_{43}-Y_{42}} & \dfrac{-Y_{33}}{Y_{32}Y_{53}-Y_{33}Y_{52}} & 0 \\ 0 & 0 & -\dfrac{1}{Y_{61}} \end{pmatrix} \qquad (27)$$

is the wave-mode generation matrix of the massless joint at point 1.

The upper-left and lower-right 3 x 3 matrices of $\underline{S}(\omega)$ given by eqn. (26) contain the reflection coefficients for the waves which strike the massless joint from the left and from the right, respectively. The upper-right and lower-left 3 x 3 matrices of $\underline{S}(\omega)$ given by eqn. (26) contain the transmission coefficients for the waves which strike the massless joint from the right and from the left, respectively. Since the scattering matrix $\underline{S}(\omega)$ given by eqn. (26) is independent of frequency, the system shown in Fig. 2a exhibits nondispersive wave scattering at point 1.

Consider the case where there are no applied loads at point 1. Substituting eqn. (26) into eqn. (25) and multiplying out give

$$\begin{Bmatrix} \overline{wL_1^-} \\ \overline{wL_2^-} \\ \overline{wL_3^-} \\ \overline{wR_3^+} \\ \overline{wR_2^+} \\ \overline{wR_1^+} \end{Bmatrix} = \begin{Bmatrix} \overline{wR_1^-} \\ \overline{wR_2^-} \\ \overline{wR_3^-} \\ \overline{wL_3^+} \\ \overline{wL_2^+} \\ \overline{wL_1^+} \end{Bmatrix} \tag{28}$$

Eqn. (28) states that longitudinal and flexural waves may pass from point L to point R (or point R to point L), through point 1, unaltered. Since each wave passing through point 1 does so unaltered, without reflecting or transmitting waves of a different type, wave-mode conversion does not occur at point 1.

Wave-Mode Input Vector

Substituting eqn. (27) into eqn. (25) and considering only waves generated at point 1 give

$$\begin{Bmatrix} \overline{w_1^+} \\ \overline{w_2^+} \\ \overline{w_3^+} \\ \overline{w_3^-} \\ \overline{w_2^-} \\ \overline{w_1^-} \end{Bmatrix}_1 = \begin{Bmatrix} G_{16}\overline{F}_N \\ G_{24}\overline{F}_M + G_{25}\overline{F}_V \\ G_{34}\overline{F}_M + G_{35}\overline{F}_V \\ G_{44}\overline{F}_M + G_{45}\overline{F}_V \\ G_{54}\overline{F}_M + G_{55}\overline{F}_V \\ G_{66}\overline{F}_N \end{Bmatrix} \tag{29}$$

where G_{ij} represents the element located at row i and column j of the wave-mode generation matrix $\underline{G}(\omega)$ given by eqn. (27). Eqn. (29) contains the longitudinal and flexural waves generated by the sinusoidal axial force $\overline{F}_N$, shear force $\overline{F}_V$ and bending moment $\overline{F}_M$ at point 1.

Joint Coupling and Scattering Matrix of "L" Lattice Junction

In this section, the joint coupling relationship for the two-dimensional rigid joint with mass and rotary inertia, shown in Fig. 1, is presented. The scattering matrix is developed and presented both analytically and graphically.

Joint Coupling Matrix

The explicit form of the joint coupling matrix for arbitrary two-dimensional rigid joints with mass and rotary inertia is given in [2]. From [2], the joint coupling relationship for the joint shown in Fig. 1 is

$$\underline{B}\begin{Bmatrix}\overline{\underline{z}}_2\\ \overline{\underline{z}}_3\end{Bmatrix}=\begin{Bmatrix}0\\0\\0\\0\\0\\0\end{Bmatrix} \tag{30}$$

where

$$\underline{B}=\begin{pmatrix} 0 & -1 & 0 & 0 & 0 & 0 & -1 & 0 & 0 & 0 & 0 & 0\\ 1 & 0 & 0 & 0 & 0 & 0 & 0 & -1 & 0 & 0 & 0 & 0\\ 0 & 0 & 1 & 0 & 0 & 0 & 0 & 0 & -1 & 0 & 0 & 0\\ 0 & 0 & -I_{zz}\omega^2 & 1 & 0 & 0 & 0 & 0 & 0 & -1 & 0 & 0\\ 0 & -m\omega^2 & 0 & 0 & (-1) & 0 & 0 & 0 & 0 & 0 & 0 & 1\\ -m\omega^2 & 0 & 0 & 0 & 0 & 1 & 0 & 0 & 0 & 0 & (1) & 0 \end{pmatrix} \tag{31}$$

is the joint coupling matrix of the rigid joint with mass, and

$$\overline{\underline{z}}_2^T=\{\overline{u}_2 \quad \overline{y}_2 \quad \overline{\psi}_2 \quad \overline{M}_2 \quad \overline{V}_2 \quad \overline{N}_2\} \tag{32}$$

$$\overline{\underline{z}}_3^T=\{\overline{u}_3 \quad \overline{y}_3 \quad \overline{\psi}_3 \quad \overline{M}_3 \quad \overline{V}_3 \quad \overline{N}_3\} \tag{33}$$

are the Fourier transformed state vectors at points 2 and 3. The two elements of the joint coupling matrix $\underline{B}$ which are enclosed in parentheses are the modified terms which ensure that the sign conventions for the joint coupling matrix and the transfer matrix are consistent.

The joint coupling relationship given by eqn. (30) contains the force dynamic and geometric compatibility requirements at the joint. Substituting eqns. (31) through (33) into eqn. (30) and writing out each scalar equation give

$$\bar{y}_2 + \bar{u}_3 = 0 \tag{34}$$

$$\bar{u}_2 - \bar{y}_3 = 0 \tag{35}$$

$$\bar{\psi}_2 - \bar{\psi}_3 = 0 \tag{36}$$

$$\bar{M}_2 - \bar{M}_3 = I_{zz}\omega^2 \bar{\psi}_2 \tag{37}$$

$$-\bar{V}_2 + \bar{N}_3 = m\omega^2 \bar{y}_2 \tag{38}$$

$$\bar{N}_2 + \bar{V}_3 = m\omega^2 \bar{u}_2 \tag{39}$$

Eqns. (34) through (36) represent the compatibility requirements at the joint and eqns. (37) through (39) represent the force dynamic requirements at the joint. Fig. 3 illustrates the internal forces of the attached members acting on the joint in accordance with eqns. (34) through (39).

Scattering Matrix

The process of transforming eqn. (30) into a scattering relationship of the form of eqn. (11) is presented below.

The state vectors at points 2 and 3 in Fig. 1 are related to the wave-mode coordinates at points 2 and 3, respectively, by

$$\underline{\bar{z}}_2 = \underline{Y}(\omega)\underline{\bar{w}}_2 \tag{40}$$

$$\underline{\bar{z}}_3 = \underline{Y}(\omega)\underline{\bar{w}}_3 \tag{41}$$

where

$$\underline{\bar{w}}_2^T = \{\bar{w}_1^+ \quad \bar{w}_2^+ \quad \bar{w}_3^+ \quad \bar{w}_3^- \quad \bar{w}_2^- \quad \bar{w}_1^-\}_2 \tag{42}$$

$$\underline{\bar{w}}_3^T = \{\bar{w}_1^+ \quad \bar{w}_2^+ \quad \bar{w}_3^+ \quad \bar{w}_3^- \quad \bar{w}_2^- \quad \bar{w}_1^-\}_3 \tag{43}$$

are the wave-mode vectors at points 2 and 3, respectively.

Substituting eqns. (40) and (41) into eqn. (30) gives

$$\underline{B}\begin{pmatrix}\underline{Y}(\omega) & 0\\ 0 & \underline{Y}(\omega)\end{pmatrix}\begin{Bmatrix}\overline{\underline{w}_2}\\ \overline{\underline{w}_3}\end{Bmatrix}=\begin{Bmatrix}0\\0\\0\\0\\0\\0\end{Bmatrix} \tag{44}$$

Substituting eqns. (14) and (31) into eqn. (44) and multiplying out give

$$\begin{pmatrix}
0 & -1 & -1 & -1 & -1 & 0\\
1 & 0 & 0 & 0 & 0 & 1\\
0 & Y_{32} & Y_{33} & -Y_{33} & -Y_{32} & 0\\
0 & Y_{42}-I_{zz}\omega^2 Y_{32} & Y_{43}-I_{zz}\omega^2 Y_{33} & Y_{43}+I_{zz}\omega^2 Y_{33} & Y_{42}+I_{zz}\omega^2 Y_{32} & 0\\
0 & -(Y_{52}+m\omega^2) & -(Y_{53}+m\omega^2) & Y_{53}-m\omega^2 & Y_{52}-m\omega^2 & 0\\
Y_{61}-m\omega^2 & 0 & 0 & 0 & 0 & -(Y_{61}+m\omega^2)
\end{pmatrix}$$

$$\begin{pmatrix}
-1 & 0 & 0 & 0 & 0 & -1\\
0 & -1 & -1 & -1 & -1 & 0\\
0 & -Y_{32} & -Y_{33} & Y_{33} & Y_{32} & 0\\
0 & -Y_{42} & -Y_{43} & -Y_{43} & -Y_{42} & 0\\
Y_{61} & 0 & 0 & 0 & 0 & -Y_{61}\\
0 & Y_{52} & Y_{53} & -Y_{53} & -Y_{52} & 0
\end{pmatrix}\begin{Bmatrix}\overline{\underline{w}_2}\\ \overline{\underline{w}_3}\end{Bmatrix}=\begin{Bmatrix}0\\0\\0\\0\\0\\0\end{Bmatrix} \tag{45}$$

From Fig. 4, two wave-mode vectors which represent waves leaving and entering the joint may be written as

$$\overline{\underline{w}}_{OUT}^{T}=\{\overline{w2}_1^- \quad \overline{w2}_2^- \quad \overline{w2}_3^- \quad \overline{w3}_3^+ \quad \overline{w3}_2^+ \quad \overline{w3}_1^+\} \tag{46}$$

$$\overline{\underline{w}}_{IN}^{T}=\{\overline{w2}_1^+ \quad \overline{w2}_2^+ \quad \overline{w2}_3^+ \quad \overline{w3}_3^- \quad \overline{w3}_2^- \quad \overline{w3}_1^-\} \tag{47}$$

A wave-mode coordinate $\overline{wn}_i^{\pm}$ represents a type i wave (i=1,2,3) which, given a plus (+) sign, travels along increasing x or, given a minus (-) sign, travels along decreasing x, at point n. For the system shown in Fig. 1, n may equal 1 through 4. For example, the wave-mode coordinate $\overline{w3}_2^+$ represents a type two wave (which is a mode 1 flexural wave) at point 3 which is propagating toward point 4.

Rearranging the order of the scalar equations of eqn. (45) gives

$$\begin{pmatrix} 0 & -1 & -1 & 0 & 0 & -1 \\ 1 & 0 & 0 & -1 & -1 & 0 \\ 0 & -Y_{32} & -Y_{33} & -Y_{33} & -Y_{32} & 0 \\ 0 & Y_{42}+I_{zz}\omega^2 Y_{32} & Y_{43}+I_{zz}\omega^2 Y_{33} & -Y_{43} & -Y_{42} & 0 \\ 0 & Y_{52}-m\omega^2 & Y_{53}-m\omega^2 & 0 & 0 & Y_{61} \\ -(Y_{61}+m\omega^2) & 0 & 0 & Y_{53} & Y_{52} & 0 \end{pmatrix}$$

$$\begin{pmatrix} 0 & -1 & -1 & 0 & 0 & -1 \\ 1 & 0 & 0 & -1 & -1 & 0 \\ 0 & Y_{32} & Y_{33} & Y_{33} & Y_{32} & 0 \\ 0 & Y_{42}-I_{zz}\omega^2 Y_{32} & Y_{43}-I_{zz}\omega^2 Y_{33} & -Y_{43} & -Y_{42} & 0 \\ 0 & -(Y_{52}+m\omega^2) & -(Y_{53}+m\omega^2) & 0 & 0 & -Y_{61} \\ Y_{61}-m\omega^2 & 0 & 0 & -Y_{53} & -Y_{52} & 0 \end{pmatrix} \begin{Bmatrix} \overline{\underline{w}}_{OUT} \\ \overline{\underline{w}}_{IN} \end{Bmatrix} = \begin{Bmatrix} 0 \\ 0 \\ 0 \\ 0 \\ 0 \\ 0 \end{Bmatrix} \quad (48)$$

Eqn. (48) is equivalent to

$$\underline{D}_{OUT} \begin{Bmatrix} \overline{w2}_1^- \\ \overline{w2}_2^- \\ \overline{w2}_3^- \\ \overline{w3}_3^+ \\ \overline{w3}_2^+ \\ \overline{w3}_1^+ \end{Bmatrix} + \underline{D}_{IN} \begin{Bmatrix} \overline{w2}_1^+ \\ \overline{w2}_2^+ \\ \overline{w2}_3^+ \\ \overline{w3}_3^- \\ \overline{w3}_2^- \\ \overline{w3}_1^- \end{Bmatrix} = \begin{Bmatrix} 0 \\ 0 \\ 0 \\ 0 \\ 0 \\ 0 \end{Bmatrix} \quad (49)$$

where

$$\underline{D}_{OUT} = \begin{pmatrix} 0 & -1 & -1 & 0 & 0 & -1 \\ 1 & 0 & 0 & -1 & -1 & 0 \\ 0 & -Y_{32} & -Y_{33} & -Y_{33} & -Y_{32} & 0 \\ 0 & Y_{42}+I_{zz}\omega^2 Y_{32} & Y_{43}+I_{zz}\omega^2 Y_{33} & -Y_{43} & -Y_{42} & 0 \\ 0 & Y_{52}-m\omega^2 & Y_{53}-m\omega^2 & 0 & 0 & Y_{61} \\ -(Y_{61}+m\omega^2) & 0 & 0 & Y_{53} & Y_{52} & 0 \end{pmatrix} \quad (50)$$

and

$$\underline{D}_{IN} = \begin{pmatrix} 0 & -1 & -1 & 0 & 0 & -1 \\ 1 & 0 & 0 & -1 & -1 & 0 \\ 0 & Y_{32} & Y_{33} & Y_{33} & Y_{32} & 0 \\ 0 & Y_{42} - I_{zz}\omega^2 Y_{32} & Y_{43} - I_{zz}\omega^2 Y_{33} & -Y_{43} & -Y_{42} & 0 \\ 0 & -(Y_{52} + m\omega^2) & -(Y_{53} + m\omega^2) & 0 & 0 & -Y_{61} \\ Y_{61} - m\omega^2 & 0 & 0 & -Y_{53} & -Y_{52} & 0 \end{pmatrix} \tag{51}$$

Rearranging eqn. (49) into the form of eqn. (11) gives

$$\begin{Bmatrix} \overline{w2_1^-} \\ \overline{w2_2^-} \\ \overline{w2_3^-} \\ \overline{w3_3^+} \\ \overline{w3_2^+} \\ \overline{w3_1^+} \end{Bmatrix} = \underline{S}(\omega) \begin{Bmatrix} \overline{w2_1^+} \\ \overline{w2_2^+} \\ \overline{w2_3^+} \\ \overline{w3_3^-} \\ \overline{w3_2^-} \\ \overline{w3_1^-} \end{Bmatrix} \tag{52}$$

where

$$\underline{S}(\omega) = -\underline{D}_{OUT}^{-1}\,\underline{D}_{IN} \tag{53}$$

is the scattering matrix of the rigid joint with mass shown in Fig. 1. Eqn. (52) is the description of the scattering at the joint shown in Fig. 1 in terms of the wave-mode coordinates. The matrix $\underline{D}_{OUT}^{-1}$ and the scattering matrix $\underline{S}(\omega)$ are determined symbolically using MACSYMA. The scattering matrix has the form

$$\underline{S}(\omega) = \begin{pmatrix} S_{11} & S_{12} & S_{13} & S_{14} & S_{15} & S_{16} \\ S_{21} & S_{22} & S_{23} & S_{24} & S_{25} & S_{26} \\ S_{31} & S_{32} & S_{33} & S_{34} & S_{35} & S_{36} \\ S_{41} & S_{42} & S_{43} & S_{44} & S_{45} & S_{46} \\ S_{51} & S_{52} & S_{53} & S_{54} & S_{55} & S_{56} \\ S_{61} & S_{62} & S_{63} & S_{64} & S_{65} & S_{66} \end{pmatrix} \tag{54}$$

The upper-left and lower-right 3 x 3 matrices of $\underline{S}(\omega)$ given by eqn. (54) contain the reflection coefficients for the waves which strike the rigid joint from point 1 and from point

4, respectively. The upper-right and lower-left 3 x 3 matrices of $\underline{S}(\omega)$ given by eqn. (54) contain the transmission coefficients for the waves which strike the rigid joint from point 4 and from point 1, respectively.

Since member 2 is semi-infinite and free of externally applied loads, there are no waves entering the joint, at point 3, from point 4. Therefore, substituting eqn. (54) into eqn. (52) and rewriting give

$$\begin{Bmatrix} \overline{w2_1^-} \\ \overline{w2_2^-} \\ \overline{w2_3^-} \\ \overline{w3_3^+} \\ \overline{w3_2^+} \\ \overline{w3_1^+} \end{Bmatrix} = \begin{pmatrix} S_{11} & S_{12} & S_{13} \\ S_{21} & S_{22} & S_{23} \\ S_{31} & S_{32} & S_{33} \\ S_{41} & S_{42} & S_{43} \\ S_{51} & S_{52} & S_{53} \\ S_{61} & S_{62} & S_{63} \end{pmatrix} \begin{Bmatrix} \overline{w2_1^+} \\ \overline{w2_2^+} \\ \overline{w2_3^+} \end{Bmatrix} \tag{55}$$

The upper 3 x 3 matrix of $\underline{S}(\omega)$ in eqn. (55) contains the reflection coefficients which the incident waves at point 2 encounter as they strike the joint. The lower 3 x 3 matrix of $\underline{S}(\omega)$ in eqn. (55) contains the transmission coefficients which the incident waves at point 2 encounter as they strike the joint. From eqn. (55), a longitudinal wave may reflect and/or transmit a longitudinal and/or flexural wave, and a flexural wave may reflect and/or transmit a longitudinal and/or flexural wave. Systems, such as the "L" lattice junction, which exhibit wave-mode conversion between longitudinal and flexural waves display a phenomenon we choose to call "wave-mode conversion of the second kind". It is manifested through the terms S_{12}, S_{13}, S_{23}, S_{21}, S_{31}, S_{32}, S_{41}, S_{42}, S_{51}, S_{53}, S_{62}, and S_{63} of the scattering matrix $\underline{S}(\omega)$. Systems which exhibit wave-mode conversion only between mode 1 and mode 2 flexural waves display "wave-mode conversion of the first kind".

From MACSYMA [6], the entries of the scattering matrix given in eqn. (55) are

$$S_{ij} = \frac{S_{ij}^N}{S_D} \qquad (i = 1,2,\ldots,6, j = 1,2,3) \tag{56}$$

where

$$S_{11}^N = -[(Y_{33}-Y_{32})^2 I_{zz} m^2\omega^6 +$$
$$2[Y_{32}Y_{53}(Y_{33}-Y_{32}) - Y_{33}Y_{52}(Y_{33}-Y_{32})]I_{zz} m\omega^4 +$$
$$2[Y_{43}(Y_{33}-Y_{32}) - Y_{42}(Y_{33}-Y_{32})]m^2\omega^4 +$$
$$[Y_{32}^2Y_{53}^2 - 2Y_{32}Y_{33}Y_{52}Y_{53} - Y_{61}^2(Y_{33}-Y_{32})^2 + Y_{33}^2Y_{52}^2]I_{zz}\omega^2 +$$
$$2[Y_{32}Y_{43}Y_{53} + Y_{42}Y_{53}(Y_{33}-2Y_{32}) + Y_{43}Y_{52}(Y_{32}-2Y_{33}) + Y_{33}Y_{42}Y_{52}]m\omega^2 +$$
$$2[Y_{33}Y_{52}(Y_{43}Y_{52} - Y_{42}Y_{53}) + Y_{32}Y_{53}(Y_{42}Y_{53} - Y_{43}Y_{52}) +$$
$$Y_{61}^2(Y_{42}(Y_{33}-Y_{32}) - Y_{43}(Y_{33}-Y_{32})) - Y_{33}Y_{42}Y_{52}Y_{53}]] \quad (57)$$

$$S_{12}^N = [2[Y_{32}Y_{53}(Y_{43}-Y_{42}) - Y_{32}Y_{52}(Y_{43}-Y_{42})]m\omega^2 +$$
$$2[Y_{42}Y_{52}(Y_{33}Y_{52} - Y_{53}(Y_{33}+Y_{32})) + Y_{32}Y_{53}Y_{61}(Y_{43}-Y_{42}) -$$
$$Y_{32}Y_{52}Y_{61}(Y_{43}-Y_{42}) + Y_{33}Y_{42}Y_{52}^2]] \quad (58)$$

$$S_{13}^N = [2(Y_{33}Y_{53}(Y_{43}-Y_{42}) - Y_{33}Y_{52}(Y_{43}-Y_{42}))m\omega^2 +$$
$$2[Y_{43}Y_{52}(Y_{33}Y_{52} - Y_{53}(Y_{33}+Y_{32})) + Y_{33}Y_{53}Y_{61}(Y_{43}-Y_{42}) -$$
$$Y_{33}Y_{52}Y_{61}(Y_{43}-Y_{42}) + Y_{32}Y_{43}Y_{53}^2]] \quad (59)$$

$$S_{21}^N = 2[Y_{61}(Y_{32}Y_{43} - Y_{33}Y_{42})m\omega^2 +$$
$$Y_{61}^2(Y_{32}Y_{43} - Y_{33}Y_{42}) - Y_{53}Y_{61}(Y_{32}Y_{43} - Y_{33}Y_{42})] \quad (60)$$

$$S_{22}^N = -[(Y_{33}^2 - Y_{32}^2)I_{zz} m^2\omega^6 +$$
$$2[Y_{32}(Y_{32}Y_{53} - Y_{33}Y_{52}) + Y_{61}(Y_{33}^2 - Y_{32}^2)]I_{zz} m\omega^4 + 2Y_{33}(Y_{43}-Y_{42})m^2\omega^4 +$$
$$[Y_{61}^2(Y_{33}^2 - Y_{32}^2) + 2Y_{32}Y_{61}(Y_{32}Y_{53} - Y_{33}Y_{52}) - Y_{32}^2Y_{53}^2]I_{zz}\omega^2 +$$
$$2[2Y_{33}Y_{61}(Y_{43}-Y_{42}) + Y_{33}Y_{42}Y_{53} - Y_{32}Y_{43}Y_{52}]m\omega^2 +$$
$$2[Y_{33}Y_{61}^2(Y_{43}-Y_{42}) + Y_{61}(Y_{33}Y_{42}Y_{53} - Y_{32}Y_{43}Y_{52}) + Y_{43}Y_{52}(Y_{32}Y_{53} - Y_{33}Y_{52})]] \quad (61)$$

$$S_{23}^N = -[2Y_{33}(Y_{33}-Y_{32})I_{zz} m^2\omega^6 +$$
$$[4Y_{33}Y_{61}(Y_{33}-Y_{32}) + 2Y_{33}(Y_{32}Y_{53} - Y_{33}Y_{52})]I_{zz} m\omega^4 + 2Y_{33}(Y_{43}-Y_{42})m^2\omega^4 +$$
$$2[Y_{33}Y_{61}^2(Y_{33}-Y_{32}) + Y_{33}Y_{61}(Y_{32}Y_{53} - Y_{33}Y_{52})]I_{zz}\omega^2 +$$
$$2[2Y_{33}Y_{61}(Y_{43}-Y_{42}) + Y_{43}Y_{53}(Y_{33}-Y_{32}) + Y_{33}Y_{42}Y_{53} - Y_{33}Y_{43}Y_{52}]m\omega^2 +$$
$$2[Y_{43}Y_{53}(Y_{32}Y_{53} - Y_{33}Y_{52}) + Y_{61}(Y_{43}Y_{53}(Y_{33}-Y_{32}) + Y_{33}Y_{42}Y_{53} - Y_{33}Y_{43}Y_{52}) +$$
$$Y_{33}Y_{61}^2(Y_{43}-Y_{42})]] \quad (62)$$

$$S_{31}^{N} = -2[Y_{61}(Y_{32}Y_{43} - Y_{33}Y_{42})m\omega^2 +$$
$$Y_{52}Y_{61}(Y_{33}Y_{42} - Y_{32}Y_{43}) + Y_{61}^2(Y_{32}Y_{43} - Y_{33}Y_{42})] \quad (63)$$

$$S_{32}^{N} = [2Y_{32}(Y_{33} - Y_{32})I_{zz}m^2\omega^6 +$$
$$2[2Y_{32}Y_{61}(Y_{33} - Y_{32}) + Y_{32}^2Y_{53} - Y_{32}Y_{33}Y_{52}]I_{zz}m\omega^4 + 2Y_{32}(Y_{43} - Y_{42})m^2\omega^4 +$$
$$2[Y_{32}Y_{61}^2(Y_{33} - Y_{32}) + Y_{32}Y_{61}(Y_{32}Y_{53} - Y_{33}Y_{52})]I_{zz}\omega^2 +$$
$$2[2Y_{32}Y_{61}(Y_{43} - Y_{42}) + Y_{32}Y_{42}Y_{53} + Y_{42}Y_{52}(Y_{33} - Y_{32}) - Y_{32}Y_{43}Y_{52}]m\omega^2 +$$
$$2[Y_{42}Y_{52}(Y_{32}Y_{53} - Y_{33}Y_{52}) + Y_{42}Y_{52}Y_{61}(Y_{33} - Y_{32}) + Y_{32}Y_{61}(Y_{42}Y_{53} - Y_{43}Y_{52}) +$$
$$Y_{32}Y_{61}^2(Y_{43} - Y_{42})]] \quad (64)$$

$$S_{33}^{N} = [(Y_{33}^2 - Y_{32}^2)I_{zz}m^2\omega^6 +$$
$$2[Y_{61}(Y_{33}^2 - Y_{32}^2) + Y_{33}(Y_{32}Y_{53} - Y_{33}Y_{52})]I_{zz}m\omega^4 + 2Y_{32}(Y_{43} - Y_{42})m^2\omega^4 +$$
$$[Y_{33}Y_{52}(Y_{33}Y_{52} - 2Y_{32}Y_{53} - 2Y_{33}Y_{61}) + Y_{32}Y_{53}(Y_{32}Y_{53} + 2Y_{33}Y_{52}) + Y_{61}^2(Y_{33}^2 - Y_{32}^2)]I_{zz}\omega^2 +$$
$$2[Y_{32}Y_{43}(2Y_{61} - Y_{52}) + Y_{42}(Y_{33}Y_{53} - 2Y_{32}Y_{61})]m\omega^2 +$$
$$2[Y_{42}Y_{53}(Y_{32}Y_{53} - Y_{33}Y_{52}) + Y_{61}(Y_{33}Y_{42}Y_{53} - Y_{32}Y_{43}Y_{52}) +$$
$$Y_{32}Y_{61}^2(Y_{43} - Y_{42})]] \quad (65)$$

$$S_{41}^{N} = -[2Y_{32}Y_{61}(Y_{33} - Y_{32})I_{zz}m\omega^4 +$$
$$2[Y_{32}Y_{61}(Y_{32}Y_{53} - Y_{33}Y_{52}) + Y_{32}Y_{61}^2(Y_{33} - Y_{32})]I_{zz}\omega^2 +$$
$$2[Y_{42}Y_{61}(Y_{33} - 2Y_{32}) + Y_{32}Y_{43}Y_{61}]m\omega^2 +$$
$$2[2Y_{32}Y_{42}Y_{61}(Y_{53} - Y_{61}) + Y_{32}Y_{43}Y_{61}(Y_{61} - Y_{52}) + Y_{33}Y_{42}Y_{61}(Y_{61} - Y_{52})]] \quad (66)$$

$$S_{42}^{N} = [2Y_{32}(Y_{43} - Y_{42})m^2\omega^4 +$$
$$2[Y_{32}Y_{42}(Y_{53} + Y_{52}) + 2Y_{32}Y_{61}(Y_{43} - Y_{42}) - Y_{52}(Y_{33}Y_{42} + Y_{32}Y_{43})]m\omega^2 +$$
$$2[Y_{32}Y_{42}Y_{53}(Y_{61} - Y_{51}) + Y_{33}Y_{42}Y_{52}(Y_{52} - Y_{61}) + Y_{32}Y_{61}^2(Y_{43} - Y_{42})]] \quad (67)$$

$$S_{43}^{N} = [2Y_{33}(Y_{43} - Y_{42})m^2\omega^4 +$$
$$2[2Y_{33}Y_{61}(Y_{43} - Y_{42}) + Y_{33}Y_{52}(Y_{42} - 2Y_{43}) + Y_{32}Y_{43}Y_{53}]m\omega^2 +$$
$$[2Y_{32}Y_{43}Y_{53}(Y_{61} - Y_{52}) + 2Y_{33}Y_{43}Y_{52}(Y_{52} - 2Y_{61}) + 2Y_{33}Y_{61}(Y_{42}Y_{52} +$$
$$Y_{43}Y_{61} - Y_{42}Y_{61})]] \quad (68)$$

$$S_{51}^{N} = [2Y_{33}Y_{61}(Y_{33} - Y_{32})I_{zz}m\omega^4 +$$

$$2[Y_{33}Y_{61}(Y_{32}Y_{53}-Y_{33}Y_{61})-Y_{33}Y_{61}(Y_{33}Y_{52}+Y_{32}Y_{61})]I_{zz}\omega^2+$$
$$2[Y_{43}Y_{61}(2Y_{33}-Y_{32})-Y_{33}Y_{42}Y_{61}]m\omega^2+$$
$$2[2Y_{33}Y_{43}Y_{61}(Y_{61}-Y_{52})+Y_{32}Y_{43}Y_{61}(Y_{53}-Y_{61})+Y_{33}Y_{42}Y_{61}(Y_{53}-Y_{61})]] \quad (69)$$

$$S_{52}^N=-[2Y_{32}(Y_{43}-Y_{42})m^2\omega^4+$$
$$2[2Y_{32}Y_{61}(Y_{43}-Y_{42})+Y_{32}Y_{53}(2Y_{42}-Y_{43})-Y_{33}Y_{42}Y_{52}]m\omega^2+$$
$$2[Y_{33}Y_{42}Y_{52}(Y_{53}-Y_{61})+Y_{32}Y_{42}Y_{53}(2Y_{61}-Y_{53})+Y_{32}Y_{61}(Y_{61}Y_{43}-$$
$$Y_{43}Y_{53}-Y_{42}Y_{61})]] \quad (70)$$

$$S_{53}^N=-[2Y_{33}(Y_{43}-Y_{42})m^2\omega^4+$$
$$2[2Y_{33}Y_{61}(Y_{43}-Y_{42})+Y_{43}Y_{53}(Y_{32}-Y_{33})+Y_{33}(Y_{42}Y_{53}-Y_{43}Y_{52})]m\omega^2+$$
$$2[Y_{33}Y_{43}Y_{52}(Y_{53}-Y_{61})+Y_{32}Y_{43}Y_{53}(Y_{61}-Y_{53})+Y_{33}Y_{61}(Y_{42}Y_{53}-$$
$$Y_{43}Y_{53}+Y_{43}Y_{61}-Y_{42}Y_{61})]] \quad (71)$$

$$S_{61}^N=2[Y_{33}Y_{42}Y_{61}(Y_{52}-Y_{53})+Y_{32}Y_{43}Y_{61}(Y_{53}-Y_{52})] \quad (72)$$

$$S_{62}^N=-[2[Y_{33}Y_{52}(Y_{32}-Y_{33})-Y_{32}Y_{53}(Y_{32}-Y_{33})]I_{zz}m\omega^4+$$
$$2[Y_{32}Y_{53}Y_{61}(Y_{33}-Y_{32})-Y_{33}Y_{52}Y_{61}(Y_{33}-Y_{32})+Y_{33}Y_{52}(Y_{33}Y_{52}-2Y_{32}Y_{53})+Y_{32}^2Y_{53}^2]I_{zz}\omega^2+$$
$$2[Y_{43}Y_{52}(Y_{32}-2Y_{33})+Y_{42}Y_{52}(2Y_{33}-Y_{32})+Y_{32}Y_{53}(Y_{43}-Y_{42})]m\omega^2+$$
$$2[Y_{33}Y_{52}^2(2Y_{43}-Y_{42})-Y_{32}Y_{52}Y_{53}(2Y_{43}-Y_{42})-Y_{33}Y_{42}Y_{52}Y_{53}+Y_{32}Y_{53}Y_{61}(Y_{43}-Y_{42})-$$
$$Y_{43}Y_{52}Y_{61}(2Y_{33}-Y_{32})+Y_{42}Y_{52}Y_{61}(2Y_{33}-Y_{32})+Y_{32}Y_{42}Y_{53}^2]] \quad (73)$$

$$S_{63}^N=-[2[Y_{32}Y_{53}(Y_{33}-Y_{32})-Y_{33}Y_{52}(Y_{33}-Y_{32})]I_{zz}m\omega^4+$$
$$2[Y_{32}Y_{53}Y_{61}(Y_{33}-Y_{32})-Y_{33}Y_{52}Y_{61}(Y_{33}-Y_{32})+Y_{33}Y_{52}(Y_{33}Y_{52}-2Y_{32}Y_{43})+Y_{32}^2Y_{53}^2]I_{zz}\omega^2+$$
$$2[Y_{33}Y_{52}(Y_{42}-Y_{43})+Y_{42}Y_{53}(Y_{33}-2Y_{32})-Y_{43}Y_{53}(Y_{33}-2Y_{32})]m\omega^2+$$
$$2[Y_{43}Y_{52}Y_{53}(Y_{33}-Y_{32})+Y_{33}Y_{52}(Y_{43}Y_{52}-2Y_{42}Y_{53})-Y_{33}Y_{52}Y_{61}(Y_{43}-Y_{42})-$$
$$Y_{43}Y_{53}Y_{61}(Y_{33}-2Y_{32})+Y_{42}Y_{53}Y_{61}(Y_{33}-2Y_{32})-Y_{32}Y_{53}^2(Y_{43}-2Y_{42})]] \quad (74)$$

and

$$S_D=[(Y_{33}-Y_{32})^2I_{zz}m^2\omega^6+$$
$$2[Y_{33}Y_{52}(Y_{32}-Y_{33})+Y_{32}Y_{53}(Y_{33}-Y_{32})+Y_{61}(Y_{33}-Y_{32})^2]I_{zz}m\omega^4+$$
$$2[Y_{42}(Y_{32}-Y_{33})+Y_{43}(Y_{33}-Y_{32})]m^2\omega^4+$$

$$[2Y_{32}Y_{53}Y_{61}(Y_{33}-Y_{32})-2Y_{33}Y_{52}Y_{61}(Y_{33}-Y_{32})-2Y_{32}Y_{33}Y_{52}Y_{53}+$$
$$Y_{33}^2Y_{52}^2+Y_{61}^2(Y_{33}-Y_{32})^2]J_{zz}\omega^2+$$
$$2[Y_{43}Y_{52}(Y_{32}-2Y_{33})+Y_{42}Y_{53}(Y_{33}-2Y_{32})+2Y_{43}Y_{61}(Y_{33}-Y_{32})-$$
$$2Y_{42}Y_{61}(Y_{33}-Y_{32})+Y_{32}Y_{43}Y_{53}+Y_{33}Y_{42}Y_{52}]m\omega^2+$$
$$2[Y_{33}Y_{43}Y_{52}^2-Y_{52}Y_{53}(Y_{32}Y_{43}+Y_{33}Y_{42})+Y_{32}Y_{42}Y_{53}^2+$$
$$Y_{42}Y_{53}Y_{61}(Y_{33}-2Y_{32})+Y_{43}Y_{52}Y_{61}(Y_{32}-2Y_{33})+Y_{32}Y_{43}Y_{53}Y_{61}+Y_{33}Y_{42}Y_{52}Y_{61}+$$
$$Y_{43}Y_{61}^2(Y_{33}-Y_{32})-Y_{42}Y_{61}^2(Y_{33}-Y_{32})]] \qquad (75)$$

The entries of the scattering matrix given by eqns. (56) through (75) are frequency dependent. Therefore, the system shown in Fig. 1 exhibits dispersive scattering as waves are reflected at and transmitted through the rigid joint with mass and rotary inertia.

The reflection and transmission coefficients given by eqns. (56) through (75) are, in general, complex quantities. Using the properties of a tubular lattice member and a rigid joint with mass given in Table 1, the magnitude and phase of each reflection and transmission coefficient are presented below as a series of plots. These properties approximate the hardware currently under development by McDonnell Douglas and NASA which will be used in the space station scheduled for orbital construction in the mid 1990's.

The magnitude is calculated as the square root of the sum of the squares of the real and imaginary parts. The phase is calculated as the arctangent of the imaginary part divided by the real part. The arctangent function used in this calculation gives a value between ±180 degrees. As a consequence, the phase plot may be read like the surface of a cylinder with its axis parallel to the abscissa, and the 180 degree and the -180 degree points on the ordinate coincident. The phase of a reflection coefficient represents a phase shift between the reflected wave and the incident wave. If positive, it represents a phase lead of the reflected wave over the incident wave; if negative, a phase lag. Likewise, the phase of a transmission coefficient

represents a phase shift between the transmitted wave and the incident wave. If positive, it represents a phase lead of the transmitted wave over the incident wave; if negative, a phase lag.

The physical joint is a spherical orb which is machined to accommodate the attachment of the lattice members. A loss of approximately one-third of its solid mass occurs due to machining. The joint mass and mass moment of inertia given in Table 1 serve as nominal values. The following plots present three curves which correspond to three values of joint mass and mass moment of inertia. In each case, the joint diameter is assumed to be the same, 0.10 meter. Therefore, the mass and mass rotary inertia are linearly related [7].

From eqn. (55), it should be noted that the longitudinal and flexural waves are naturally coupled as a consequence of the perpendicular geometry of the system. For the properties of a tubular lattice member given in Table 1, the cutoff frequency ω_c [1,8] of the mode 2 flexural wave is approximately 105,000 radians per second. The cutoff frequency ω_c is a frequency below which the mode 2 flexural wave is an evanescent wave and above which the mode 2 flexural wave is a propagating wave. The specific value of the cutoff frequency is strongly dependent on the shear related properties of the lattice member, as illustrated by eqn. (57) in [1]. Although it may not be predominate, the effect of the cutoff frequency is apparent in all of the reflection and transmission coefficient plots. In addition, for frequencies $0 < \omega < \omega_c$, each magnitude curve exhibits a peak or a valley. It can be shown, by calculations not shown here, that the magnitude and frequency at which the phenomenon occurs is sensitive to the joint mass moment of inertia and the shear related properties of the lattice members. A physical interpretation of this phenomenon and the possible existence of a characteristic equation which identifies the frequency at which it occurs is unclear at this time and suggests further study.

Figs. 5a and 5b give the magnitude and phase of the scattering matrix reflection coefficient S_{11}. The reflection coefficient S_{11} represents the amplitude ratio of reflected longitudinal waves due to incident longitudinal waves at point 2 for various frequencies, reference Fig. 1. As the frequency ω approaches zero, the magnitude of S_{11} approaches unity and the phase approaches zero degrees. This suggests that a longitudinal wave propagating along member 1, toward the joint, will perceive the junction as a free-end boundary condition and the wave will be reflected accordingly. As the frequency ω approaches infinity, the magnitude of S_{11} approaches unity and the phase approaches -180 degrees. Figs. 5a and 5b illustrate the dynamics between incident longitudinal waves and reflected longitudinal waves at point 2.

Figs. 6a and 6b give the magnitude and phase of the scattering matrix reflection coefficient S_{12}. The reflection coefficient S_{12} represents the amplitude ratio of reflected longitudinal waves due to incident mode 1 flexural waves at point 2 for various frequencies, reference Fig. 1. As the frequency ω approaches zero, the magnitude of S_{12} approaches zero and the phase approaches 90 degrees. As the frequency ω approaches infinity, the magnitude of S_{12} approaches zero and the phase approaches -180 degrees. Figs. 6a and 6b illustrate the dynamics of wave-mode conversion between incident mode 1 flexural waves and reflected longitudinal waves at point 2.

Figs. 7a and 7b give the magnitude and phase of the scattering matrix reflection coefficient S_{13}. The reflection coefficient S_{13} represents the amplitude ratio of reflected longitudinal waves due to incident mode 2 flexural waves at point 2 for various frequencies, reference Fig. 1. As the frequency ω approaches zero, the magnitude and phase of S_{13} both approach zero. As the frequency ω approaches infinity, the magnitude and phase of S_{13} approach zero. Figs. 7a and 7b illustrate the dynamics of wave-mode conversion between incident mode 2 flexural waves and reflected longitudinal waves at point 2.

Figs. 8a and 8b give the magnitude and phase of the scattering matrix reflection coefficient S_{21}. The reflection coefficient S_{21} represents the amplitude ratio of reflected mode 1 flexural waves due to incident longitudinal waves at point 2 for various frequencies, reference Fig. 1. As the frequency ω approaches zero, the magnitude of S_{21} approaches 0.5 and the phase approaches 90 degrees. As the frequency ω approaches infinity, the magnitude of S_{21} approaches zero and the phase approaches -180 degrees. Figs. 8a and 8b illustrate the dynamics of wave-mode conversion between incident longitudinal waves and reflected mode 1 flexural waves at point 2.

Figs. 9a and 9b give the magnitude and phase of the scattering matrix reflection coefficient S_{22}. The reflection coefficient S_{22} represents the amplitude ratio of reflected mode 1 flexural waves due to incident mode 1 flexural waves at point 2 for various frequencies, reference Fig. 1. As the frequency ω approaches zero, the magnitude of S_{22} approaches approximately 0.7071 and the phase approaches -135 degrees. As the frequency ω approaches infinity, the magnitude of S_{22} approaches unity and the phase approaches -180 degrees. Figs. 9a and 9b illustrate the dynamics between incident mode 1 flexural waves and reflected mode 1 flexural waves at point 2.

Figs. 10a and 10b give the magnitude and phase of the scattering matrix reflection coefficient S_{23}. The reflection coefficient S_{23} represents the amplitude ratio of reflected mode 1 flexural waves due to incident mode 2 flexural waves at point 2 for various frequencies, reference Fig. 1. As the frequency ω approaches zero, the magnitude of S_{23} approaches approximately 0.7071 and the phase approaches -135 degrees. As the frequency ω approaches infinity, the magnitude of S_{23} approaches 2.0 and the phase approaches -180 degrees. Figs. 10a and 10b illustrate the dynamics of wave-mode conversion between incident mode 2 flexural waves and reflected mode 1 flexural waves at point 2.

Figs. 11a and 11b give the magnitude and phase of the scattering matrix reflection coefficient S_{31}. The reflection coefficient S_{31} represents the amplitude ratio of reflected mode 2 flexural waves due to incident longitudinal waves at point 2 for various frequencies,

reference Fig. 1. As the frequency ω approaches zero, the magnitude of S_{31} approaches 0.5 and the phase approaches -90 degrees. As the frequency ω approaches infinity, the magnitude and phase of S_{31} approach zero. Figs. 11a and 11b illustrate the dynamics of wave-mode conversion between incident longitudinal waves and reflected mode 2 flexural waves at point 2.

Figs. 12a and 12b give the magnitude and phase of the scattering matrix reflection coefficient S_{32}. The reflection coefficient S_{32} represents the amplitude ratio of reflected mode 2 flexural waves due to incident mode 1 flexural waves at point 2 for various frequencies, reference Fig. 1. As the frequency ω approaches zero, the magnitude of S_{32} approaches approximately 0.7071 and the phase approaches 135 degrees. As the frequency ω approaches infinity, the magnitude S_{32} approaches zero and the phase approaches -180 degrees. Figs. 12a and 12b illustrate the dynamics of wave-mode conversion between incident mode 1 flexural waves and reflected mode 2 flexural waves at point 2.

Figs. 13a and 13b give the magnitude and phase of the scattering matrix reflection coefficient S_{33}. The reflection coefficient S_{33} represents the amplitude ratio of reflected mode 2 flexural waves due to incident mode 2 flexural a. . ' point 2 for various frequencies, reference Fig. 1. As the frequency ω approaches zero, the magnitude of S_{33} approaches approximately 0.7071 and the phase approaches 135 degrees. As the frequency ω approaches infinity, the magnitude S_{33} approaches unity and the phase approaches zero. Figs. 13a and 13b illustrate the dynamics between incident mode 2 flexural waves and reflected mode 2 flexural waves at point 2.

Figs. 14a and 14b give the magnitude and phase of the scattering matrix transmission coefficient S_{41}. The transmission coefficient S_{41} represents the amplitude ratio of transmitted mode 2 flexural waves at point 3 due to incident longitudinal waves at point 2 for various frequencies, reference Fig. 1. As the frequency ω approaches zero, the magnitude of S_{41} approaches approximately 1.120 and the phase approaches approximately -27 degrees. As the frequency ω approaches infinity, the magnitude of S_{41} approaches zero and the phase

approaches -90 degrees. Figs. 14a and 14b illustrate the dynamics of wave-mode conversion between incident longitudinal waves at point 2 and transmitted mode 2 flexural waves at point 3.

Figs. 15a and 15b give the magnitude and phase of the scattering matrix transmission coefficient S_{42}. The transmission coefficient S_{42} represents the amplitude ratio of transmitted mode 2 flexural waves at point 3 due to incident mode 1 flexural waves at point 2 for various frequencies, reference Fig. 1. As the frequency ω approaches zero, the magnitude of S_{42} approaches approximately 0.7071 and the phase approaches 135 degrees. As the frequency ω approaches infinity, the magnitude of S_{42} approaches zero and the phase approaches 90 degrees. Figs. 15a and 15b illustrate the dynamics of wave-mode conversion between incident mode 1 flexural waves at point 2 and transmitted mode 2 flexural waves at point 3.

Figs. 16a and 16b give the magnitude and phase of the scattering matrix transmission coefficient S_{43}. The transmission coefficient S_{43} represents the amplitude ratio of transmitted mode 2 flexural waves at point 3 due to incident mode 2 flexural waves at point 2 for various frequencies, reference Fig. 1. As the frequency ω approaches zero, the magnitude of S_{43} approaches approximately 0.7071 and the phase approaches 45 degrees. As the frequency ω approaches infinity, the magnitude of S_{43} approaches zero and the phase approaches -90 degrees. Figs. 16a and 16b illustrate the dynamics between incident mode 2 flexural waves at point 2 and transmitted mode 2 flexural waves at point 3.

Figs. 17a and 17b give the magnitude and phase of the scattering matrix transmission coefficient S_{51}. The transmission coefficient S_{51} represents the amplitude ratio of transmitted mode 1 flexural waves at point 3 due to incident longitudinal waves at point 2 for various frequencies, reference Fig. 1. As the frequency ω approaches zero, the magnitude of S_{51} approaches approximately 1.120 and the phase approaches approximately 27 degrees. As the frequency ω approaches infinity, the magnitude of S_{51} approaches zero and the phase

approaches -90 degrees. Figs. 17a and 17b illustrate the dynamics of wave-mode conversion between incident longitudinal waves at point 2 and transmitted mode 1 flexural waves at point 3.

Figs. 18a and 18b give the magnitude and phase of the scattering matrix transmission coefficient S_{52}. The transmission coefficient S_{52} represents the amplitude ratio of transmitted mode 1 flexural waves at point 3 due to incident mode 1 flexural waves at point 2 for various frequencies, reference Fig. 1. As the frequency ω approaches zero, the magnitude of S_{52} approaches approximately 0.7071 and the phase approaches -45 degrees. As the frequency ω approaches infinity, the magnitude of S_{52} approaches zero and the phase approaches -90 degrees. Figs. 18a and 18b illustrate the dynamics between incident mode 1 flexural waves at point 2 and transmitted mode 1 flexural waves at point 3.

Figs. 19a and 19b give the magnitude and phase of the scattering matrix transmission coefficient S_{53}. The transmission coefficient S_{53} represents the amplitude ratio of transmitted mode 1 flexural waves at point 3 due to incident mode 2 flexural waves at point 2 for various frequencies, reference Fig. 1. As the frequency ω approaches zero, the magnitude of S_{53} approaches approximately 0.7071 and the phase approaches -135 degrees. As the frequency ω approaches infinity, the magnitude of S_{53} approaches zero and the phase approaches 90 degrees. Figs. 19a and 19b illustrate the dynamics of wave-mode conversion between incident mode 2 flexural waves at point 2 and transmitted mode 1 flexural waves at point 3.

Figs. 20a and 20b give the magnitude and phase of the scattering matrix transmission coefficient S_{61}. The transmission coefficient S_{61} represents the amplitude ratio of transmitted longitudinal waves at point 3 due to incident longitudinal waves at point 2 for various frequencies, reference Fig. 1. As the frequency ω approaches zero, the magnitude of S_{61} approaches zero and the phase approaches 45 degrees. As the frequency ω approaches infinity, the magnitude of S_{61} approaches zero and the phase approaches -90 degrees. Figs. 20a and 20b illustrate the dynamics between incident longitudinal waves at point 2 and transmitted longitudinal waves at point 3.

Figs. 21a and 21b give the magnitude and phase of the scattering matrix transmission coefficient S_{62}. The transmission coefficient S_{62} represents the amplitude ratio of transmitted longitudinal waves at point 3 due to incident mode 1 flexural waves at point 2 for various frequencies, reference Fig. 1. As the frequency ω approaches zero, the magnitude of S_{62} approaches zero and the phase approaches approximately -153 degrees. As the frequency ω approaches infinity, the magnitude S_{62} approaches zero and the phase approaches 90 degrees. Figs. 21a and 21b illustrate the dynamics of wave-mode conversion between incident mode 1 flexural waves at point 2 and transmitted longitudinal waves at point 3.

Figs. 22a and 22b give the magnitude and phase of the scattering matrix transmission coefficient S_{63}. The transmission coefficient S_{63} represents the amplitude ratio of transmitted longitudinal waves at point 3 due to incident mode 2 flexural waves at point 2 for various frequencies, reference Fig. 1. As the frequency ω approaches zero, the magnitude of S_{63} approaches zero and the phase approaches approximately -117 degrees. As the frequency ω approaches infinity, the magnitude S_{63} approaches zero and the phase approaches 90 degrees. Figs. 22a and 22b illustrate the dynamics of wave-mode conversion between incident mode 2 flexural waves at point 2 and transmitted longitudinal waves at point 3.

At arbitrary frequencies, the dynamic behavior between the incident and the reflected and transmitted waves can be difficult to interpret in physical terms. Therefore, studying the limiting values of the reflection and transmission coefficients may enhance understanding and confidence in the analysis. In this light, from the series of plots presented above, the following observations are noted.

• As the frequency ω approaches zero, the reflection and transmission coefficients given by $S(\omega)$ approach either zero or a constant nonzero value. A zero value indicates that reflection or transmission does not occur between the corresponding wave types. A nonzero value indicates that static coupling exists between the corresponding wave types and point locations.

• As the frequency ω approaches zero, a longitudinal wave which strikes the joint along member 1 is reflected as if the joint end of member 1 were a free-end boundary condition. As the frequency ω approaches infinity, a longitudinal wave which strikes the joint along member 1 is reflected as if the joint end of member 1 were a fixed-end boundary condition.

• As the frequency ω approaches zero, an incident mode 1 or mode 2 flexural wave, at point 2, will not result in a reflected or transmitted longitudinal wave into member 1 or member 2, respectively. However, an incident longitudinal wave, at point 2, will result in a reflected and transmitted mode 1 and mode 2 flexural wave in member 1 and member 2, respectively.

• As the frequency ω approaches infinity, each incident wave will encounter complete reflection at the joint with no transmission. This behavior is expected since a joint with mass and rotary inertia should appear as a fixed-end boundary condition at ultra-high frequencies regardless of the number or orientation of any adjacent members attached to the joint.

• In general, each wave which strikes the joint, at point 2, will result in the reflection of three different waves. For example, an incident longitudinal (type one) wave at point 2 will, in general, result in the reflection of a longitudinal wave, a mode 1 flexural (type two) wave and a mode 2 flexural (type three) wave. These waves will then propagate along member 1 in the direction of decreasing x, refer to Fig. 1.

• In general, each wave which strikes the joint, at point 2, will result in the transmission of three different waves, at point 3. For example, an incident longitudinal wave at point 2 will, in general, result in the transmission of a longitudinal wave, a mode 1 flexural wave and a mode 2 flexural wave. These waves will then propagate along member 2 in the direction of increasing x, refer to Fig. 1.

In summary, over various frequencies, the dynamic behavior between each incident wave and each reflected and transmitted wave is diverse and unique. In this analysis, a longitudinal (type one) wave, a mode 1 flexural (type two) wave and/or a mode 2 flexural (type three) wave may strike the joint at point 2. In general, at any given frequency ω, each

type of wave which strikes the joint may result in three reflected waves and three transmitted waves. This accounts for the eighteen scattering matrix terms given by eqn. (55) which are presented and illustrated above in Figs. 5 through 22.

Frequency Response Functions of "L" Lattice Junction Assembly

In this section, the frequency response of each state variable at point 4 due to applied sinusoidal loading at point 1 will be determined and presented analytically for the "L" lattice assembly shown in Fig. 1.

The wave-mode coordinates for longitudinal and flexural waves generated at point 1 are given by eqn. (29). The wave-mode vector at point 1 is related to the wave-mode vector at point 2 according to

$$\overline{\underline{w}}_2 = \underline{W}(\omega)\overline{\underline{w}}_1 \tag{76}$$

where [1,4,5]

$$\underline{W}(\omega) = \begin{pmatrix} e^{-j\lambda_1} & 0 & \cdot & \cdot & \cdot & 0 \\ 0 & e^{-j\lambda_2} & & & & \cdot \\ \cdot & & e^{-\lambda_3} & & & \cdot \\ \cdot & & & e^{\lambda_3} & & \cdot \\ \cdot & & & & e^{j\lambda_2} & 0 \\ 0 & \cdot & \cdot & \cdot & 0 & e^{j\lambda_1} \end{pmatrix} \tag{77}$$

is the wave-mode propagation matrix for member 1.

Substituting eqns. (29) and (77) into eqn. (76) and considering only waves which propagate toward the rigid joint with mass and rotary inertia give

$$\begin{Bmatrix} \overline{w}_1^+ \\ \overline{w}_2^+ \\ \overline{w}_3^+ \end{Bmatrix}_2 = \begin{Bmatrix} e^{-j\lambda_1} G_{16} \overline{F}_N \\ e^{-j\lambda_2}(G_{24}\overline{F}_M + G_{25}\overline{F}_V) \\ e^{-\lambda_3}(G_{34}\overline{F}_M + G_{35}\overline{F}_V) \end{Bmatrix} \tag{78}$$

Eqn. (78) contains the longitudinal and flexural waves at point 2 which strike the joint from point 1.

Considering only waves transmitted through the joint, substituting eqn. (78) into eqn. (55) and writing out each scalar equation give, after some manipulation,

$$\overline{w3}_1^+ = e^{-j\lambda_1} S_{61} G_{16} \overline{F}_N + e^{-j\lambda_2} S_{62}(G_{24}\overline{F}_M + G_{25}\overline{F}_V) + e^{-\lambda_3} S_{63}(G_{34}\overline{F}_M + G_{35}\overline{F}_V) \tag{79}$$

$$\overline{w3}_2^+ = e^{-j\lambda_1} S_{51} G_{16} \overline{F}_N + e^{-j\lambda_2} S_{52} (G_{24} \overline{F}_M + G_{25} \overline{F}_V) + e^{-\lambda_3} S_{53} (G_{34} \overline{F}_M + G_{35} \overline{F}_V) \quad (80)$$

$$\overline{w3}_3^+ = e^{-j\lambda_1} S_{41} G_{16} \overline{F}_N + e^{-j\lambda_2} S_{42} (G_{24} \overline{F}_M + G_{25} \overline{F}_V) + e^{-\lambda_3} S_{43} (G_{34} \overline{F}_M + G_{35} \overline{F}_V) \quad (81)$$

$$\overline{w3}_3^- = 0 \quad (82)$$

$$\overline{w3}_2^- = 0 \quad (83)$$

$$\overline{w3}_1^- = 0 \quad (84)$$

Eqns. (79) through (81) are the wave-mode coordinates at point 3 which represent the waves generated by externally applied sinusoidal loading at point 1. The wave-mode coordinates at point 3 are related to the wave-mode coordinates at point 4 according to

$$\underline{\overline{w}}_4 = \underline{W}(\omega) \underline{\overline{w}}_3 \quad (85)$$

Substituting eqn. (77) and eqns. (79) through (81) into eqn. (85) and writing out each scalar equation give

$$\overline{w4}_1^+ = e^{-j2\lambda_1} S_{61} G_{16} \overline{F}_N + e^{-j(\lambda_1+\lambda_2)} S_{62} (G_{24} \overline{F}_M + G_{25} \overline{F}_V) + e^{-(\lambda_3+j\lambda_1)} S_{63} (G_{34} \overline{F}_M + G_{35} \overline{F}_V) \quad (86)$$

$$\overline{w4}_2^+ = e^{-j(\lambda_1+\lambda_2)} S_{51} G_{16} \overline{F}_N + e^{-j2\lambda_2} S_{52} (G_{24} \overline{F}_M + G_{25} \overline{F}_V) + e^{-(\lambda_3+j\lambda_2)} S_{53} (G_{34} \overline{F}_M + G_{35} \overline{F}_V) \quad (87)$$

$$\overline{w4}_3^+ = e^{-(\lambda_3+j\lambda_1)} S_{41} G_{16} \overline{F}_N + e^{-(\lambda_3+j\lambda_2)} S_{42} (G_{24} \overline{F}_M + G_{25} \overline{F}_V) + e^{-2\lambda_3} S_{43} (G_{34} \overline{F}_M + G_{35} \overline{F}_V) \quad (88)$$

$$\overline{w4}_3^- = 0 \quad (89)$$

$$\overline{w4}_2^- = 0 \quad (90)$$

$$\overline{w4}_1^- = 0 \quad (91)$$

The wave-mode coordinates at point 4 are related to the Fourier transformed state variables at point 4 according to

$$\underline{\overline{z}}_4 = \underline{Y}(\omega) \underline{\overline{w}}_4 \quad (92)$$

Substituting eqn. (14) and eqns. (86) through (91) into eqn. (92) and multiplying out each scalar equation give

$$\overline{u}_4(\omega) = e^{-j2\lambda_1} S_{61} G_{16} \overline{F}_N +$$
$$\left[e^{-j(\lambda_1+\lambda_2)} S_{62} G_{24} + e^{-(\lambda_3+j\lambda_1)} S_{63} G_{34} \right] \overline{F}_M +$$

$$\left[e^{-j\left(\lambda_1+\lambda_2\right)}S_{62}G_{25}+e^{-\left(\lambda_3+j\lambda_1\right)}S_{63}G_{35}\right]\overline{F}_V \tag{93}$$

$$\overline{y}_4(\omega)=\left[e^{-j\left(\lambda_1+\lambda_2\right)}S_{51}G_{16}+e^{-\left(\lambda_3+j\lambda_1\right)}S_{41}G_{16}\right]\overline{F}_N+$$

$$\left[e^{-\left(\lambda_3+j\lambda_2\right)}(S_{42}G_{24}+S_{53}G_{34})+e^{-2\lambda_3}S_{43}G_{34}+e^{-j2\lambda_2}S_{52}G_{24}\right]\overline{F}_M+$$

$$\left[e^{-\left(\lambda_3+j\lambda_2\right)}(S_{42}G_{25}+S_{53}G_{35})+e^{-2\lambda_3}S_{43}G_{35}+e^{-j2\lambda_2}S_{52}G_{25}\right]\overline{F}_V \tag{94}$$

$$\overline{\psi}_4(\omega)=\left[e^{-j\left(\lambda_1+\lambda_2\right)}Y_{32}S_{51}G_{16}+e^{-\left(\lambda_3+j\lambda_1\right)}Y_{33}S_{41}G_{16}\right]\overline{F}_N+$$

$$\left[e^{-\left(\lambda_3+j\lambda_2\right)}(Y_{33}S_{42}G_{24}+Y_{32}S_{53}G_{34})+e^{-2\lambda_3}Y_{33}S_{43}G_{34}+e^{-j2\lambda_2}Y_{32}S_{52}G_{24}\right]\overline{F}_M+$$

$$\left[e^{-\left(\lambda_3+j\lambda_2\right)}(Y_{33}S_{42}G_{25}+Y_{32}S_{53}G_{35})+e^{-2\lambda_3}Y_{33}S_{43}G_{35}+e^{-j2\lambda_2}Y_{32}S_{52}G_{25}\right]\overline{F}_V \tag{95}$$

$$\overline{M}_4(\omega)=\left[e^{-j\left(\lambda_1+\lambda_2\right)}Y_{42}S_{51}G_{16}+e^{-\left(\lambda_3+j\lambda_1\right)}Y_{43}S_{41}G_{16}\right]\overline{F}_N+$$

$$\left[e^{-\left(\lambda_3+j\lambda_2\right)}(Y_{43}S_{42}G_{24}+Y_{42}S_{53}G_{34})+e^{-2\lambda_3}Y_{43}S_{43}G_{34}+e^{-j2\lambda_2}Y_{42}S_{52}G_{24}\right]\overline{F}_M+$$

$$\left[e^{-\left(\lambda_3+j\lambda_2\right)}(Y_{43}S_{42}G_{25}+Y_{42}S_{53}G_{35})+e^{-2\lambda_3}Y_{43}S_{43}G_{35}+e^{-j2\lambda_2}Y_{42}S_{52}G_{25}\right]\overline{F}_V \tag{96}$$

$$\overline{V}_4(\omega)=\left[e^{-j\left(\lambda_1+\lambda_2\right)}Y_{52}S_{51}G_{16}+e^{-\left(\lambda_3+j\lambda_1\right)}Y_{53}S_{41}G_{16}\right]\overline{F}_N+$$

$$\left[e^{-\left(\lambda_3+j\lambda_2\right)}(Y_{53}S_{42}G_{24}+Y_{52}S_{53}G_{34})+e^{-2\lambda_3}Y_{53}S_{43}G_{34}+e^{-j2\lambda_2}Y_{52}S_{52}G_{24}\right]\overline{F}_M+$$

$$\left[e^{-\left(\lambda_3+j\lambda_2\right)}(Y_{53}S_{42}G_{25}+Y_{52}S_{53}G_{35})+e^{-2\lambda_3}Y_{53}S_{43}G_{35}+e^{-j2\lambda_2}Y_{52}S_{52}G_{25}\right]\overline{F}_V \tag{97}$$

$$\overline{N}_4(\omega) = e^{-j2\lambda_1} Y_{61} S_{61} G_{16} \overline{F}_N +$$
$$\left[e^{-j(\lambda_1+\lambda_2)} Y_{61} S_{62} G_{24} + e^{-(\lambda_3+j\lambda_1)} Y_{61} S_{63} G_{34} \right] \overline{F}_M +$$
$$\left[e^{-j(\lambda_1+\lambda_2)} Y_{61} S_{62} G_{25} + e^{-(\lambda_3+j\lambda_1)} Y_{61} S_{63} G_{35} \right] \overline{F}_V \qquad (98)$$

Eqns. (93) through (98) represent the frequency response functions of each Fourier transformed state variable at point 4 due to sinusoidally applied loads at point 1. Given the magnitude and frequency of the applied loads at point 1, the magnitude and phase of each state variable at point 4 of the "L" lattice assembly, shown in Fig. 1, may be determined.

It is important to note that, using eqn. (85), the wave-mode vector at any location along member 2 may be determined by substituting in the appropriate wave-mode propagation matrix $\underline{W}(\omega)$. Therefore, once the wave-mode vector at point 3 is known, the frequency response function of each Fourier transformed state variable at any location along member 2 may be determined using the above procedures.

From eqns. (93) through (98), the time domain response of each state variable at point 4 may be obtained using one of two methods. One method is to perform contour integration in the complex plane to determine the inverse Fourier transform of the state variable. An alternate approach is to utilize the concepts of digital signal processing to determine the inverse discrete Fourier transform of the state variable. The first method is particularly favored when the equations are of known tabulated form. For cases when the time domain applied loading is of arbitrary shape, or whose transform is not tabulated, the digital approach is recommended.

Conclusions and Recommendations

The objective of this report was to illustrate the concepts and features of wave-mode coordinate analysis by studying the behavior of waves propagating through an "L" lattice junction. A system of two identical semi-infinite perpendicular lattice members joined by a rigid joint with mass and rotary inertia was considered. The system was subjected to sinusoidal loading at a point along one of the lattice members. Each lattice member was modeled as a combined longitudinal rod and Timoshenko beam.

An applied sinusoidal axial force $\overline{F}_N$, shear force $\overline{F}_V$ and bending moment $\overline{F}_M$ along a continuous lattice member may generate up to three independent waves. These are: one, a longitudinal (type one) wave; two, a mode 1 flexural (type two) wave and; three, a mode 2 flexural (type three) wave.

As the frequency ω approaches zero, a longitudinal wave which strikes the joint along member 1 is reflected as if the joint end of member 1 were a free-end boundary condition. As the frequency ω approaches infinity, a longitudinal wave which strikes the joint along member 1 is reflected as if the joint end of member 1 were a fixed-end boundary condition.

As the frequency ω approaches infinity, each incident wave will encounter complete reflection at the joint with no transmission. This behavior is expected since a joint with mass and rotary inertia should appear as a fixed-end boundary condition at ultra-high frequencies regardless of the number or orientation of any adjacent members attached to the joint.

In general, each wave which strikes the joint, at point 2, will result in the reflection of three waves, at point 2. For example, an incident longitudinal wave will, in general, result in the reflection of a longitudinal wave, a mode 1 flexural wave and a mode 2 flexural wave, all of which will propagate along member 1 in the direction of decreasing x, refer to Fig. 1. In general, each wave which strikes the joint, at point 2, will result in the transmission of three waves, at point 3. For example, an incident longitudinal wave will, in general, result in the transmission of a longitudinal wave, a mode 1 flexural wave and a mode 2 flexural wave, all

of which will propagate along member 2 in the direction of increasing x, refer to Fig. 1. In summary, at any given frequency ω, each type of wave which strikes the joint may result in three reflected waves and three transmitted waves In this analysis, a longitudinal wave, a mode 1 flexural wave and/or a mode 2 flexural wave may strike the joint at point 2. This accounts for the eighteen scattering matrix terms given by eqn. (55) which were presented and illustrated.

The following recommendations are presented as suggestions for future research :

1 - For frequencies $0 < \omega < \omega_c$, each reflection and transmission coefficient exhibits a peak or a valley in its magnitude plot. A physical interpretation of this phenomenon and the possible existence of a characteristic equation which identifies the frequency at which each peak and valley will occur is unclear and suggests further investigation.

2 - As the frequency ω approaches zero, static coupling exists between member 1 and member 2. This is illustrated by the nonzero reflection and transmission coefficients near zero frequency. It is desirable to have a physical interpretation of these finite nonzero values of the reflection and transmission coefficients. Therefore, it is recommended that further work be conducted in this area in order to attain a better understanding of these quasi-static effects.

3 - The wave propagation analysis of the "L" lattice junction is an important step in understanding the behavior of propagating waves in large space structures. However, there are joint geometries of greater complexity that must eventually be addressed. It is recommended that a wave propagation analysis be performed, using wave-mode coordinates, of a "T" lattice junction.

4 - It is desirable to obtain the time domain response of each state variable at an arbitrary location along the "L" lattice assembly. It is recommended that a procedure which utilizes the concepts of digital signal processing be pursued in order to provide time domain responses from the frequency response functions obtained using wave-mode coordinates.

5 - Finally, it is recommended that the results presented in this report be verified experimentally.

Wave-mode coordinate analysis is an effective tool in studying the behavior of propagating waves through an "L" lattice junction. It provides a well structured and relatively straightforward procedure to determine the reflection and transmission coefficients for longitudinal and flexural waves which may strike the joint. In addition, the frequency response of each transformed state variable may be determined at any location in the "L" lattice assembly. Unlike finite element methods, the wave-mode coordinate approach to wave propagation analysis does not require remodelling in order to increase analysis accuracy or to obtain solutions at arbitrary locations. This is a very attractive feature which emphasizes the analysis capabilities and versatility of wave-mode coordinate analysis.

References

[1] J.H. Williams,Jr. and D.S. Webb, "Wave-Mode Coordinate Analysis of a Combined Longitudinal Rod and Timoshenko Beam Lattice Member", AFOSR Technical Report, September 1988.

[2] J.H. Williams,Jr., H.K. Yeung and R.J. Nagem, "Joint Coupling Matrices for Wave Propagation Analysis of Large Space Structures", AFOSR Technical Report, April 1986.

[3] E.C. Pestel and F.A. Leckie, Matrix Methods in Elastomechanics, McGraw-Hill, Inc., 1963.

[4] D.S. Webb, "The Transfer, Wave-Mode, and Wave-Mode Propagation Matrix of the Timoshenko Beam", Composite Materials and Nondestructive Evaluation Laboratory Report, Massachusetts Institute of Technology, November 1987.

[5] R.J. Nagem, "Wave-Mode Coordinates for an Elastic Longitudinal Rod", Composite Materials and Nondestructive Evaluation Laboratory Report, Massachusetts Institute of Technology, December 1985.

[6] MACSYMA Reference Manuals - Volumes I and II, The Mathlab Group, Laboratory for Computer Science, Massachusetts Institute of Technology, Version Ten, January 1983.

[7] R.D. Blevins, Formulas for Natural Frequency and Mode Shape, Robert E. Krieger Publishing Company, 1984.

[8] S.H. Crandall, D.C. Karnopp, E.F. Kurtz,Jr. and D.C. Pridmore-Brown, Dynamics of Mechanical and Electromechanical Systems, McGraw-Hill, Inc., 1968.

[9] J.H. Williams,Jr., R.J. Nagem and H.K. Yeung, "Wave-Mode Coordinates and Scattering Matrices for Dynamic Analysis of Large Space Structures", AFOSR Technical Report, October 1986.

Table 1 Geometric and material properties of aluminum lattice "L" joint assembly.

Aluminum Alloy Lattice "L" Joint Assembly	
Tubular Lattice Member	
Outside Diameter :	0.0750 m
Wall Thickness :	0.0125 m
Cross-Sectional Area (A) :	2.45E-03 m^2 †
Section Moment of Ineria (I) :	1.25E-06 m^4
Shear Correction Coefficient (κ) :	0.568
Mass Density (ρ) :	2.70E+03 Kg/m^3
Section Rotary Inertia (J) :	3.37E-03 Kg-m
Tensile Modulus (E) :	7.00E+10 N/m^2
Shear Modulus (G) :	2.60E+10 N/m^2
Rigid Joint	
Joint Diameter :	0.100 m
Mass (m) :	1.000 Kg ‡
Mass Moment of Inertia (I_{zz}) :	1.00E-03 $Kg\text{-}m^2$ ‡

† E-03 ≡ 10^{-3}
‡ Assumes joint is spherical and approximately two-thirds solid.

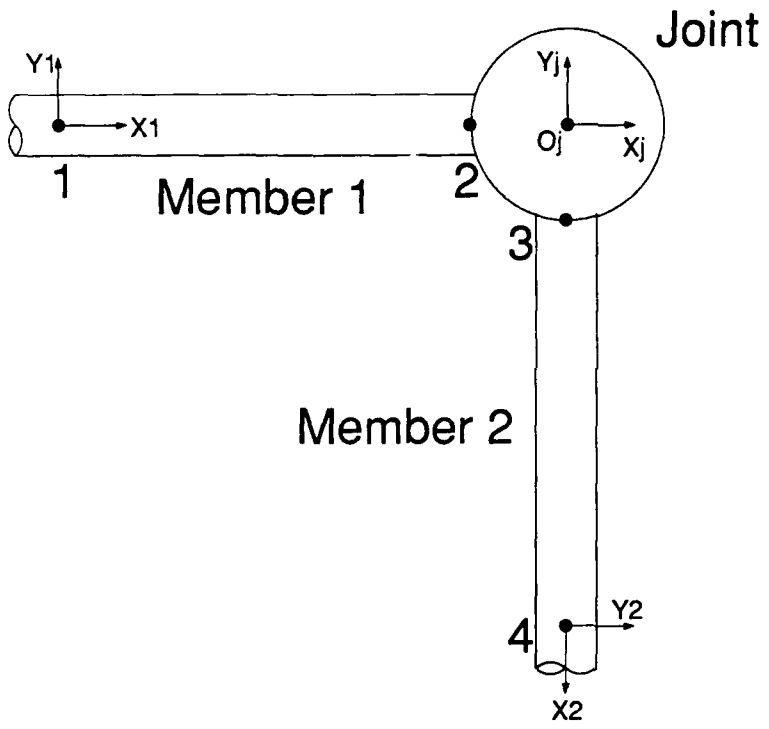

Fig. 1 Local coordinate systems of "L" lattice joint assembly.

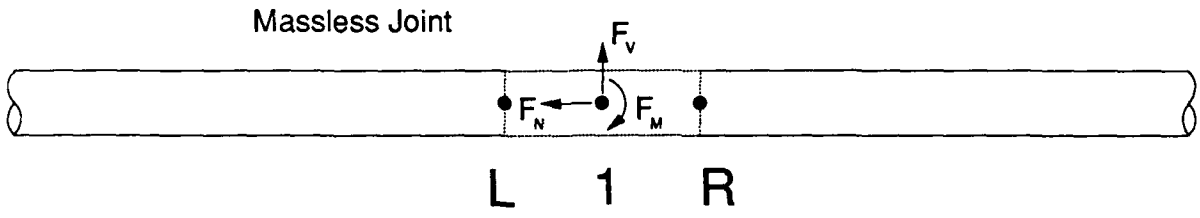

Fig. 2a Simulated rigid massless joint with no spatial extent at point of applied loading along lattice member.

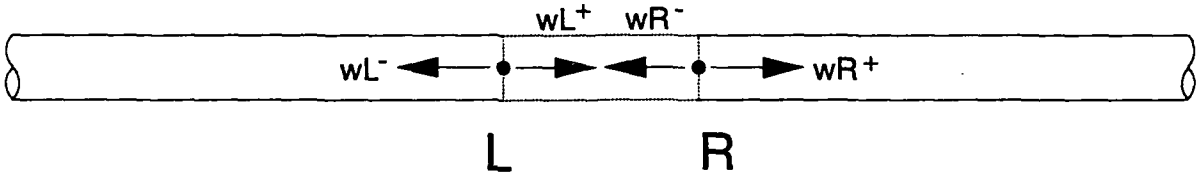

Fig. 2b Wave-mode coordinates entering and leaving simulated rigid massless joint at point of applied loading.

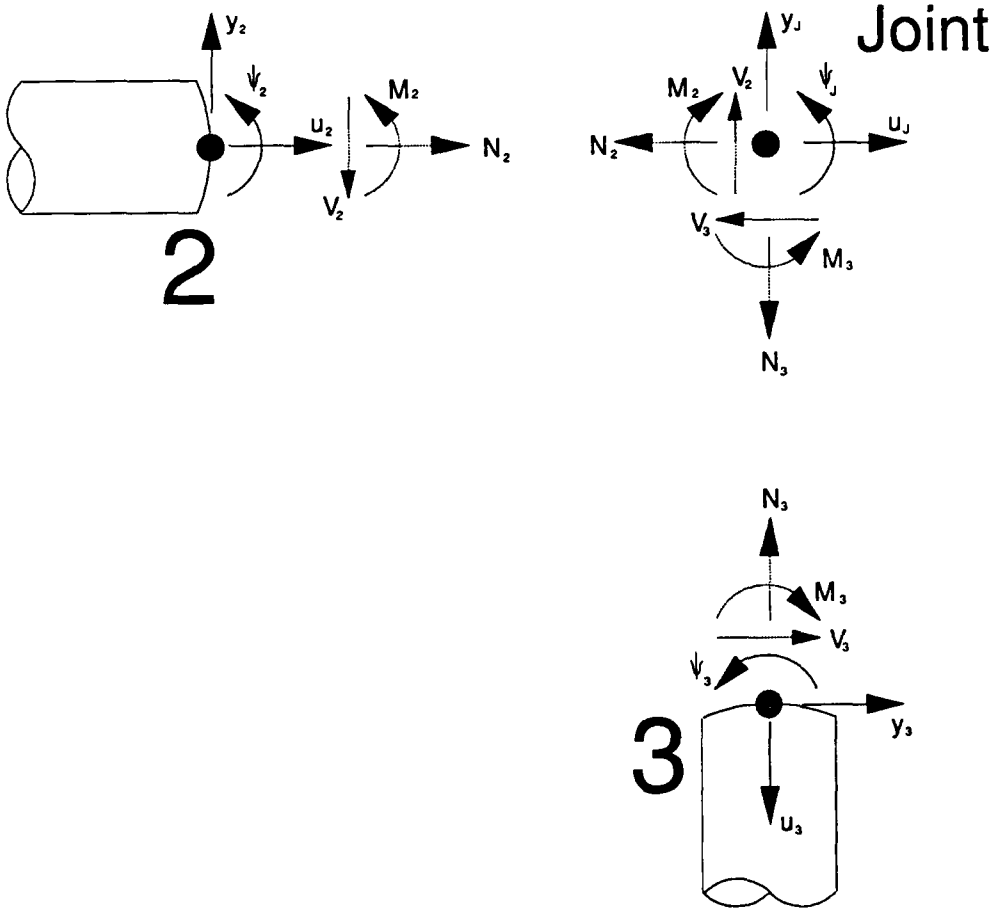

Fig. 3 Components of state vectors at "L" lattice joint with mass and rotary inertia.

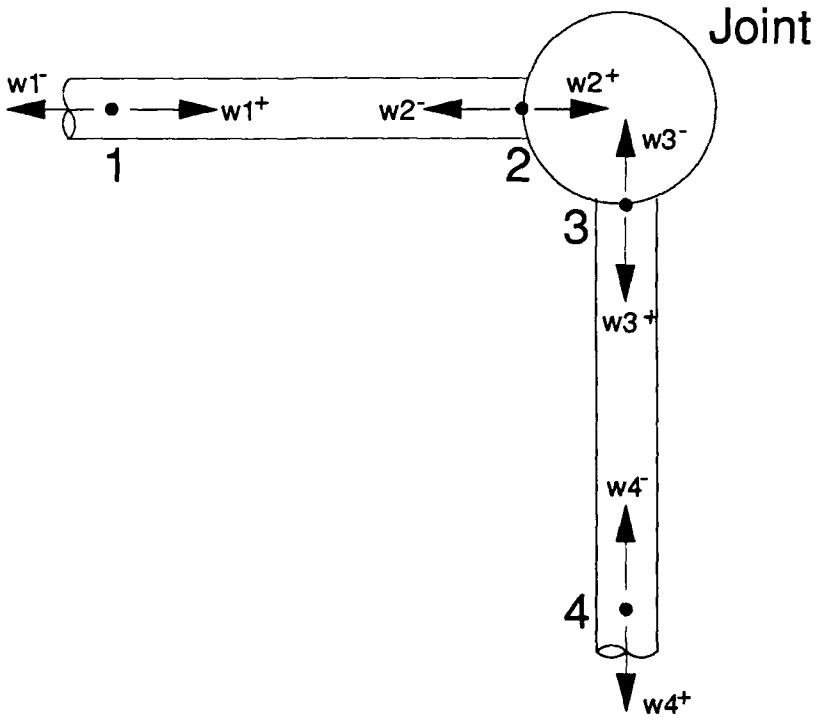

Fig. 4 Wave-mode coordinates entering and leaving rigid "L" joint with mass and rotary inertia.

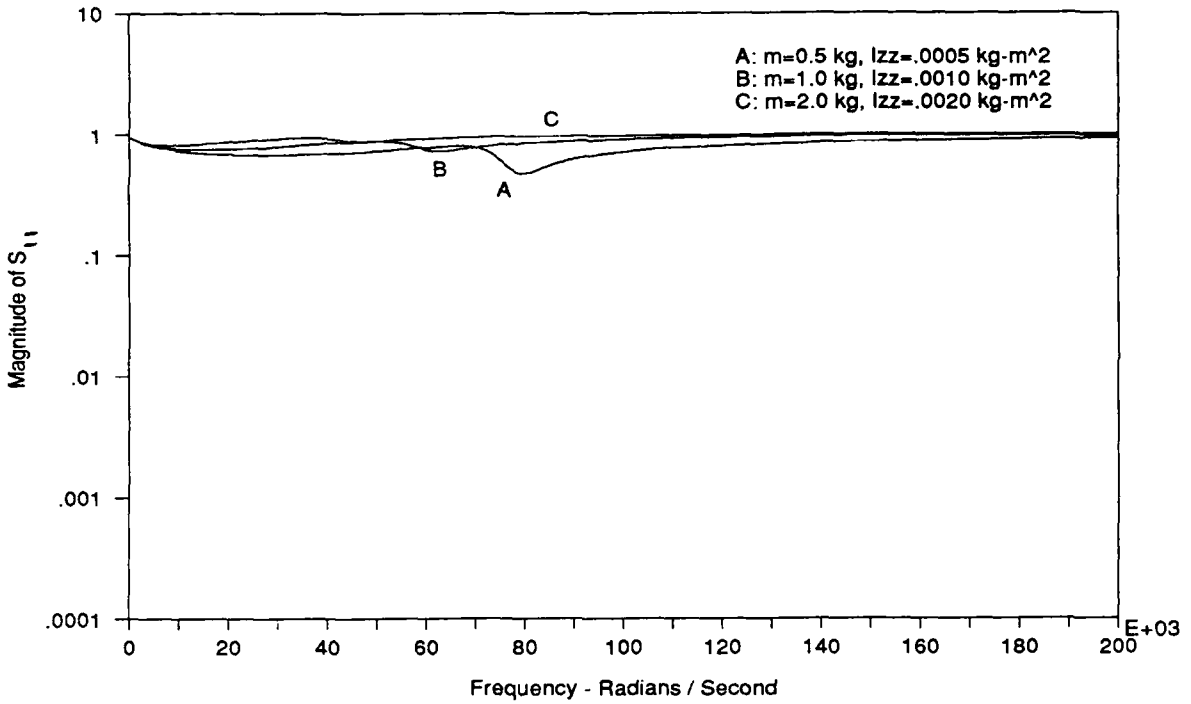

Fig. 5a Magnitude of scattering matrix reflection coefficient S_{11}.

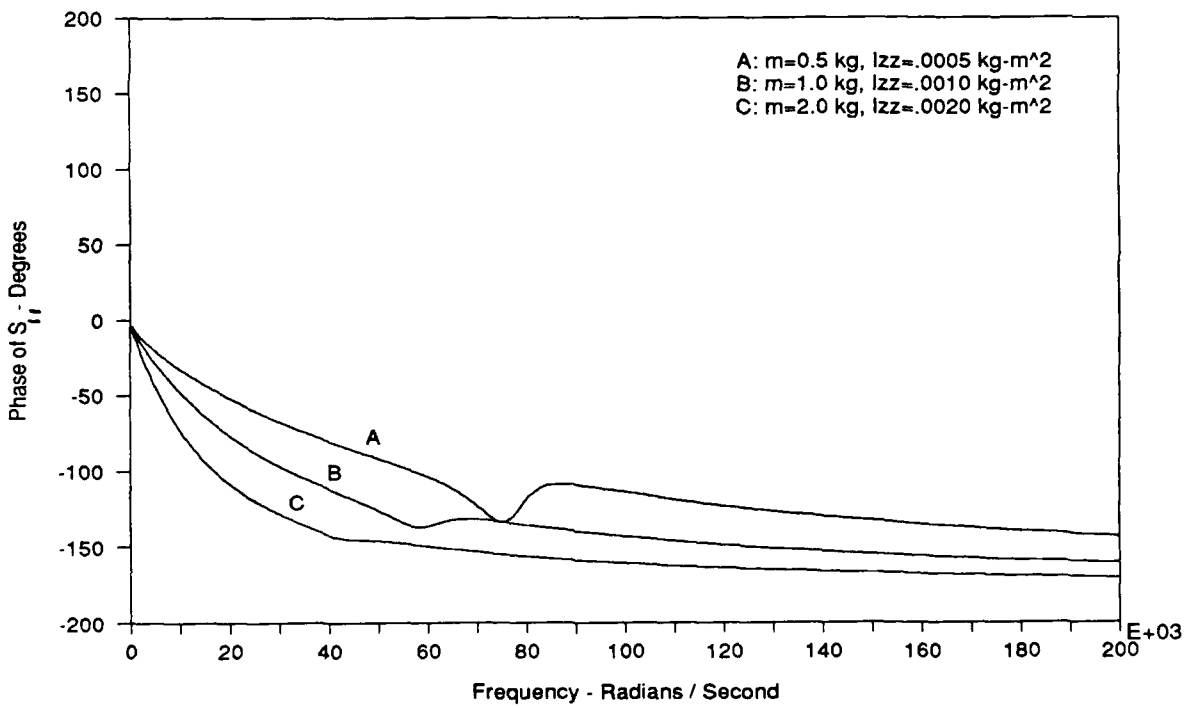

Fig. 5b Phase of scattering matrix reflection coefficient S_{11}.

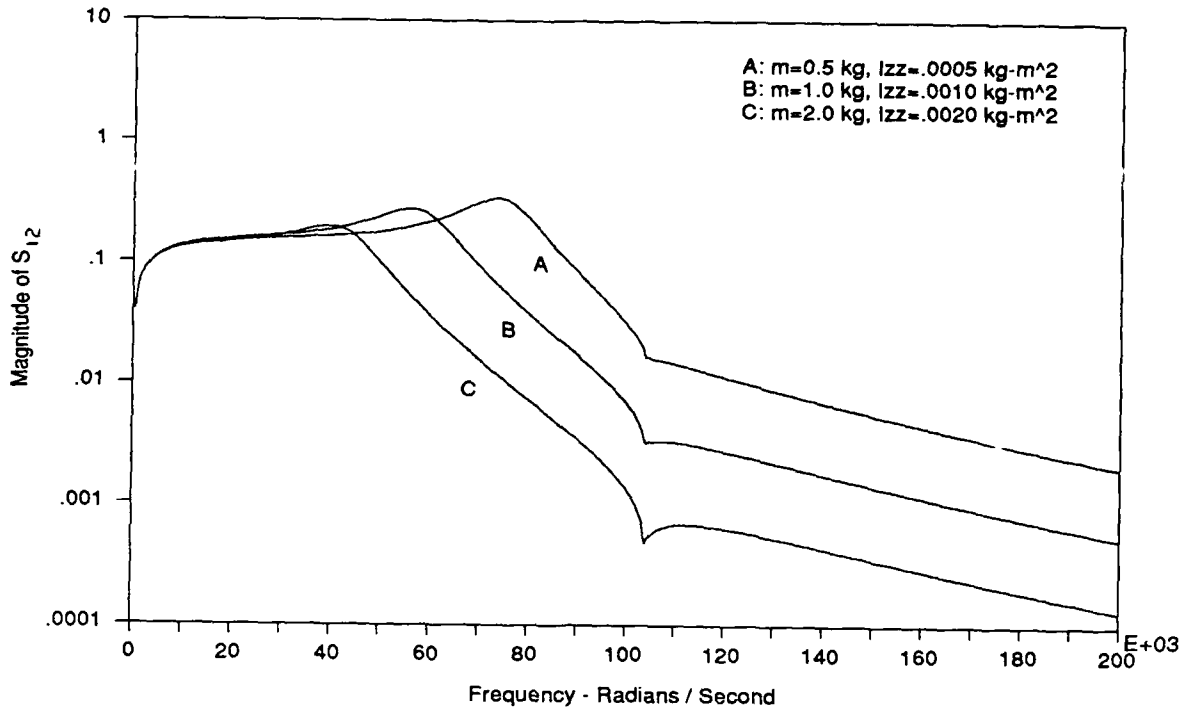

Fig. 6a Magnitude of scattering matrix reflection coefficient S_{12}.

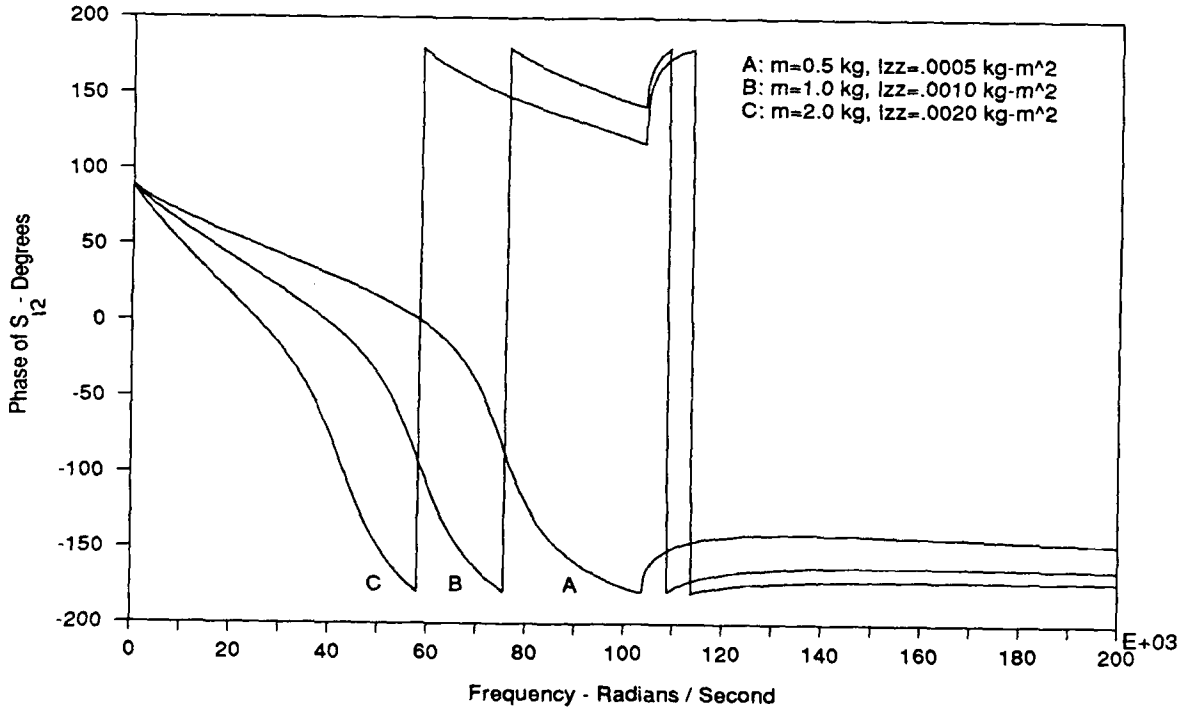

Fig. 6b Phase of scattering matrix reflection coefficient S_{12}.

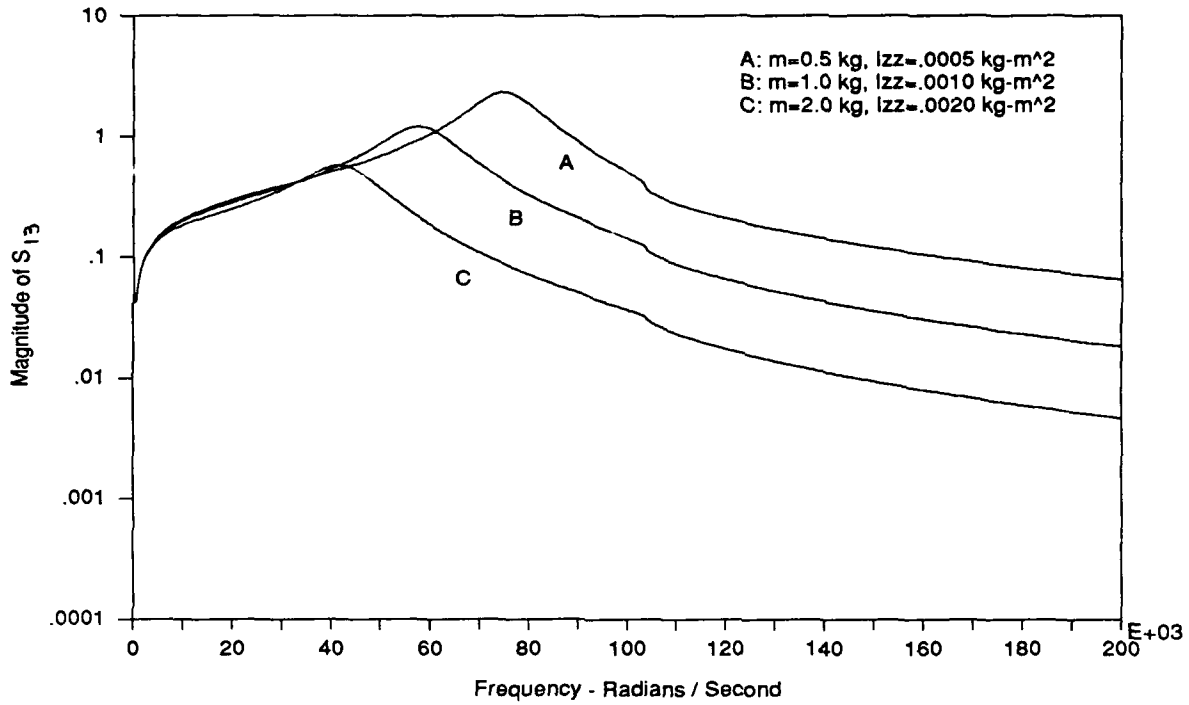

Fig. 7a Magnitude of scattering matrix reflection coefficient S_{13}.

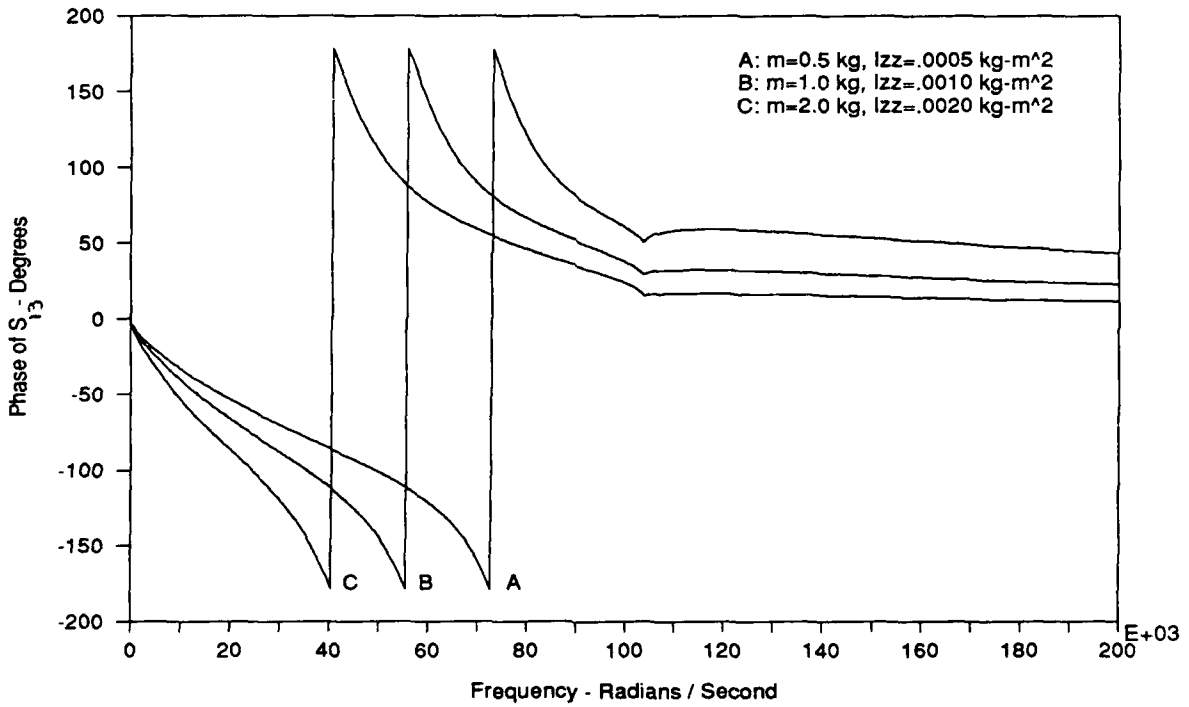

Fig. 7b Phase of scattering matrix reflection coefficient S_{13}.

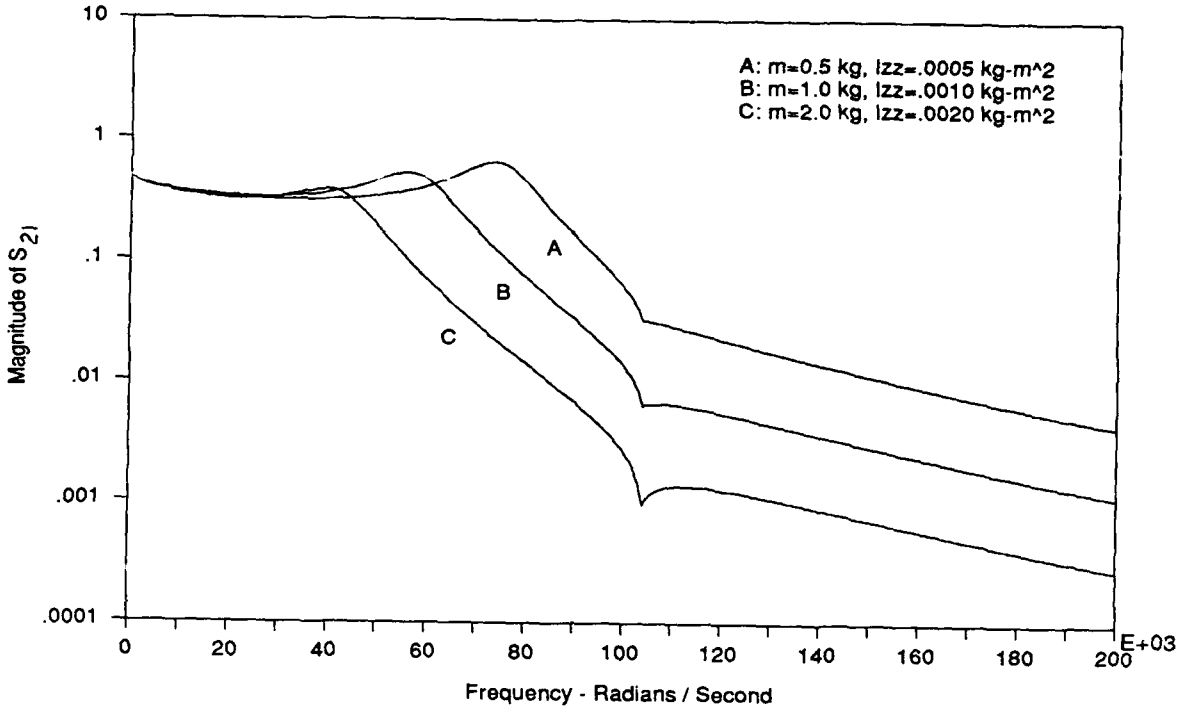

Fig. 8a Magnitude of scattering matrix reflection coefficient S_{21}.

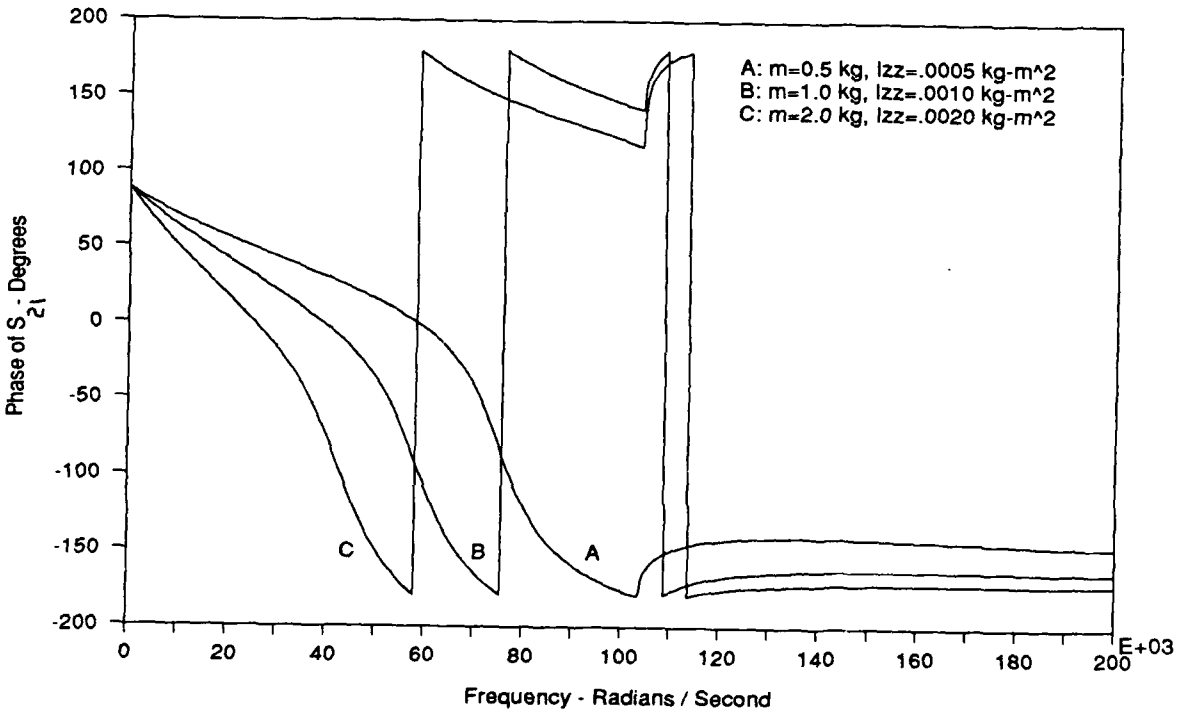

Fig. 8b Phase of scattering matrix reflection coefficient S_{21}.

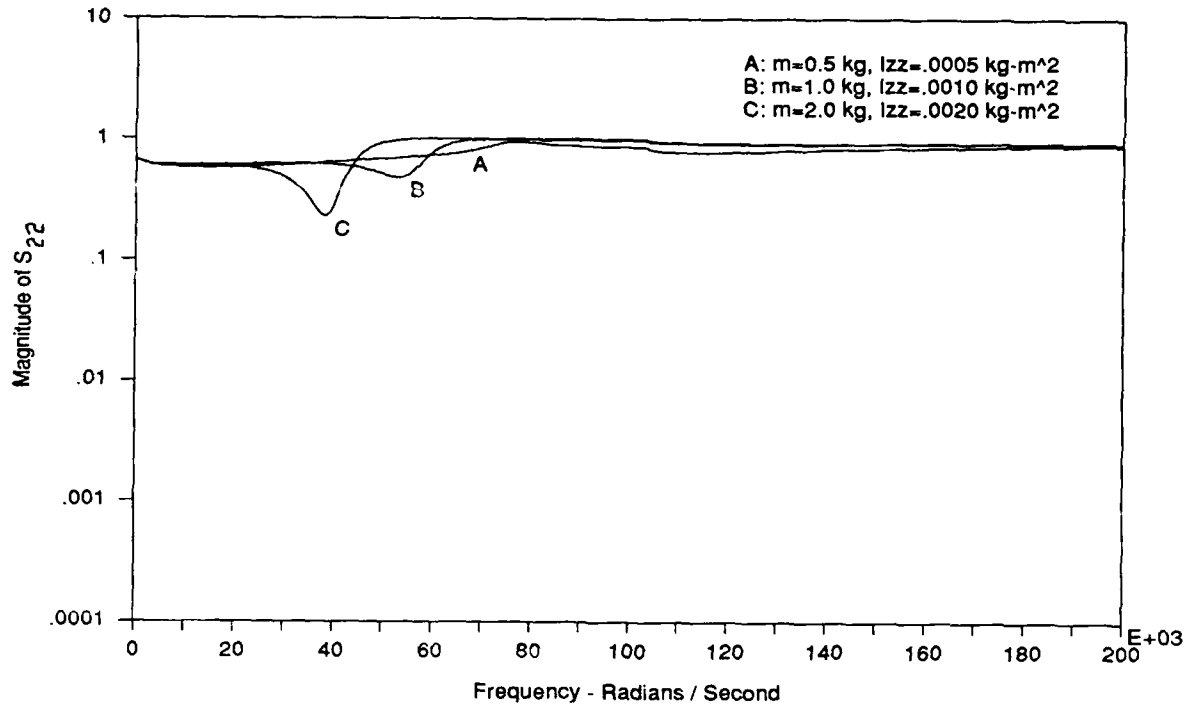

Fig. 9a Magnitude of scattering matrix reflection coefficient S_{22}.

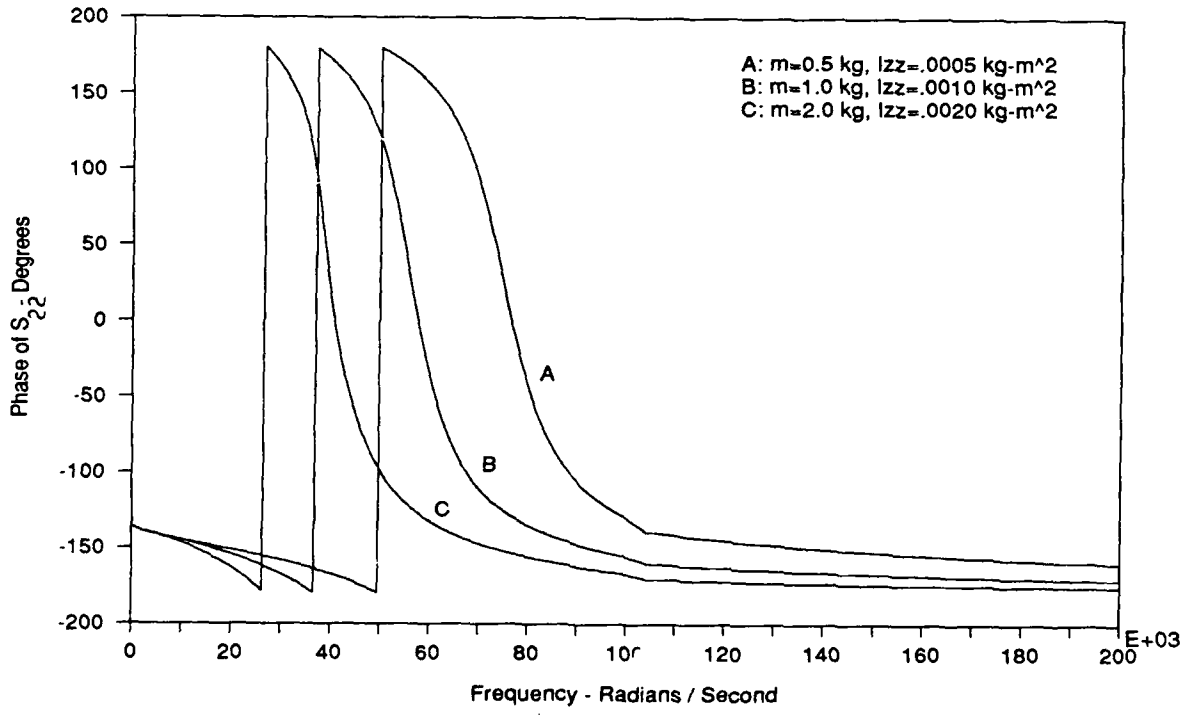

Fig. 9b Phase of scattering matrix reflection coefficient S_{22}.

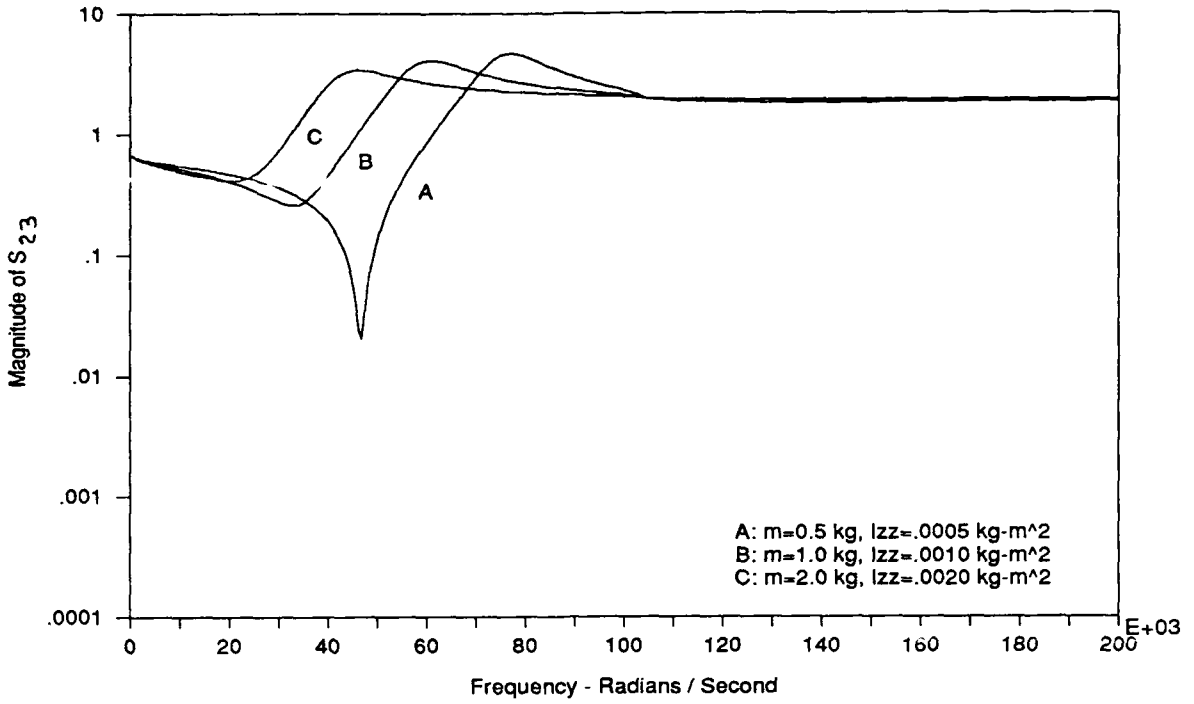

Fig. 10a Magnitude of scattering matrix reflection coefficient S_{23}.

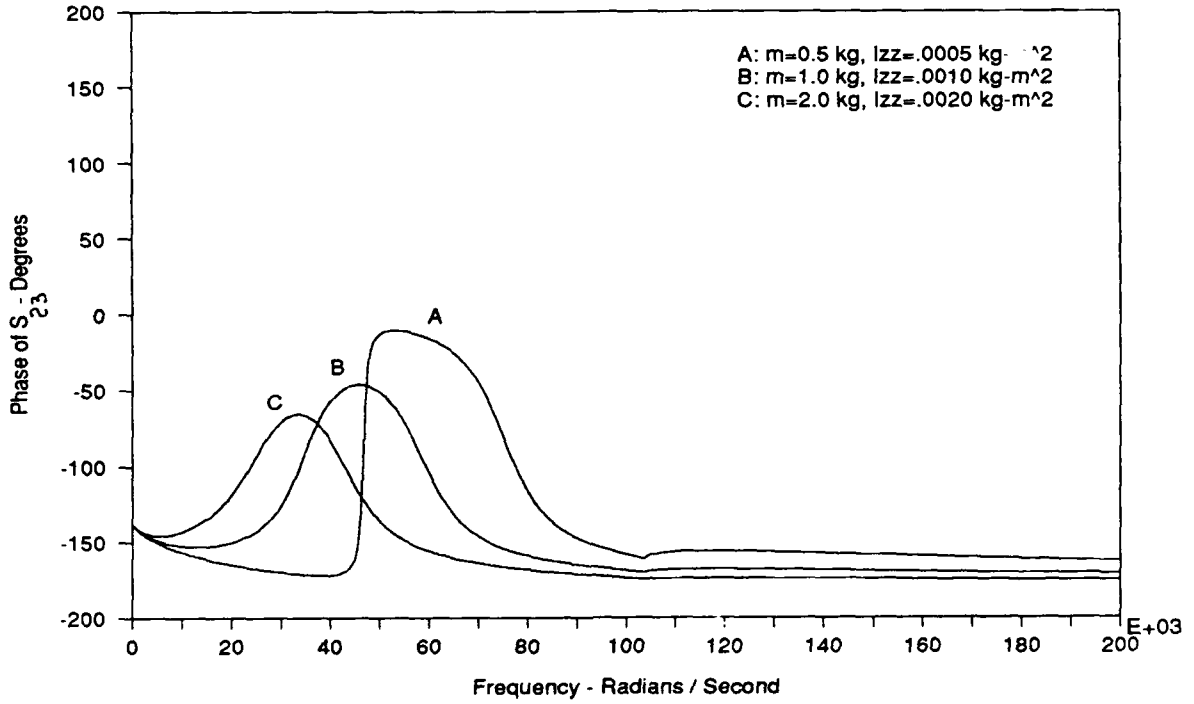

Fig. 10b Phase of scattering matrix reflection coefficient S_{23}.

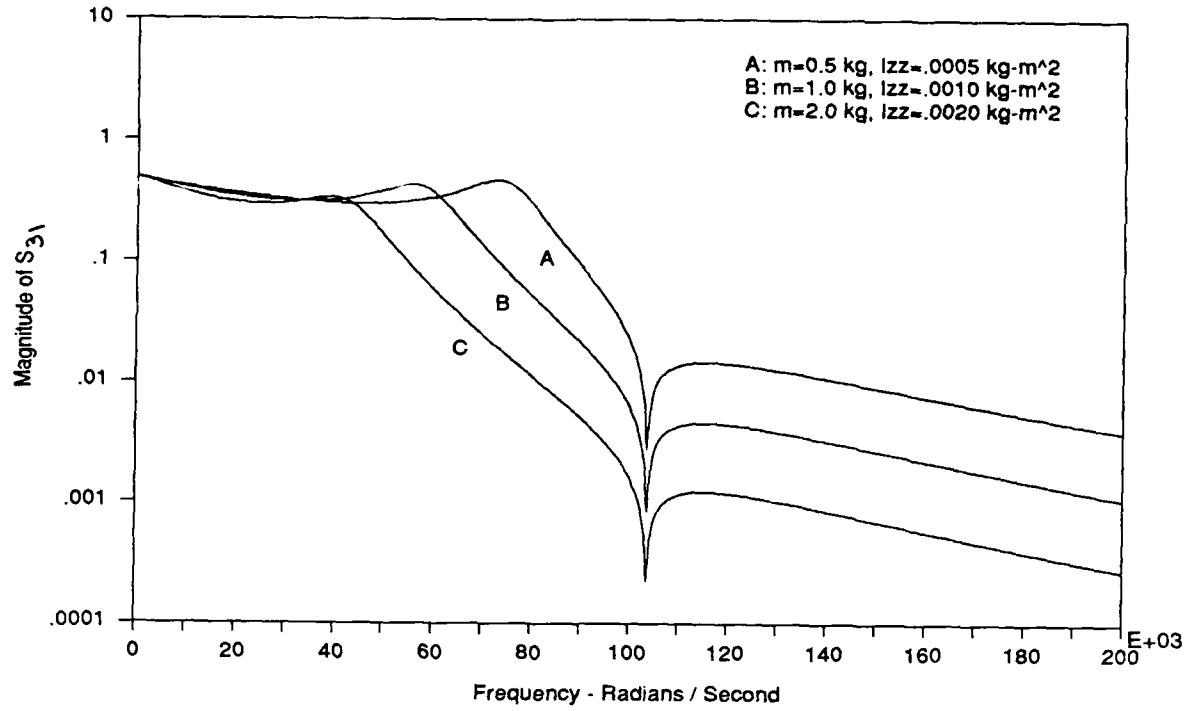

Fig. 11a Magnitude of scattering matrix reflection coefficient S_{31}.

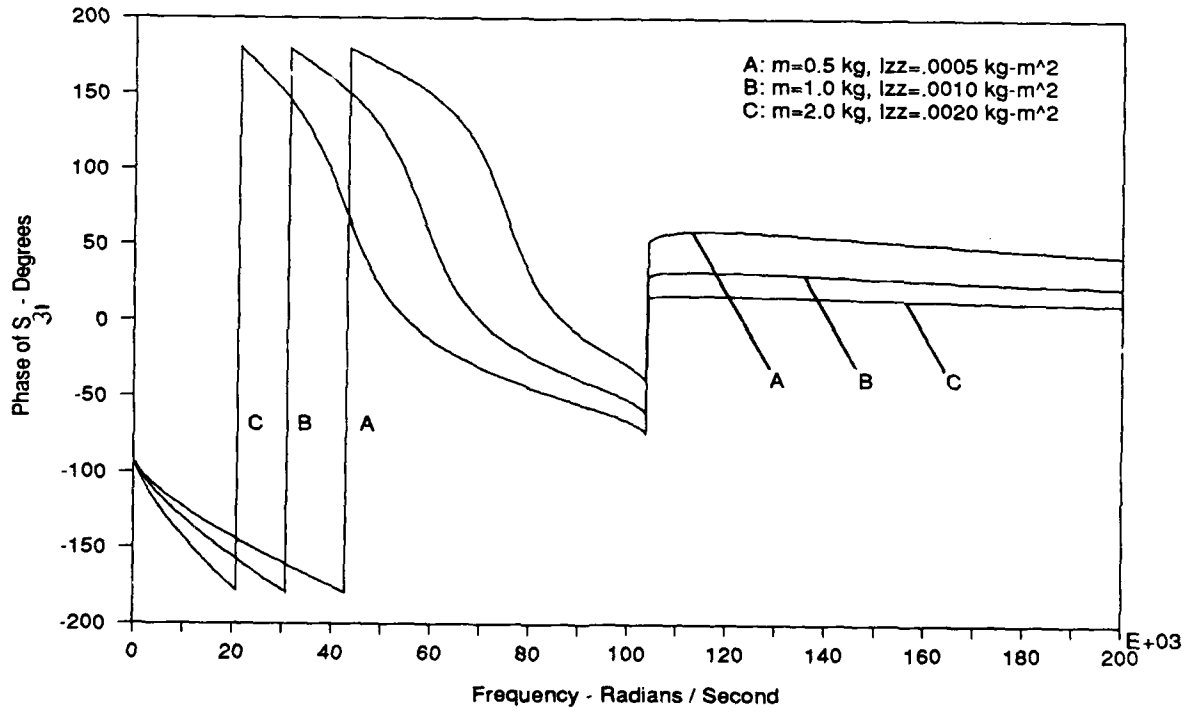

Fig. 11b Phase of scattering matrix reflection coefficient S_{31}.

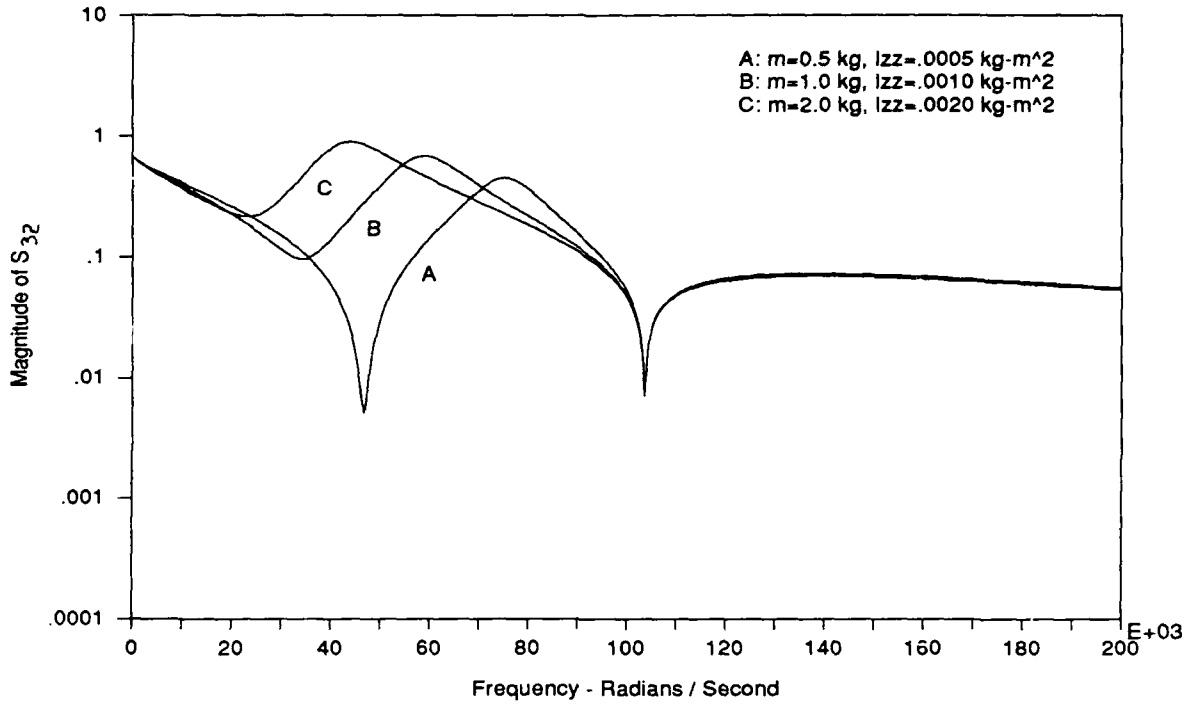

Fig. 12a Magnitude of scattering matrix reflection coefficient S_{32}.

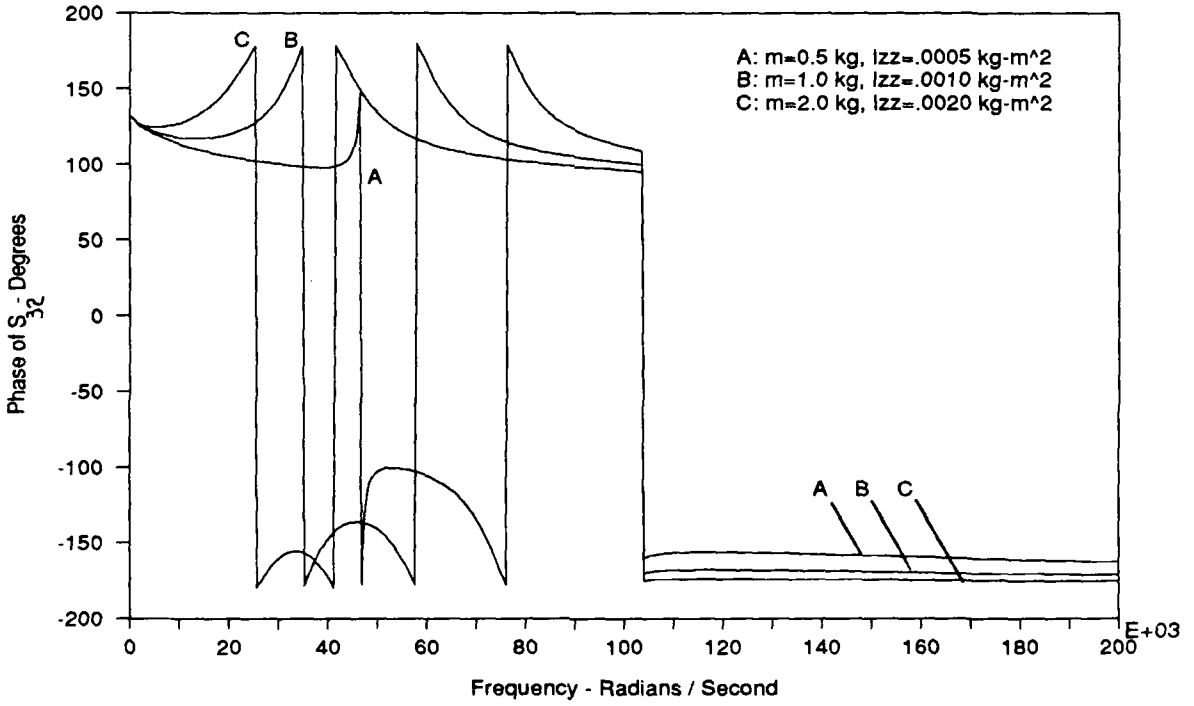

Fig. 12b Phase of scattering matrix reflection coefficient S_{32}.

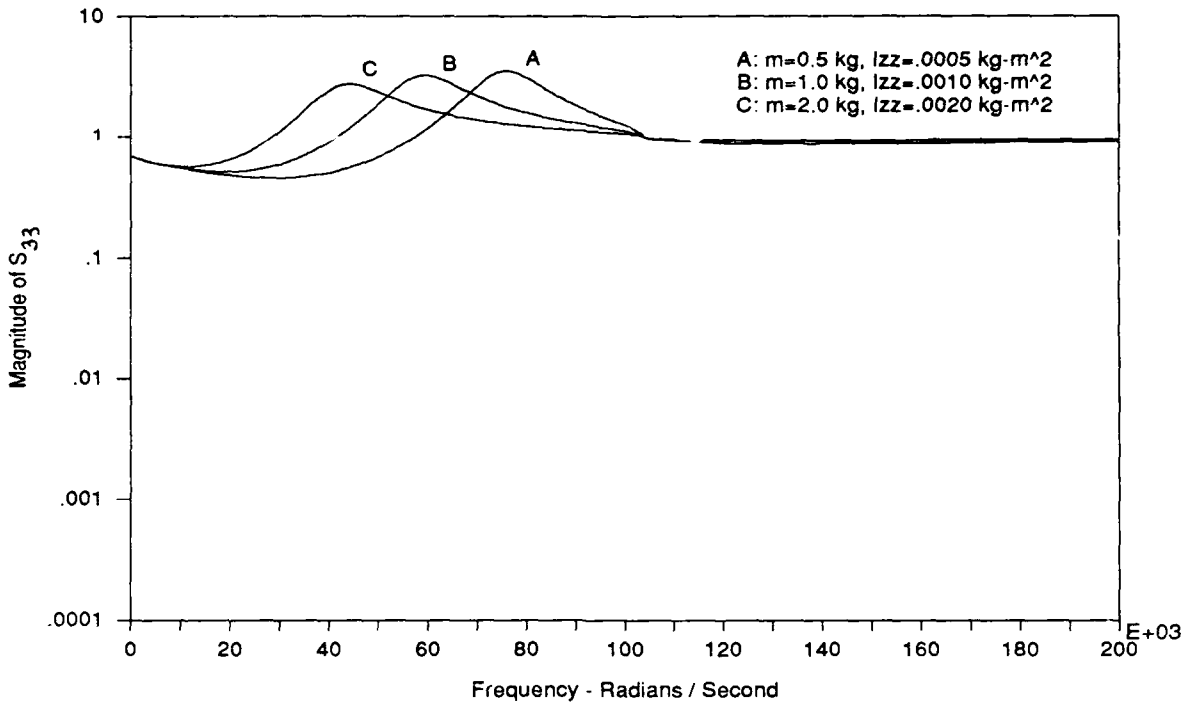

Fig. 13a Magnitude of scattering matrix reflection coefficient S_{33}.

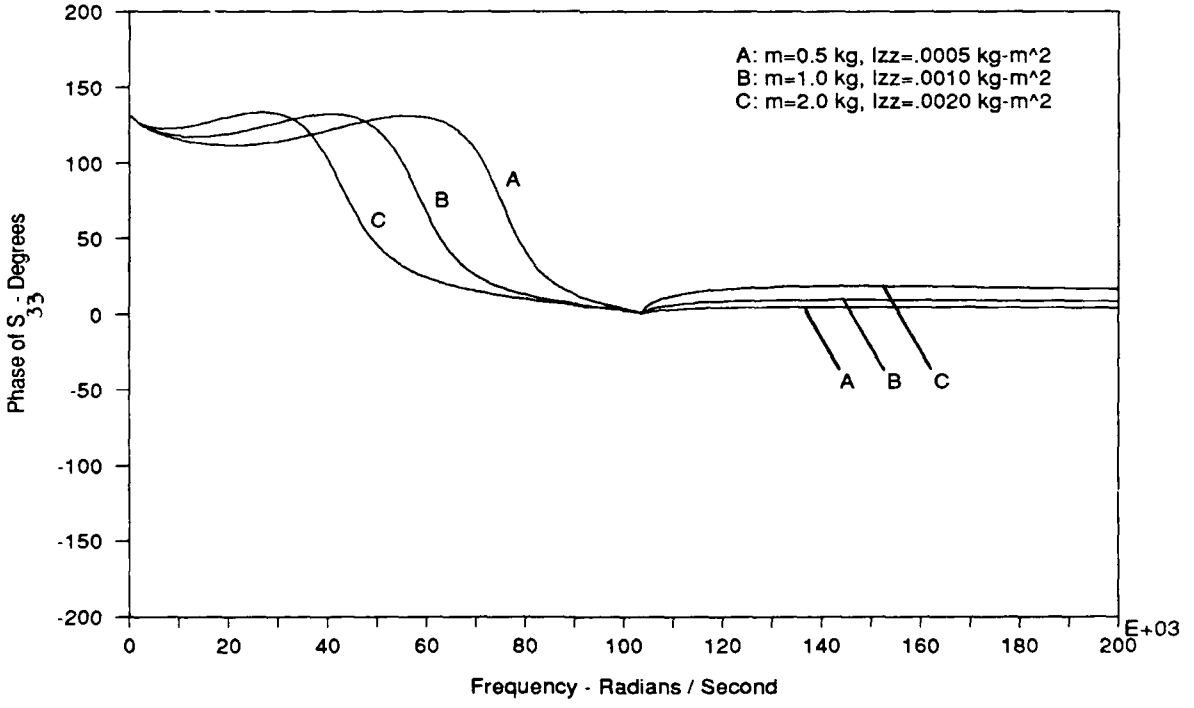

Fig. 13b Phase of scattering matrix reflection coefficient S_{33}.

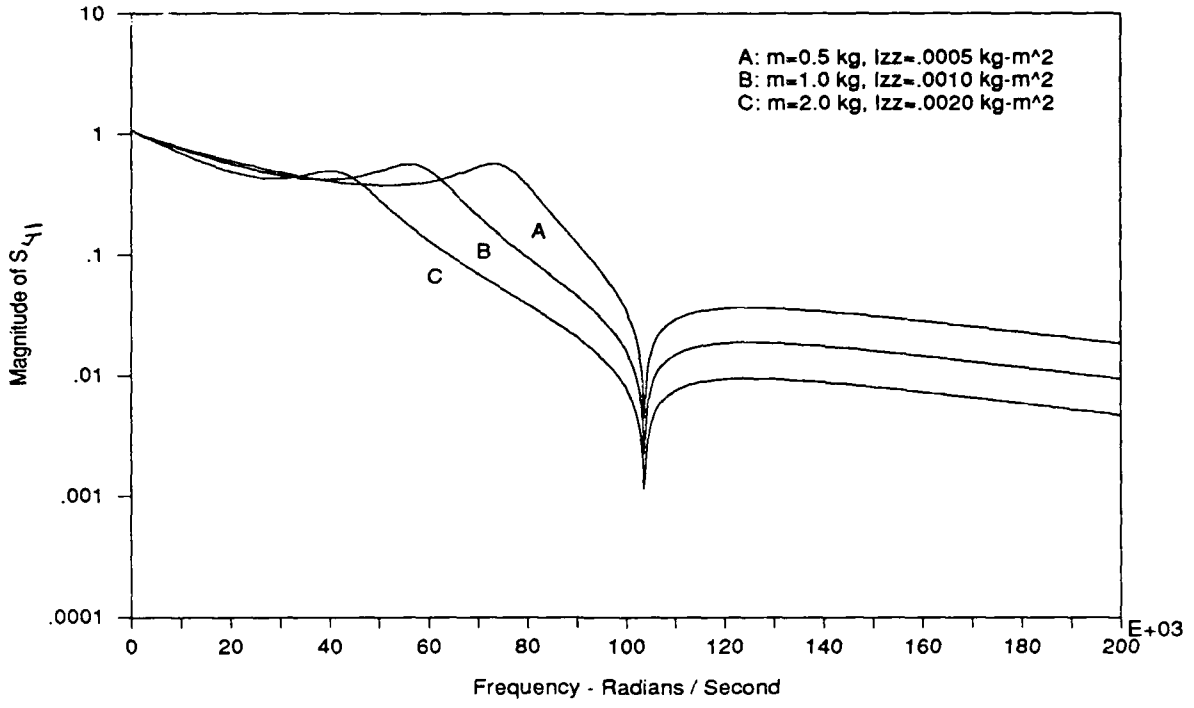

Fig. 14a Magnitude of scattering matrix transmission coefficient S_{41}.

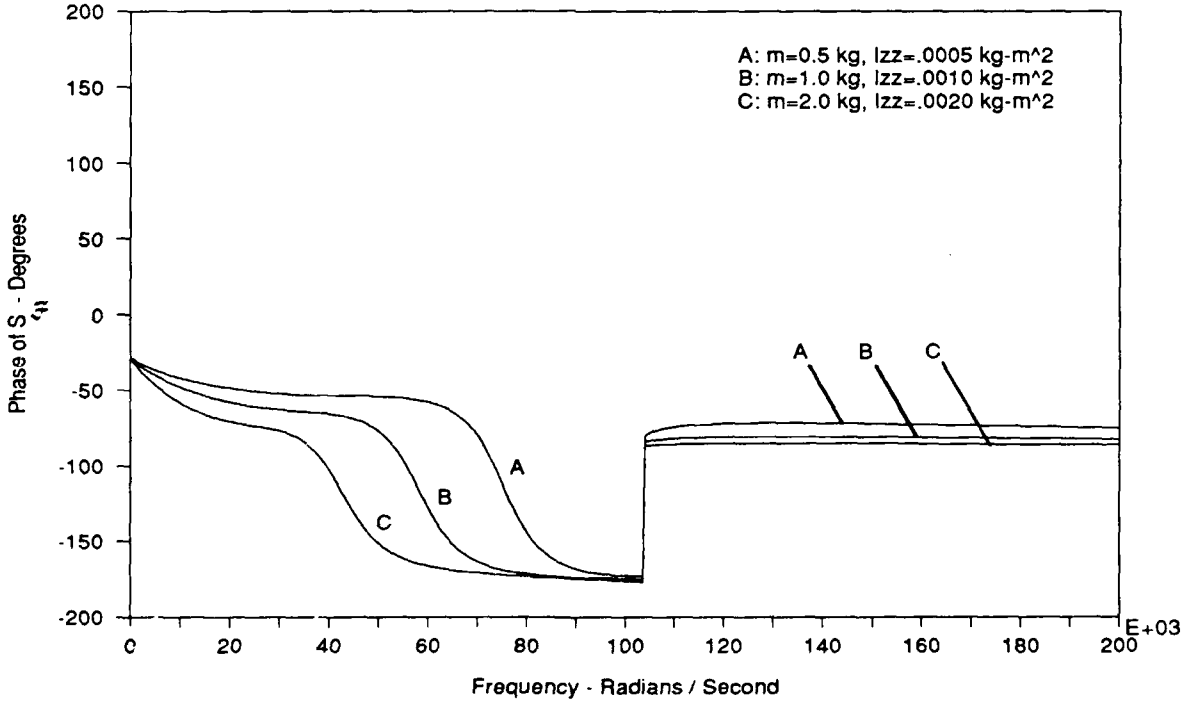

Fig. 14b Phase of scattering matrix transmission coefficient S_{41}.

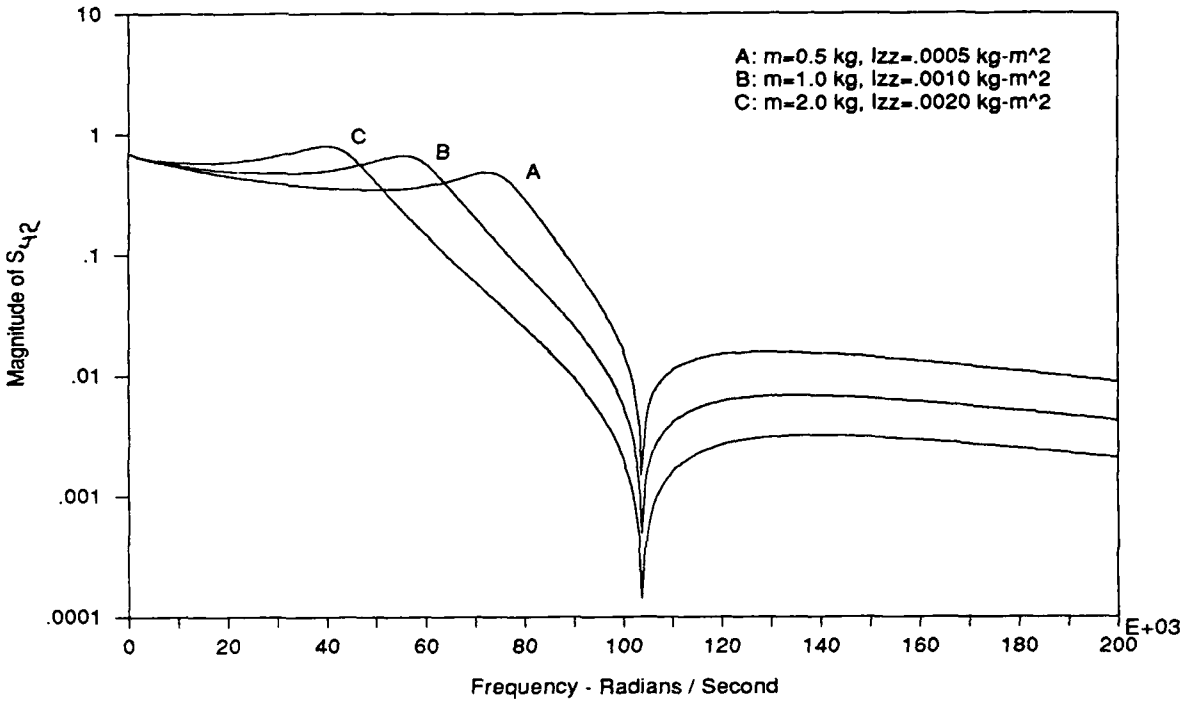

Fig. 15a Magnitude of scattering matrix transmission coefficient S_{42}.

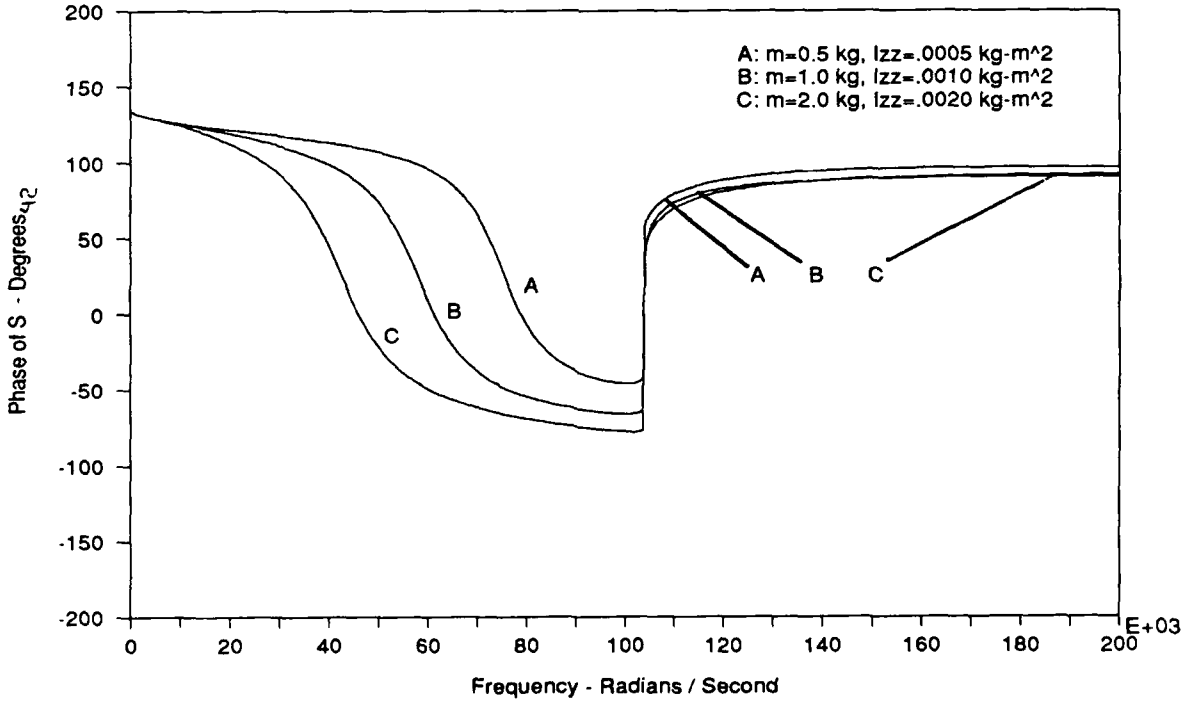

Fig. 15b Phase of scattering matrix transmission coefficient S_{42}.

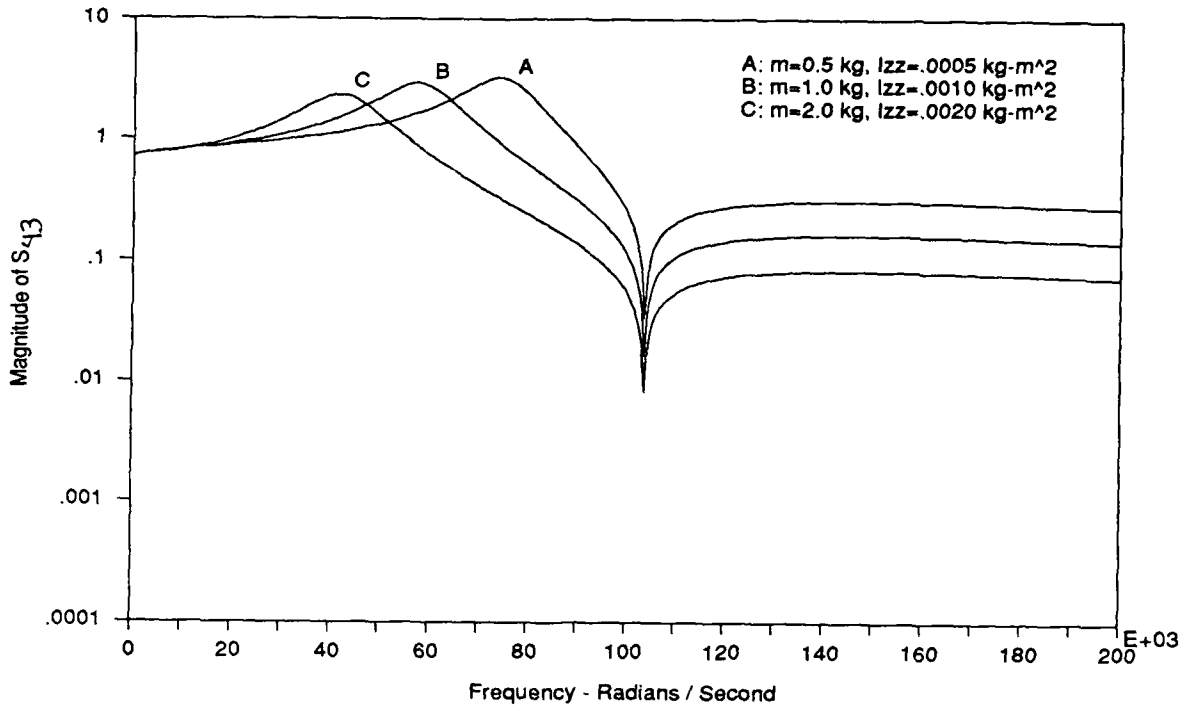

Fig. 16a Magnitude of scattering matrix transmission coefficient S_{43}.

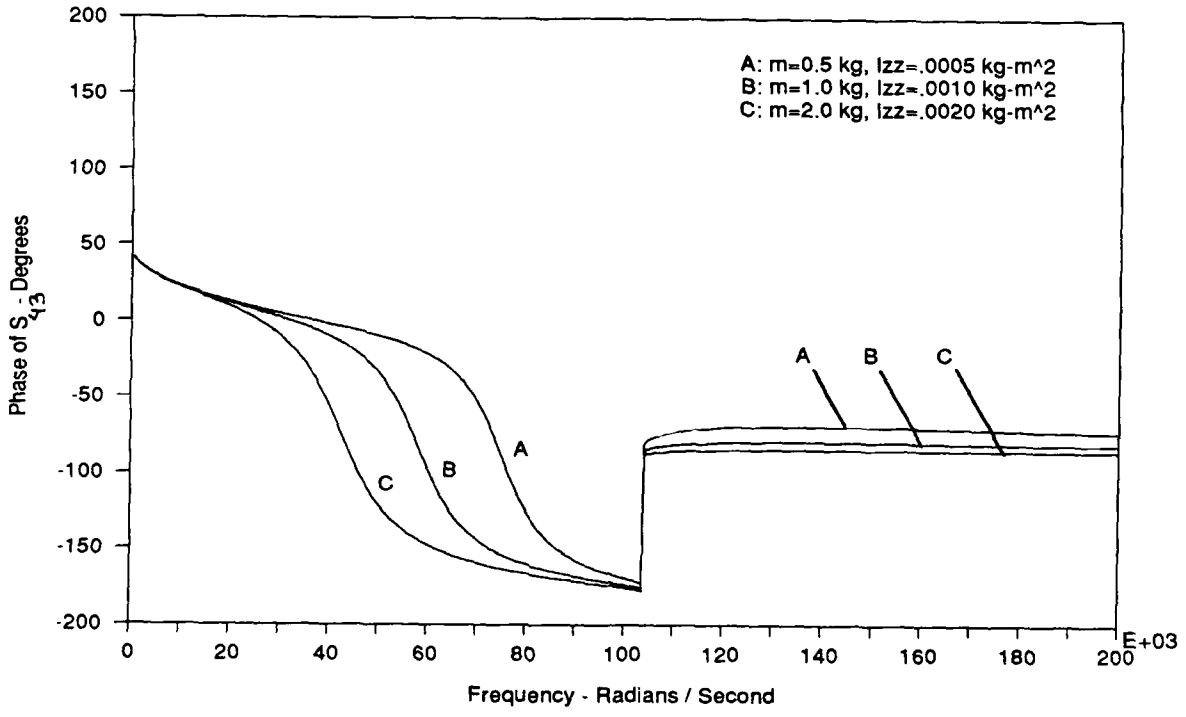

Fig. 16b Phase of scattering matrix transmission coefficient S_{43}.

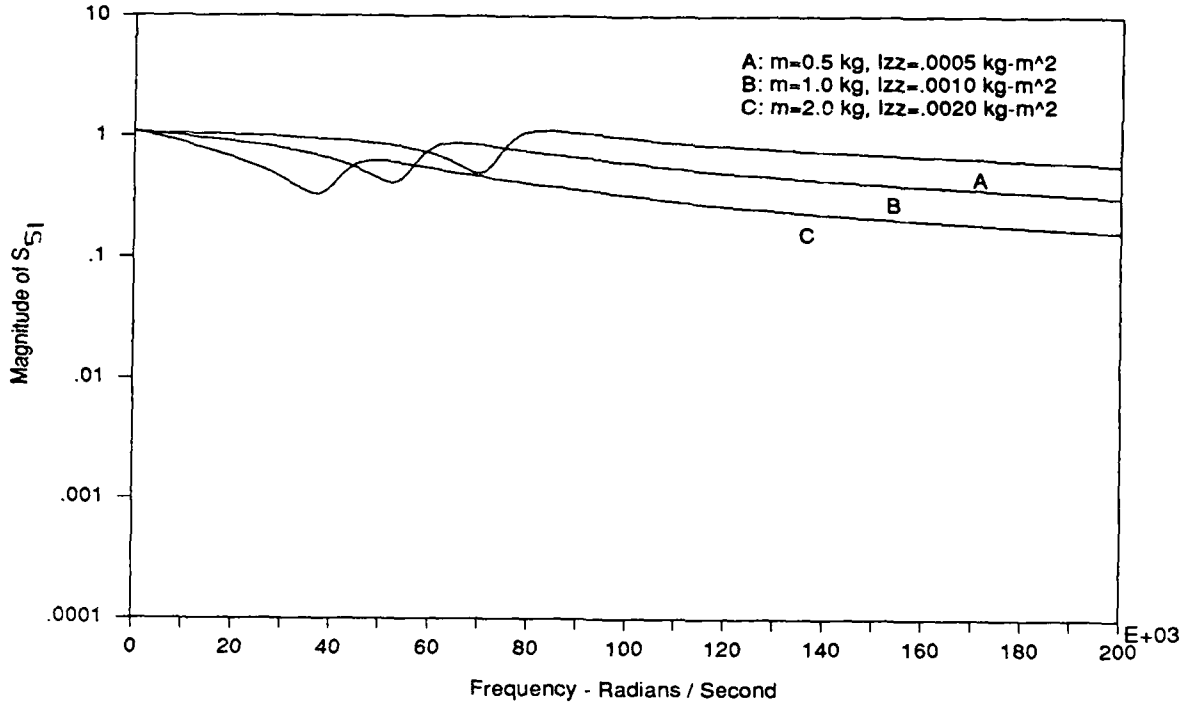

Fig. 17a Magnitude of scattering matrix transmission coefficient S_{51}.

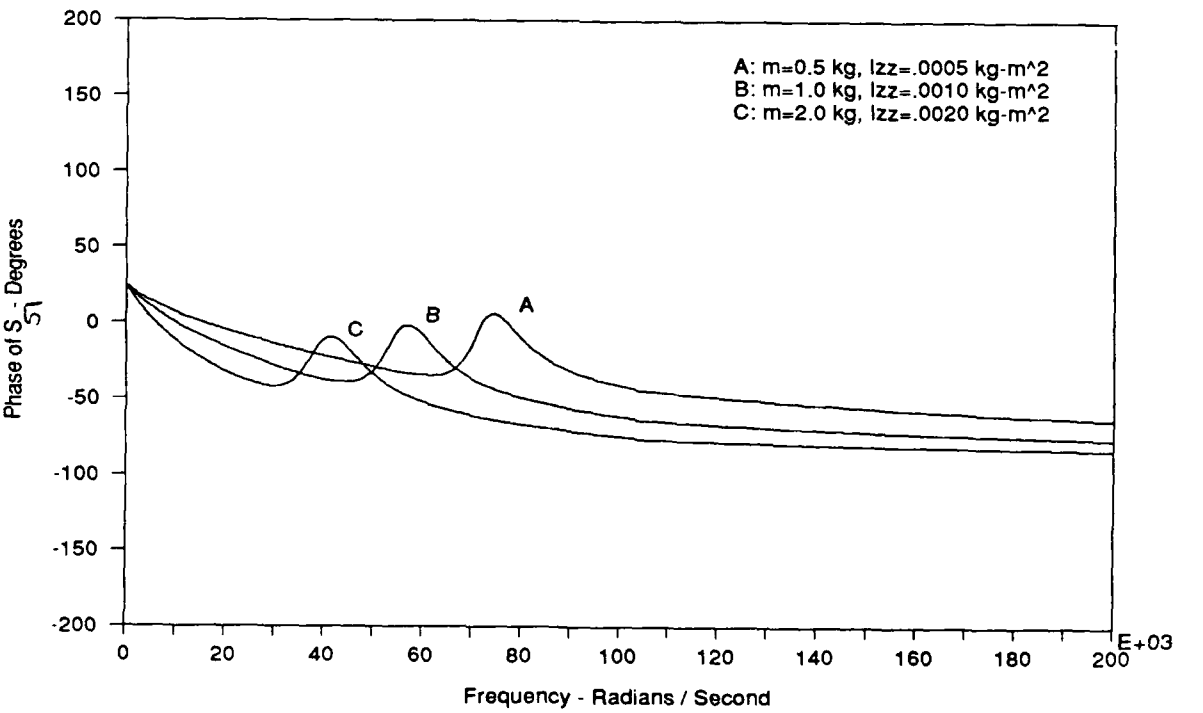

Fig. 17b Phase of scattering matrix transmission coefficient S_{51}.

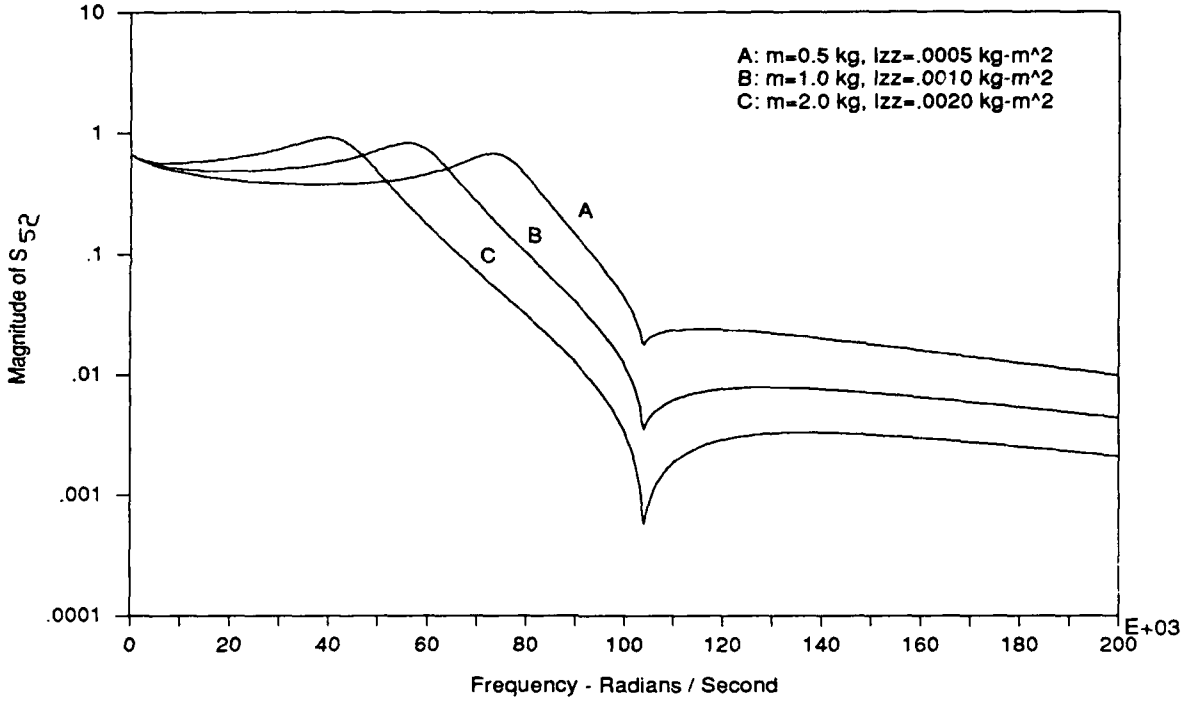

Fig. 18a Magnitude of scattering matrix transmission coefficient S_{52}.

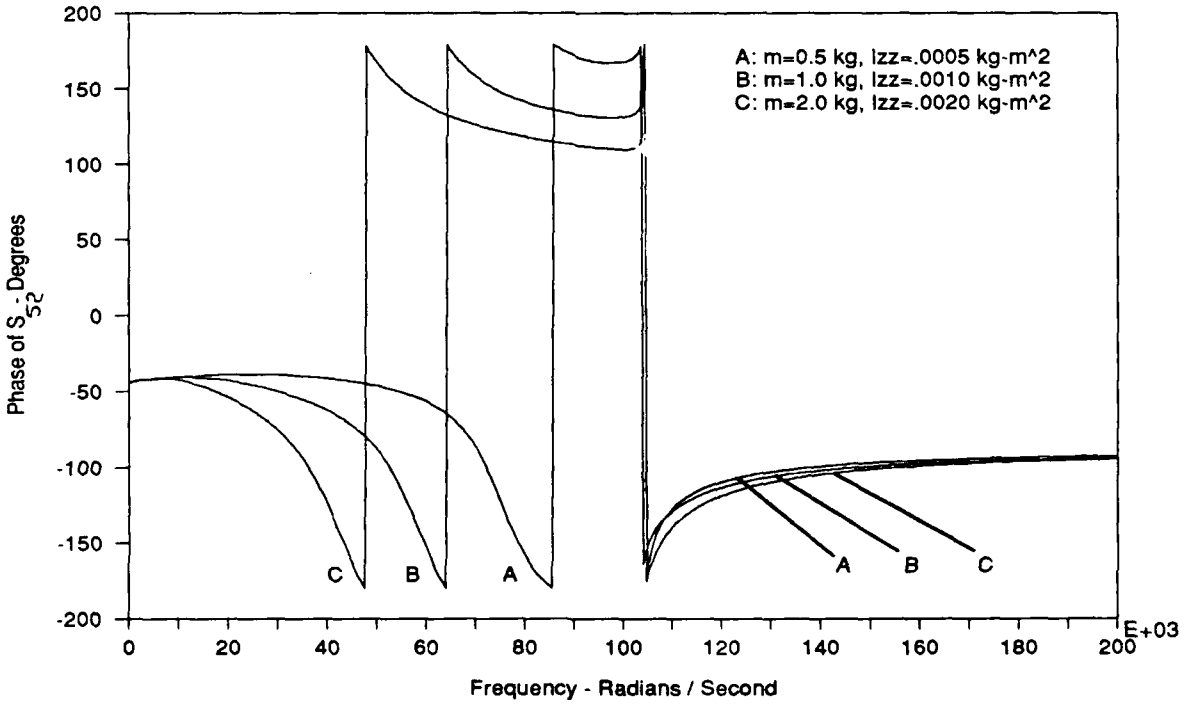

Fig. 18b Phase of scattering matrix transmission coefficient S_{52}.

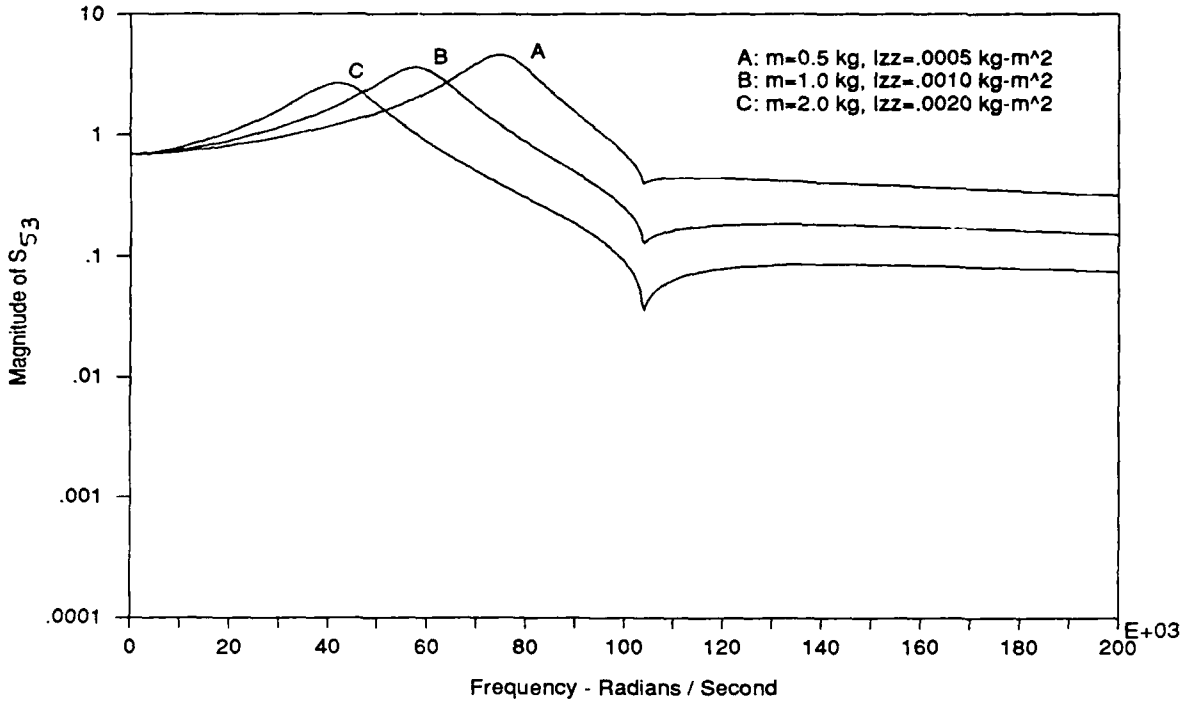

Fig. 19a Magnitude of scattering matrix transmission coefficient S_{53}.

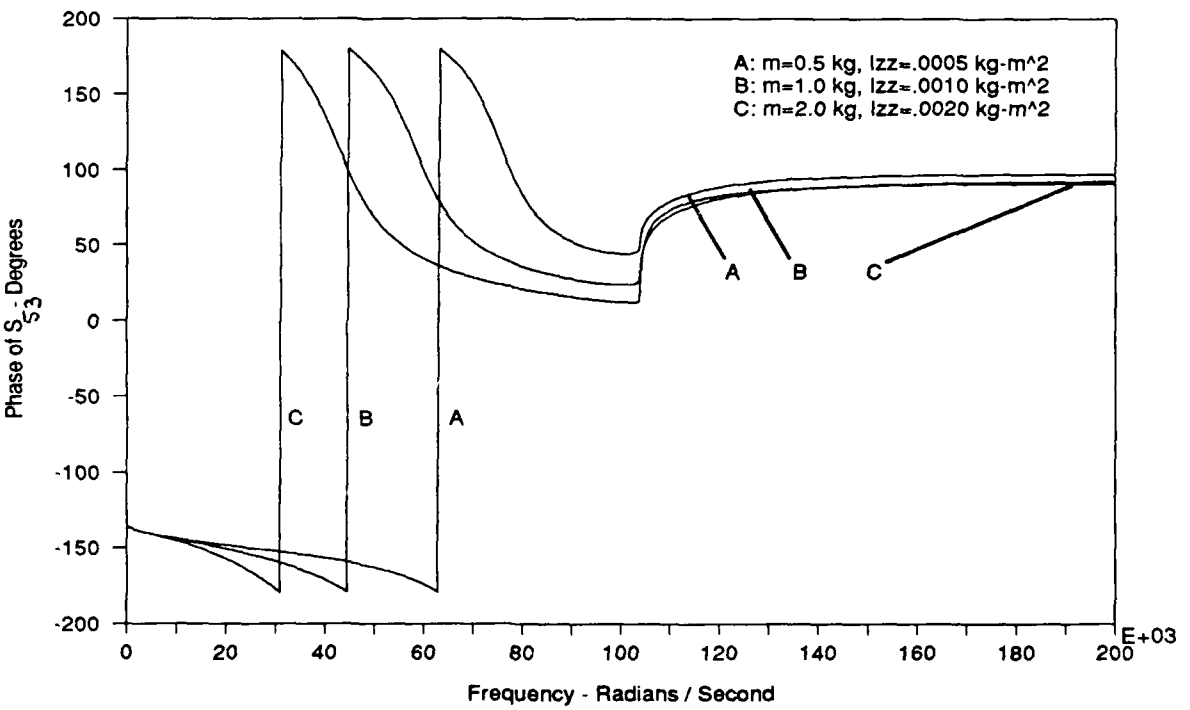

Fig. 19b Phase of scattering matrix transmission coefficient S_{53}.

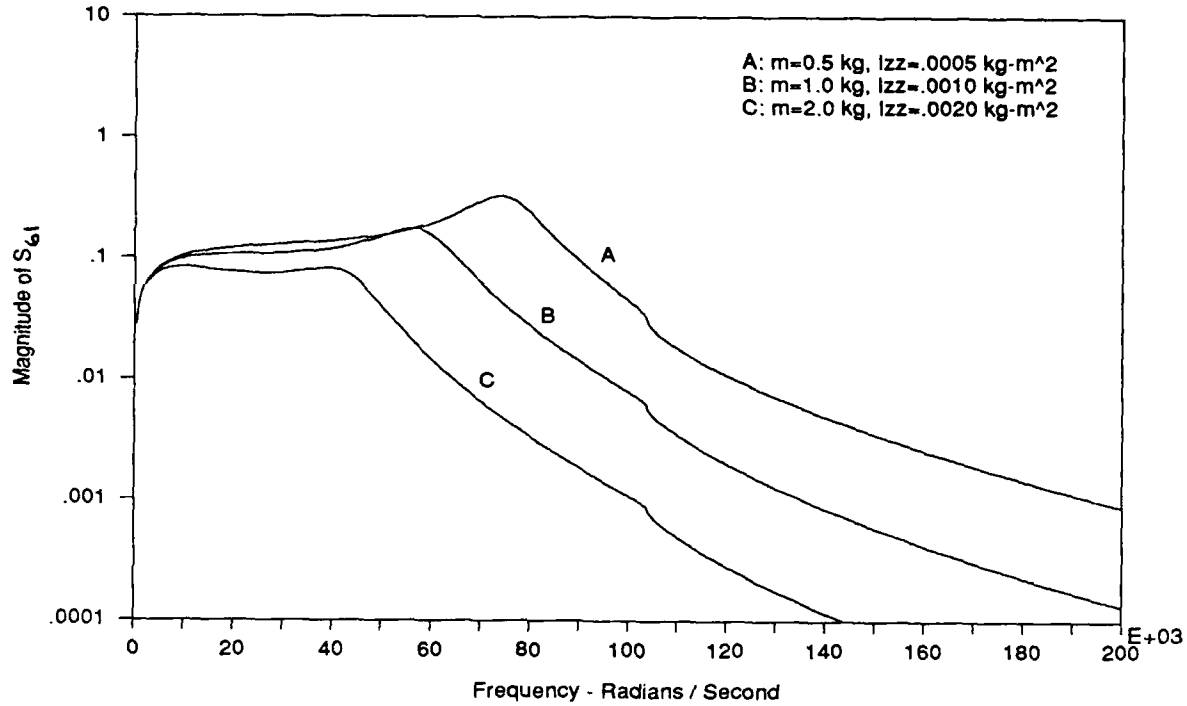

Fig. 20a Magnitude of scattering matrix transmission coefficient S_{61}.

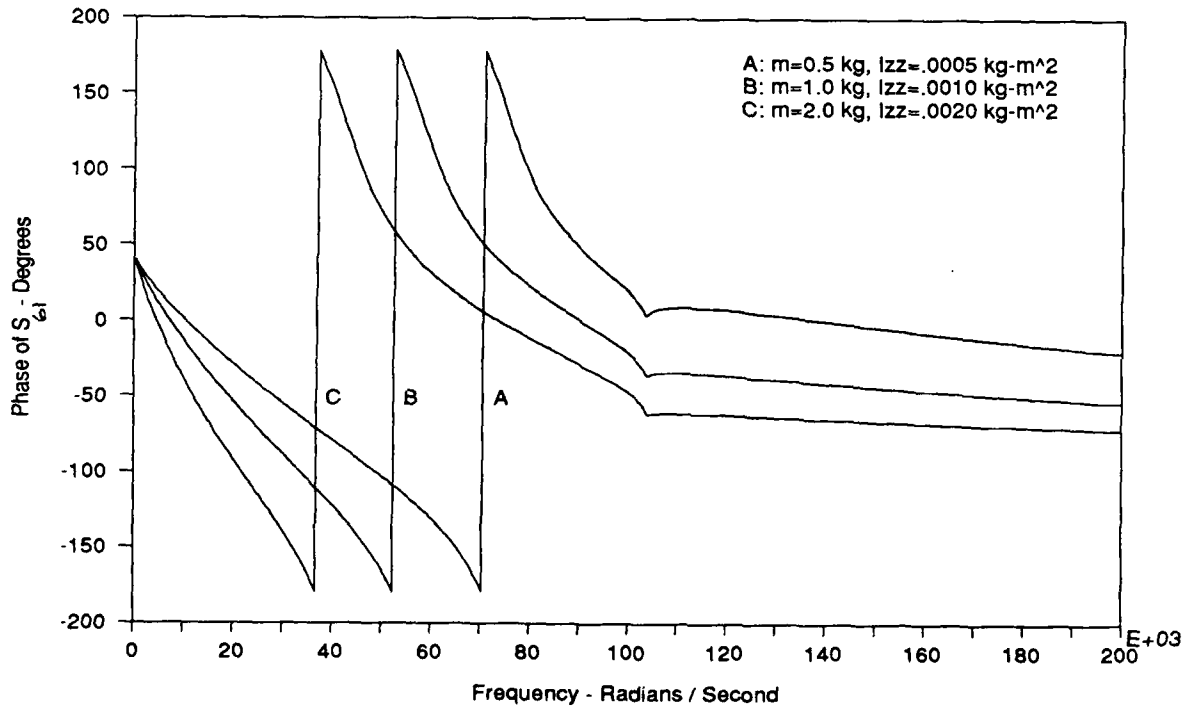

Fig. 20b Phase of scattering matrix transmission coefficient S_{61}.

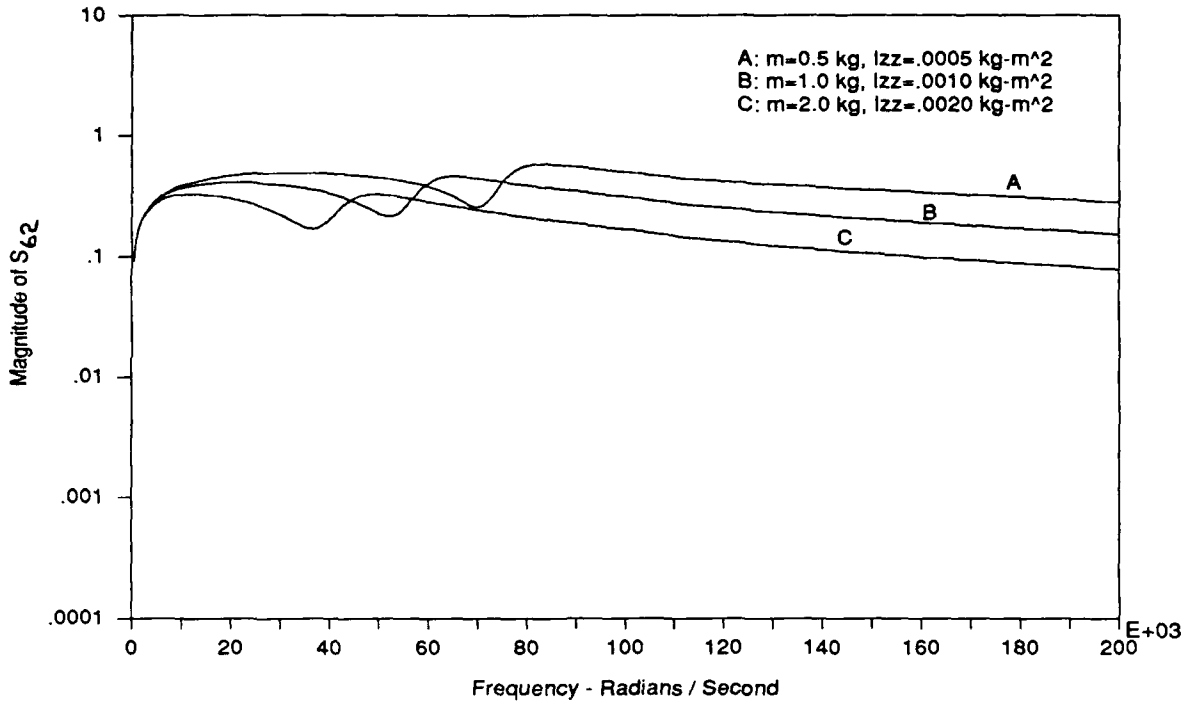

Fig. 21a Magnitude of scattering matrix transmission coefficient S_{62}.

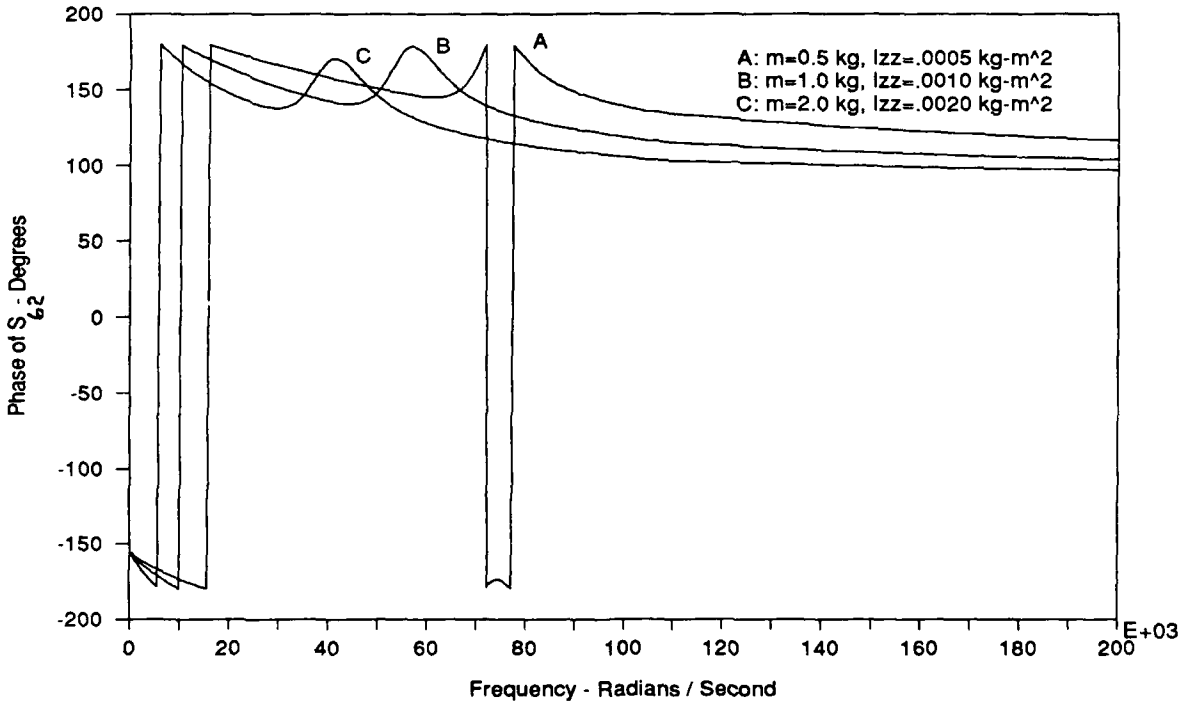

Fig. 21b Phase of scattering matrix transmission coefficient S_{62}.

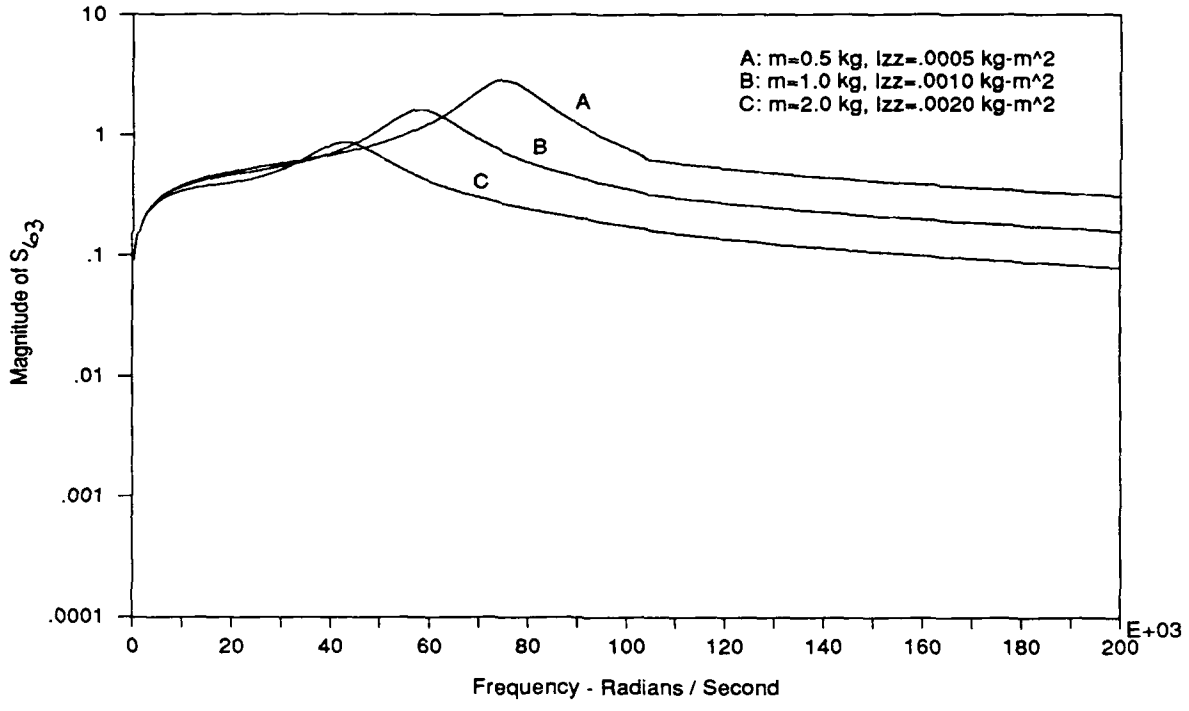

Fig. 22a Magnitude of scattering matrix transmission coefficient S_{63}.

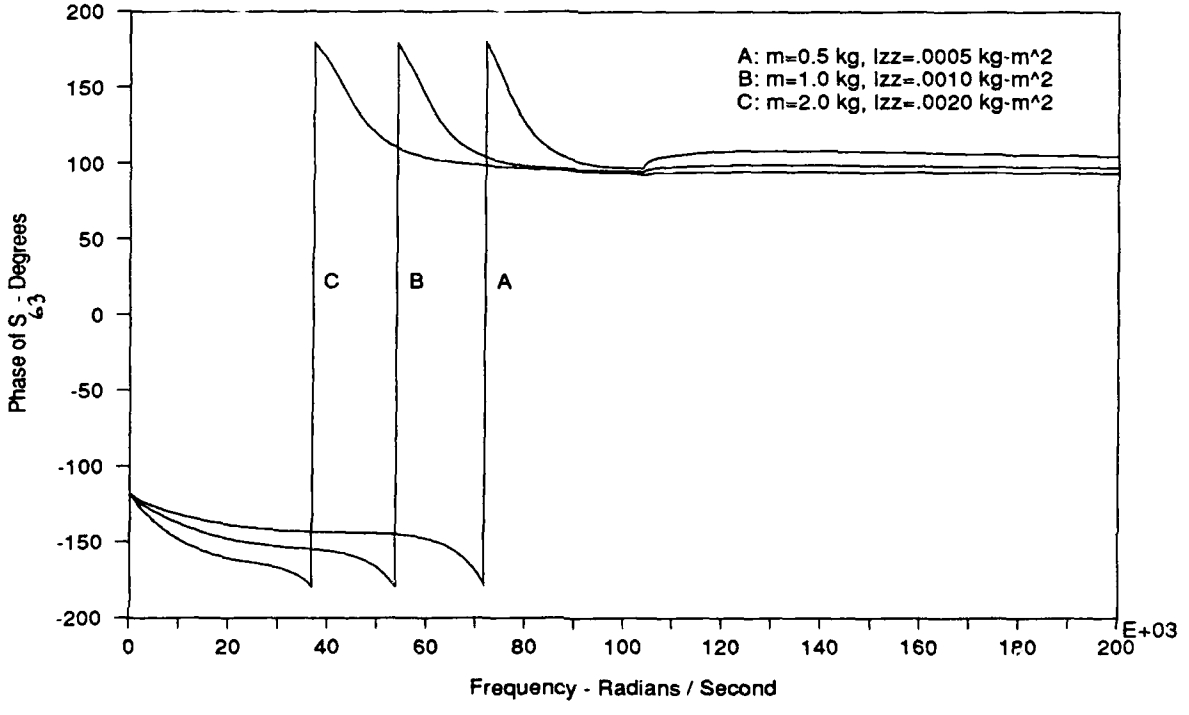

Fig. 22b Phase of scattering matrix transmission coefficient S_{63}.

Appendix A :

Summary of Wave-Mode Coordinate Analysis
of One-Dimensional Continuous Lattice Member

In this appendix, a summary of the concepts and nomenclature of wave-mode coordinate analysis used to study wave propagation in continuous one-dimensional lattice members is presented. The lattice member is modeled as an elastic longitudinal rod for axial motion and a Timoshenko beam for flexural motion. A more detailed discussion of the major developments that follow are discussed in [A1].

State Vector

A section of the lattice member is shown in Fig. A1, which illustrates the local coordinate system defining the positive orientation of axial displacement u, transverse displacement y, rotation ψ, axial force N, shear force V and moment M. The member is assumed to be uniform, with cross-sectional area A, section moment of inertia I, tensile modulus E, shear modulus G, mass density ρ and a shear correction coefficient κ.

The Fourier transformed state vector at point 1 and point 2 are

$$\underline{\bar{z}}^T(x_1,\omega) = \{\bar{u}_1 \quad \bar{y}_1 \quad \bar{\psi}_1 \quad \bar{M}_1 \quad \bar{V}_1 \quad \bar{N}_1\} \tag{A1}$$

$$\underline{\bar{z}}^T(x_2,\omega) = \{\bar{u}_2 \quad \bar{y}_2 \quad \bar{\psi}_2 \quad \bar{M}_2 \quad \bar{V}_2 \quad \bar{N}_2\} \tag{A2}$$

where the superscript ^{T} indicates a matrix transpose operation. An overbar signifies a Fourier transform and an underbar signifies a column vector or matrix.

Transfer Matrix

The Fourier transformed state vector at point 1 and point 2 are related by the transfer matrix relationship

$$\underline{\bar{z}}(x_2,\omega) = \underline{T}(\omega)\underline{\bar{z}}(x_1,\omega) \tag{A3}$$

where $\underline{T}(\omega)$ is the transfer matrix of order n, where n is the (even) number of components of the state vectors. The transfer matrix for the combined longitudinal rod and Timoshenko beam lattice member shown in Fig. A1 is

$$\underline{T}(\omega)=\begin{pmatrix} \cos\lambda_1 & 0 & 0 \\ 0 & c_0-\sigma c_2 & l[c_1-(\sigma+\tau)c_3] \\ 0 & \dfrac{\beta^4 c_3}{l} & c_0-\tau c_2 \\ 0 & \dfrac{\beta^4 EI\,c_2}{l^2} & \dfrac{EI}{l}[(\beta^4+\tau^2)c_3-\tau c_1] \\ 0 & \dfrac{\beta^4 EI}{l^3}(c_1-\sigma c_3) & \dfrac{\beta^4 EI\,c_2}{l^2} \\ \dfrac{-\mu l w^2}{\lambda_1}\sin\lambda_1 & 0 & 0 \end{pmatrix}$$

$$\begin{pmatrix} 0 & 0 & \dfrac{l}{EA\lambda_1}\sin\lambda_1 \\ \dfrac{l^2 c_2}{EI} & \dfrac{l^3}{\beta^4 EI}[(\beta^4+\sigma^2)c_3-\sigma c_1] & 0 \\ \dfrac{l}{EI}(c_1-\tau c_3) & \dfrac{l^2 c_2}{EI} & 0 \\ c_0-\tau c_2 & l[c_1-(\sigma+\tau)c_3] & 0 \\ \dfrac{\beta^4 c_3}{l} & c_0-\sigma c_2 & 0 \\ 0 & 0 & \cos\lambda_1 \end{pmatrix} \qquad (A4)$$

where

$$l = x_2 - x_1 \qquad (A5)$$

$$\mu = \rho A \qquad (A6)$$

$$J = \rho I \qquad (A7)$$

$$\sigma = \frac{\mu l^2 \omega^2}{\kappa A G} \qquad (A8)$$

$$\tau = \frac{J l^2 \omega^2}{EI} \qquad (A9)$$

$$\beta^4 = \frac{\mu l^4 \omega^2}{EI} \qquad (A10)$$

$$\lambda_1 = \omega l \sqrt{\frac{\rho}{E}} \tag{A11}$$

$$\lambda_2 = \sqrt{\sqrt{\beta^4 + \frac{(\sigma-\tau)^2}{4}} + \frac{(\sigma+\tau)}{2}} \tag{A12}$$

$$\lambda_3 = \sqrt{\sqrt{\beta^4 + \frac{(\sigma-\tau)^2}{4}} - \frac{(\sigma+\tau)}{2}} \tag{A13}$$

$$\Lambda = \frac{1}{\lambda_2^2 + \lambda_3^2} \tag{A14}$$

$$c_0 = \Lambda(\lambda_2^2 \cosh\lambda_3 + \lambda_3^2 \cos\lambda_2) \tag{A15}$$

$$c_1 = \Lambda\left(\frac{\lambda_2^2}{\lambda_3}\sinh\lambda_3 + \frac{\lambda_3^2}{\lambda_2}\sin\lambda_2\right) \tag{A16}$$

$$c_2 = \Lambda(\cosh\lambda_3 - \cos\lambda_2) \tag{A17}$$

$$c_3 = \Lambda\left(\frac{\sinh\lambda_3}{\lambda_3} - \frac{\sin\lambda_2}{\lambda_2}\right) \tag{A18}$$

The eigenvalues and eigenvectors of the transfer matrix $\underline{T}(\omega)$ form the wave-mode propagation matrix and the wave-mode matrix, respectively, of the lattice member.

Wave-Mode Propagation Matrix

There are n eigenvalues of the transfer matrix $\underline{T}(\omega)$. For uniform lattice members, the eigenvalues occur in pairs, where the eigenvalues of an eigenpair are algebraic inverses of each other. Each eigenpair represents an independent wave which may propagate along the lattice member. Therefore, there are $n/2$ possible independent propagating waves which may traverse the lattice member. The physical interpretation of the fact that the eigenvalues of $\underline{T}(\omega)$ occur in pairs is that identical waves may propagate in the direction of increasing x or in the direction of decreasing x. The wave-mode propagation matrix is an n x n diagonal matrix whose diagonal elements are the eigenvalues of $\underline{T}(\omega)$. The wave-mode propagation matrix of the lattice member shown in Fig. A1 is

$$\underline{W}(\omega) = \begin{pmatrix} e^{-j\lambda_1} & 0 & \cdot & \cdot & \cdot & 0 \\ 0 & e^{-j\lambda_2} & & & & \cdot \\ \cdot & & e^{-\lambda_3} & & & \cdot \\ \cdot & & & e^{\lambda_3} & & \cdot \\ \cdot & & & & e^{j\lambda_2} & 0 \\ 0 & \cdot & \cdot & \cdot & 0 & e^{j\lambda_1} \end{pmatrix} \tag{A19}$$

From eqn. (A19), there are three eigenpairs and, therefore, three independent propagating waves which may simultaneously exist in the lattice member. The eigenvalues located at (*row, column*) locations (1,1) and (6,6) of $\underline{W}(\omega)$ represent longitudinal (type one) waves which may propagate along the lattice member toward increasing and decreasing x, respectively. The eigenvalues located at locations (2,2) and (5,5) of $\underline{W}(\omega)$ represent mode 1 flexural (type two) waves which may propagate along the lattice member toward increasing and decreasing x, respectively. The eigenvalues located at locations (3,3) and (4,4) of $\underline{W}(\omega)$ represent mode 2 flexural (type three) waves which may propagate along the lattice member toward increasing and decreasing x, respectively.

Wave-Mode Matrix

For each eigenvalue of $\underline{T}(\omega)$, given by $\underline{W}(\omega)$, there exists an eigenvector. The eigenvectors of $\underline{T}(\omega)$ are the columns of the wave-mode matrix. The wave-mode matrix for the lattice member shown in Fig. A1 is

$$\underline{Y}(\omega)=\begin{pmatrix} 1 & 0 & 0 \\ 0 & 1 & 1 \\ 0 & -j\dfrac{(\lambda_2^2-\sigma)}{l\lambda_2} & -\dfrac{(\lambda_3^2+\sigma)}{l\lambda_3} \\ 0 & -EI\dfrac{(\lambda_2^2-\sigma)}{l^2} & EI\dfrac{(\lambda_3^2+\sigma)}{l^2} \\ 0 & j\dfrac{EI\beta^4}{l^3\lambda_2} & -\dfrac{EI\beta^4}{l^3\lambda_3} \\ -j\dfrac{AE\lambda_1}{l} & 0 & 0 \end{pmatrix}$$

$$\begin{pmatrix} 0 & 0 & 1 \\ 1 & 1 & 0 \\ \dfrac{(\lambda_3^2+\sigma)}{l\lambda_3} & j\dfrac{(\lambda_2^2-\sigma)}{l\lambda_2} & 0 \\ EI\dfrac{(\lambda_3^2+\sigma)}{l^2} & -EI\dfrac{(\lambda_2^2-\sigma)}{l^2} & 0 \\ \dfrac{EI\beta^4}{l^3\lambda_3} & -j\dfrac{EI\beta^4}{l^3\lambda_2} & 0 \\ 0 & 0 & j\dfrac{AE\lambda_1}{l} \end{pmatrix} \qquad (A20)$$

The wave-mode matrix $\underline{Y}(\omega)$ exhibits features analogous to the modal matrix of discrete vibratory systems [A.]. Each column in $\underline{Y}(\omega)$ represents the normalized modal configuration of each Fourier transformed state variable for each type of wave.

Wave-Mode Vector

A new vector $\overline{\underline{w}}(x,\omega)$ is defined according to

$$\overline{\underline{w}}(x,\omega)=\underline{Y}^{-1}(\omega)\overline{\underline{z}}(x,\omega) \qquad (A21)$$

where $\overline{\underline{w}}(x,\omega)$, a column vector of length n, is called the wave-mode vector. The components of $\overline{\underline{w}}(x,\omega)$ are called wave-mode coordinates. The wave-mode vector at point 2 is related to the wave-mode vector at point 1 according to

$$\overline{\underline{w}}(x_2,\omega)=\underline{W}(\omega)\overline{\underline{w}}(x_1,\omega) \qquad (A22)$$

Writing out eqn. (A22) gives

$$\begin{Bmatrix} \overline{w}_1^+ \\ \overline{w}_2^+ \\ \overline{w}_3^+ \\ \overline{w}_3^- \\ \overline{w}_2^- \\ \overline{w}_1^- \end{Bmatrix}_2 = \begin{pmatrix} e^{-j\lambda_1} & 0 & \cdot & \cdot & \cdot & 0 \\ 0 & e^{-j\lambda_2} & & & & \cdot \\ \cdot & & e^{-\lambda_3} & & & \cdot \\ \cdot & & & e^{\lambda_3} & & \cdot \\ \cdot & & & & e^{j\lambda_2} & 0 \\ 0 & \cdot & \cdot & \cdot & 0 & e^{j\lambda_1} \end{pmatrix} \begin{Bmatrix} \overline{w}_1^+ \\ \overline{w}_2^+ \\ \overline{w}_3^+ \\ \overline{w}_3^- \\ \overline{w}_2^- \\ \overline{w}_1^- \end{Bmatrix}_1 \qquad (A23)$$

Eqn. (A23) is the diagonalized form of the transfer matrix relationship given by eqn. (A3). The components $\overline{w}_1^+$, $\overline{w}_2^+$ and $\overline{w}_3^+$ represent longitudinal, mode 1 flexural, and mode 2 flexural waves, respectively, which propagate along the lattice member toward increasing x. Similarly, $\overline{w}_1^-$, $\overline{w}_2^-$ and $\overline{w}_3^-$ represent longitudinal, mode 1 flexural, and mode 2 flexural waves, respectively, which propagate along the lattice member toward decreasing x.

Finally, from eqn. (A21), it follows that the Fourier transformed state vector at any specific location along the lattice member may be determined from the wave-mode vector at that location according to

$$\underline{\overline{z}}(x,\omega) = \underline{Y}(\omega)\underline{\overline{w}}(x,\omega) \qquad (A24)$$

In summary, the concepts of wave-mode coordinate analysis are developed in the frequency domain through the Fourier transform. From wave-mode coordinate analysis, the combined longitudinal rod and Timoshenko beam lattice member, shown in Fig. A1, will support as many as three independent propagating waves. The waves that the lattice member will support include a longitudinal (type one) wave, a mode 1 flexural (type two) wave and a mode 2 flexural (type three) wave.

References

[A1] J.H. Williams,Jr. and D.S. Webb, "Wave-Mode Coordinate Analysis of a Combined Longitudinal Rod and Timoshenko Beam Lattice Member", AFOSR Technical Report, September 1988.

[A2] E.C. Pestel and F.A. Leckie, Matrix Methods in Elastomechanics, McGraw-Hill, Inc., 1963.

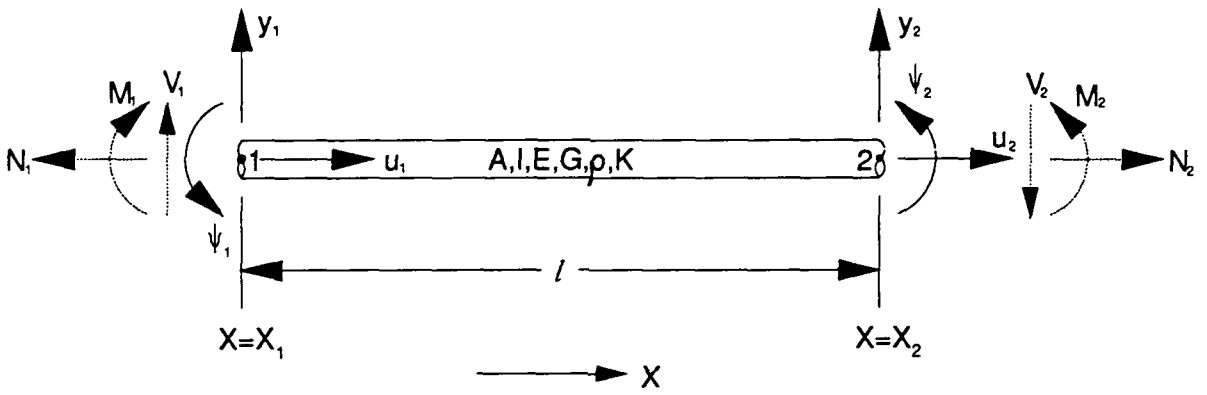

Fig. A1 Local coordinate system and state variables of lattice member.